USAFSAM-TR-85-44-PT-1

AD-A167 955

EVALUATION OF NONINVASIVE MEASUREMENT METHODS AND SYSTEMS FOR APPLICATION IN VITAL SIGNS DETECTION:
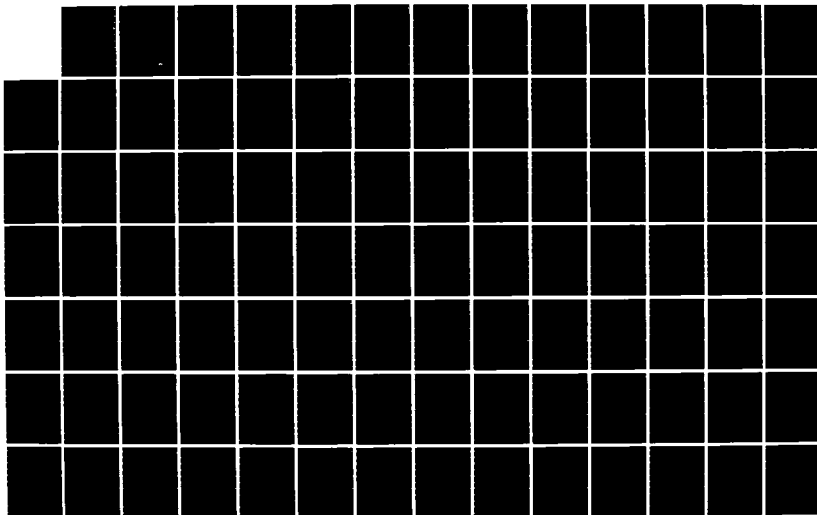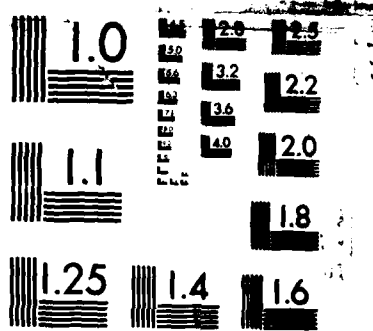
Part 1. Literature Review

Charles S. Lessard, Ph.D.
Wing Chan Wong, M.S.

Bioengineering Program
Industrial Engineering Department
Texas A&M University
College Station, TX 77843

March 1986

Final Report for Period May 1983 — September 1984

DTIC
ELECTE
MAY 30 1986
S   D
B

UNG FILE COPY

86 5 30 002

AD-A167955

REPORT DOCUMENTATION PAGE

1a. REPORT SECURITY CLASSIFICATION Unclassified		1b. RESTRICTIVE MARKINGS		
2a. SECURITY CLASSIFICATION AUTHORITY		3. DISTRIBUTION/AVAILABILITY OF REPORT Approved for public release; distribution is unlimited.		
2b. DECLASSIFICATION/DOWNGRADING SCHEDULE				
4. PERFORMING ORGANIZATION REPORT NUMBER(S)		5. MONITORING ORGANIZATION REPORT NUMBER(S) USAFSAM-TR-85-44-PT-1		
6a. NAME OF PERFORMING ORGANIZATION Bioengineering Program Industrial Engineering Dept.	6b. OFFICE SYMBOL (If applicable)	7a. NAME OF MONITORING ORGANIZATION USAF School of Aerospace Medicine (VNC)		
6c. ADDRESS (City, State and ZIP Code) Texas A&M University College Station, TX 77843		7b. ADDRESS (City, State and ZIP Code) Aerospace Medical Division (AFSC) Brooks Air Force Base, TX 78235-5301		
8a. NAME OF FUNDING/SPONSORING ORGANIZATION	8b. OFFICE SYMBOL (If applicable)	9. PROCUREMENT INSTRUMENT IDENTIFICATION NUMBER F33615-83-D-0602		

8c. ADDRESS (City, State and ZIP Code)	10. SOURCE OF FUNDING NOS.			
	PROGRAM ELEMENT NO.	PROJECT NO.	TASK NO.	WORK UNIT NO.
	62202F	2729	02	05

11. TITLE (Include Security Classification) EVALUATION OF NONINVASIVE MEASUREMENT METHODS AND SYSTEMS FOR APPLICATION IN VITAL SIGNS DETECTION: Part 1. Literature Review

12. PERSONAL AUTHOR(S)
Lessard, Charles S.; and Wong, Wing Chan

13a. TYPE OF REPORT Final Report	13b. TIME COVERED FROM May 1983 TO Sep 1984	14. DATE OF REPORT (Yr., Mo., Day) 1986, March	15. PAGE COUNT 143

16. SUPPLEMENTARY NOTATION

17.	COSATI CODES		18. SUBJECT TERMS (Continue on reverse if necessary and identify by block number)
FIELD	GROUP	SUB. GR.	Chemical defense Noninvasive medical techniques
06	12		Vital signs Cardiac sounds Respiratory sounds
15	02		

19. ABSTRACT (Continue on reverse if necessary and identify by block number)

The principal aim of this study was to evaluate current literature on noninvasive methods and instruments to provide recommendations on direction of technical development which could lead to a system or device for measuring vital signs of incapacitated military personnel in a toxic field environment. The specific aims of the study were:

(1) to determine the set of physiological parameters most likely to give the condition of an individual;

(2) to evaluate current noninvasive techniques and medical instruments to perform the desired life sign detection in a field environment without violating the integrity of the chemical protective garment; and

(3) to recommend areas of technological development that may lead to a noninvasive system or instrument for measurement or monitoring of vital life signs.

20. DISTRIBUTION/AVAILABILITY OF ABSTRACT	21. ABSTRACT SECURITY CLASSIFICATION		
UNCLASSIFIED/UNLIMITED ☒ SAME AS RPT. ☐ DTIC USERS ☐	Unclassified		
22a. NAME OF RESPONSIBLE INDIVIDUAL Yasu Tai Chen, M.S.	22b. TELEPHONE NUMBER (Include Area Code) (512) 536-2921	22c. OFFICE SYMBOL USAFSAM/VNC	

DD FORM 1473, 83 APR   EDITION OF 1 JAN 73 IS OBSOLETE.

19. ABSTRACT (Continued)

The physiological measures considered primary vital life signs in order of priority are respiratory rate or frequency contents of respiratory sounds, heart rate from raw cardiac (ECG) signal or heart sounds, blood pressure, and core temperature.

The second specific aim of the study was to evaluate current noninvasive techniques and systems which could perform desired life signs detection in a field environment without violating the integrity of the protective garment. The most promising methods/systems in order of utility ranking were electromechanical measurements of respiratory and cardiac sounds, dry electrodes, and infrared technology.

The last specific aim of the study was to recommend areas of technological development which may lead to the desired field system. The two most promising areas are given in order of payoff. Biomagnetic field measurements with a miniaturized, direct-current (DC), superconducting quantum interference device (SQUID) with a second derivative gradiometer coil configuration and a self-contained cryogenic pump system offer the most advanced high-technology area for noncontact, through the protective garment measurements of the magneto-cardiogram. Development of this system is considered the highest risk with highest payoff results. The second new technology area is in the area of bioelectric field measurements, with sensing antennas to measure variation in the electric field resulting from what appears to be body mechanical movement, e.g., respiration and heart activity of the charged body surface. This method is lower risk with lower payoff in utility results.

Accession For

NTIS   CRA&I
DTIC TAB
Unannounced
Justification

By
Distribution/

Availability Codes

Dist   Avail and/or
            Special

A-1

DTIC
SELECTED
MAY 30 1986
B

TABLE OF CONTENTS

List of Figures

List of Figures (Continued)

List of Tables

Table

CHAPTER 1

INTRODUCTION

In the event of chemical warfare, military medical technicians must be able to identify and treat victims exposed to harmful chemical agents. To determine which victims are in need of immediate treatment, a diagnostic tool is needed to help technicians in the performance of triage. As a preface to the design of such a diagnostic tool, this report will review technologies currently available which may be used to identify life signs at the first echelon of medical attention in a toxic environment.

Scope of Research

This study is divided into two parts. The first part requires a detailed search and evaluation of current literature on noninvasive methods and instrumentation techniques to measure vital life signs. The second part describes the fabrication of a prototype system. Emphasis is on providing insight and recommendations on direction of technical development which could lead to a noninvasive system for measurement or monitoring of vital life signs in a field environment. Minimum emphasis was placed on fabrication of the prototype because of funding limitations.

Specific Aims

The specific aims of the study were:
(1) to determine the set of physiological parameters most likely to give the condition of an individual,

(2) to evaluate current noninvasive techniques and medical instruments to perform the desired life sign detection in a field environment without violating the integrity of the chemical protective garment, and

(3) to recommend areas of technological development which may lead to a noninvasive system or instrument for measurement or monitoring of vital life signs.

Approach

The review of various methods for the expansion of man's senses to acquire vital life signs under a specific scenario leads to several viewpoints from which to approach the subject of biomedical instrumentation. One approach is from the physical phenomena that are to be measured, such as, bioelectric potentials, biomechanical sound waves, electromagnetic (biomagnetic field), and thermal radiations from the body. Another approach is from the measurement techniques of each physiological

system. For vital life signs measurement and assessment this reduces to the three principal systems: cardiovascular, pulmonary, and nervous. From a physician's viewpoint, the latter may be more familiar and therefore preferred; whereas, from an engineer's viewpoint, the former is more familiar and can be associated with the principle of transduction, i.e., resistive, inductive, capacitive, piezo-electric, mechanical force, pressure, etc.

This report is approached from the biomedical engineers' view, i.e., the application of engineering science and technology to medical problems. The chapters which follow, therefore, will be presented in the order of physical phenomena to be measured. This style of presentation has an advantage in that measurement techniques which are applicable to more than one physiological system can be discussed in the same section. This will be the case where the same transducer may be used for more than one system (in special cases, the measurements may be simultaneously obtained). The order of presentation will be from the more commonly used methods and instruments to the more advanced methods and systems still under study or development. Chapters 3 and 4 will discuss bio-potential systems, i.e., electrodes for electrocardiogram (ECG) recordings. Emphasis is placed on the dry or capacitive coupled electrodes and high impedance preamplifier systems. Chapter 5 deals with the latest studies in the electric fields. Chapters 6 through 9 cover noninvasive electro-mechanical devices. These devices include the electronic stethoscope for respiratory or cardic sounds analysis. Chapter 8 reviews the auscultatory method of indirect blood pressure measurements. Chapter 9 discusses ultrasonics. Chapters 10 and 11 review the use of electromagnetic radiations from the body, i.e., infrared and microwaves. Chapters 12 and 13 examine the latest state of the methods resulting from detection of biomagnetic fields from the body. Chapter 14 discusses the trend in imaging system. Chapter 15 is a discussion and evaluation of the utility value of the various methods and systems presented in previous chapters. Conclusions and recommendations are presented in Chapter 16.

CHAPTER 2

DIAGNOSIS OF CHEMICAL CASUALTIES

Although there are a variety of chemical agents used to incapacitate military personnel, the most prevalent and dangerous are nerve agents [1]. A group of highly toxic organophosphates include the G-agents and V-agents, available in both liquid and vaporous forms. These agents may be absorbed through any body surface including the skin, eyes, respiratory tract, gastrointestinal tract, and membranes of the nose and mouth. The respiratory tract is the most rapid and efficient route of absorption [1].

The primary mechanism of action of nerve agents is via the inhibition of cholinesterase enzymes throughout the body [2]. Such inhibition results in the accumulation of excessive concentrations of acetylcholine (ACH) at its various sites of action which include cholinergic motor neurons, preganglionic (cholinergic) fibers of the sympathetic, and pre- and post-ganglionic fibers of the parasympathic nervous endings [3-5]. The accumulation of ACH at these sites results in both muscarine-like and nicotine-like signs and symptoms. Accumulation of ACH in the brain and spinal cord results in characteristic central nervous system (CNS) symptoms [1].

Following inhalation of a nerve agent, respiratory symptoms begin before the systemic effects, but other muscarine-like, nicotine-like, and CNS effects may develop [1]. Local ocular effects, as well as respiratory effects, begin within one to several minutes after exposure, before there is any evidence of systemic absorption. The earliest ocular effect is pupillary constriction, sometimes unequal, and redness of the eyes or twitching of the eyelids. The earliest effects on the respiratory tract, following minimal exposure, are a watery nasal discharge, nasal hyperemia, prolonged wheezing expiration suggestive of bronchoconstriction and increased bronchial secretion. At about six to eight times the minimal symptomatic exposure, enough nerve agent is absorbed to produce more severe local ocular and respiratory effects as well as systemic effects [1].

As the nerve agent is absorbed into the systemic circulation, muscarine-like effects occur with excessive bronchial secretion causing coughing, airway obstruction, and respiratory distress. Bronchial secretions run out the sides of the mouth. Laryngeal spasm may add to respiratory difficulties, and the victim may become cyanotic. Following inhalation of nerve agent vapor, the respiratory manifestations predominate over the other muscarine-like effects which include sweating, increased peristalsis, abdominal cramps, nausea and vomiting, diarrhea, urinary frequency (sometimes involuntary), increased lacrimation, and occasional slight bradycardia [1].

With the appearance of nicotine-like systemic effects, involuntary muscular twitching and muscle cramps may occur. The skin may be pale and blood pressure slightly elevated due to vasoconstriction. If the exposure has been sufficient, twitching movements appear in all parts of the body

3

followed by severe generalized muscular weakness, including the muscles of respiration. The respiratory movements become more labored, shallow and rapid, then slow, and finally become intermittent or cease entirely. Unless artificial respiration is started promptly, the subject may die of anoxia [1].

With the appearance of moderate symptoms, CNS effects may be found in abnormalities of the electroencephalogram (EEG). These abnormalities are characterized by irregularities in rhythm, variations in potential, and intermittent bursts of abnormally slow waves of elevated voltage similar to those seen in patients with epilepsy [1]. The conscious patient becomes confused and slurs his speech. He may become comatose; his reflexes may disappear; and his respiration may become Cheyne-Stokes in character. These symptoms may be followed by generalized convulsions. Depression of the circulatory centers may also occur, causing the blood pressure, which previously may have been elevated, to fall. Cardiac rhythm may become irregular [1].

Common symptomatic indicators of the degree of the subject's exposure and seriousness of his condition may be determined from this review of signs and symptoms resulting from exposure to nerve agents. Common indicators include pulmonary edema and respiratory distress, muscular twitching, pupillary constriction, vasoconstriction, bradycardia, and abnormal EEG. Of these, the most universal indicator of either muscarinic, nicotinic, or CNS effects is respiratory distress.

Vital Signs

A swift, correct physiological assessment is essential for adequate emergency care. Such an assessment may be made by determining the patient's vital signs; however, vital signs and their parameters are rarely defined quantitatively.

According to *Webster's Dictionary* [6], vital delineates those things concerned with or characterized by life; whereas, a sign denotes objective evidence observed or interpreted by a bystander. Thus vital signs may be regarded as those discernible signs of life which are intrinsic to the state of well being of the human body. Most sources agree that temperature, pulse (heart rate), respiration, and blood pressure constitute the major vital signs [7-10]. Although many consider pupillary reflex and level of consciousness also vital signs, they are not vital to life and will not be included in this report. Therefore, the determination of the main vital signs (pulse, respiration, blood pressure, and temperature) enable medical personnel to generally assess a patient's condition. It is logical to prioritize vital signs, by the accepted assessment and treatment of emergency cases, i.e., ABC--airway, breathing, cardiac [11,12]. Therefore, respiration and cardiac (rate, action, etc.) are primary signs in respective order, whereas, blood pressure and temperature are secondary signs. It should be noted that vital signs interact such that one particular vital life sign should not be used to determine a patient's condition.

In an optimum situation, a medic, physician, etc. would deal with one injured/ill person at a time and use all medical technology and knowledge now available. However, this is not always possible and sometimes even a facsimile of the care one would like to administer is not possible. In the event of a disaster, moreover, one must determine a system so that the greatest number of patients with optimum function may be saved [13].

Triage

When such a situation with multiple patients occurs, triage may be used as a system for denoting priority. Triage involves distinguishing between an individual dying from an uncontrollable, irreparable condition and a less spectacularly injured person for whom immediate treatment may be life or function saving [2].

The concept of triage involves categorization of patients according to a priority for further assessment and treatment. The military concept of triage differs from the concept applied by nonmilitary medical personnel in that the military concept is aimed at maximizing the return of personnel to duty whereas the nonmilitary concept is to maximize survivability of disaster victims. Assignment of priority is dependent, therefore, on triage concept in use. Thus, any vital life signs detection system should be designed to provide information that will assist in categorizing and assigning a priority for care within this triage concept.

A complete survey of all patients is imperative before management of their respective conditions. This encompasses establishment of adequate airway, checking for presence of pulse and responsiveness, and realization of the presence of shock. Then categorization of patients according to priority and assignment of personnel to complete the assessment and treatment on that basis may be done [14]. Those that must be treated at the scene and transported immediately, receive the highest priority. These may include: airway and breathing difficulties, cardiac arrest, uncontrolled or suspected severe hidden bleeding, open chest or abdominal wounds, severe head injuries, and severe shock. Second priority encompasses: burns, major multiple fractures, and back injuries with or without spinal cord damage. Casualties that have minor fractures or other injuries of a minor nature, obvious mortal wounds, and the obvious dead receive the lowest priority and are treated last [13].

This system works well for most nonmilitary disaster situations; however, warfare and the advent of chemicals and other toxics require modification of the basic nonmilitary triage system because of the specialized situation. For example, once a chemical hazard has been determined personnel will don available protective suits [1]. This suit not only inhibits penetration by a chemical agent, but also inhibits the assessment of one's physiological condition and the rendering of necessary aid, e.g., establishment of adequate airway. Thus, realization of the need for an instrument or technique to measure vital signs through such protective garment becomes obvious. The need for a swift determination of a victim's physiological status is of utmost importance.

5

The first major steps of triage should be followed. These include assignment of the person in charge to control the medical scene followed by a survey. This initial survey should include realization of exposure to harmful chemical agents. The most common indications of contamination include miosis, respiratory distress, muscular twitching, cardiovascular dysfunction (e.g. bradydysrhythmias), salivation, and gastrointestinal dysfunction. Presently, the administration of 2 to 6 mg of atropine intramuscularly in an uncontaminated area of the thigh or upper arm is used to control the body's reaction to the nerve agent [1]. Anticonvulsant drugs should be administered as necessary.

Casualties should be categorized and assigned a priority dependent on the military concept of triage. Paramedical personnel should take into account travel time and adequacy of care available to the patient before determining priority. If the situation becomes emergent, those with burns but minimal chemical exposure, minor fractures without spinal cord damage, and other assorted minor injuries and contamination should be transported first. If there is no means of clearing out bronchial secretions or giving artificial respiration through the protective mask and the patient is unconscious and in respiratory distress, lowest priority should be deemed. Likewise, those with rapidly deteriorating conditions and those obviously dead comprise the lowest priority.

References

1. Air Force Manual 160-12. Treatment of Chemical Warfare Agent Casualties, pp. 1-7. USAFSAM Handout DM-7, August 1979.

2. Flint, T., and H. D. Cain. Emergency Treatment and Management, p 688. Philadelphia: W.B. Saunders Co., 1975.

3. Guyton, A. C. Textbook of Medical Physiology. Sixth Edition. Philadelphia: W.B. Saunders Co., 1981.

4. Ruch, T.C. and H. D. Patton, Physiology and Biophysics, 19th Ed., Philadelphia: W.B. Saunders Co., 1965.

5. Selkurt, E. E., Physiology, 2nd Ed., Boston: Little, Brown and Co., 1966.

6. Woolf, H. B., Editor-in-Chief. Webster's New Collegiate Dictionary. Springfield, Mass: G. & C. Merriam Co., 1973.

7. Phillips, C. Paramedic Skills Manual. Bowie, Md: Prentice Hall Publishing and Communications Co., 1980.

8. Darmody, W. R., and J. E. Tintinalli. Management of the Unconscious Patient, Volume 1. St Louis: C.V. Mosby Co., 1976.

9. Grant, H. D., and R. H. Murray. Emergency Care. Bowie, Md: Prentice Hall Co., 1978.

10. Thygerson, A. Trauma Premier Part II Head Injuries. *Emergency* 14:27 (1982).

11. Eisenbert, M. S., and M. Copass. Manual of Emergency Medical Therapeutics. Philadelphia: W.B. Saunders Co., 1978.

12. Hafen, B. O., and K. J. Karren. Prehospital Emergency Care and Crises Intervention. Englewood, Colo: Morton Publishing Co., 1981.

13. American Academy of Orthopaedic Surgeons. Emergency Care and Transportation of the Sick and Injured, Third Edition. Menasha, Wis: George Banta Co., Inc., 1981.

14. Abbot, J., M. Gifford, C. Chipman. J. Englken, and P. Rosen. Protocols for Prehospital Emergency Medical Care. Baltimore: Williams and Wilkins Co., 1980.

CHAPTER 3

ELECTRODES

In a living organism the functioning of many systems is often accompanied by a pattern of electrical signals [11]. These potentials can be monitored, measured, and/or recorded if some type of interface is introduced to transport the signal from the body to the electronic measuring apparatus [10]. Such a signal may then be used to monitor a particular physiological process. The conventional means for carrying out this function are biopotential electrodes [10]. As *Webster's Dictionary* states, "an electrode acts as a conductor to establish electrical contact with a nonmetallic portion of a circuit," in this case the human body [4]. In essence, the electrode operates as an electrochemical transducer to change ionic current into an electronic current [2,10]. This current is a feasible mode by which the physiological monitoring of a particular body function, specifically the electrical activity of the heart, can be obtained.

The conventional method for recording voltage variations associated with the beating of the heart is the conducting electrode pair [7,11]. "Despite the many configurations and names applied to electrodes used to measure bioelectric events, there are basically two functional types, extracellular and intracellular" [13]. Only extracellular electrodes will be discussed in this report.

There are two basic types of extracellular electrodes, i.e., nonpolarizable and polarizable. Perfectly nonpolarizable electrodes freely permit current to pass across the electrode-electrolyte interface without requiring energy to make the transition. An electrolyte is a conducting medium containing readily available ions, e.g., water with salts or acids, gels with salts, etc. On the other hand, perfectly polarizable electrodes are those in which no actual charge crosses the electrode-electrolyte interface when a current is applied. The transfer of ionic charge which does pass is a displacement current and the electrode actually functions as a capacitor [10]. When electrodes are applied to a subject, a galvanic cell is created and the pair of electrodes act as transducers [12,13].

The particular charge distribution that occurs when an electrode comes in contact or close proximity with an electrolyte or the subject causes the electrode to acquire a potential [13]. The electrical stability of an electrolyte is related to the stability of the region of charge gradient. The region of charge gradient is the charge layer that exists at the interface between the electrode and the subject under observation. Stabilization of this interface and prevention of movement artifacts is of major concern in design consideration. The interface includes not only an electrode-electrolyte interface (if used) but also the skin and its underlying tissue fluids [12]. Therefore, "distortionless insertion of the event into a recording apparatus requires special consideration of the electrodes and the input impedance of the amplifier" [12].

Wet Electrode Electrolytes

The term "wet" is applied to electrodes that employ an electrolyte, e.g., a paste, jelly, or some other type of conducting medium through which a current, either ionic or electrical, may pass between the skin and electrode. Such a medium is believed to enter the integument and gradually shunt the skin's impedance, thus lowering overall impedance [2]. Electrolytes may also reduce some movement artifact; however, this is true only with the recessed type of electrode where the electrode-electrolyte interface is not in contact with the skin of the subject [12].

Despite the advantages of using an electrolyte, there are many drawbacks. Although the whole idea behind an electrolyte is the passage of current or merely ionic activity, increased electrochemical noise at the electrode site does deteriorate the biopotential being measured [1]. These electrical artifacts cause severe reliability problems [5]. Also, it has been realized that paste is not only irritating to the skin, but also requires careful skin preparation to obtain clinically useful results [3,5]. Olson et al. stated that "further studies are needed to find a gel (electrolyte) which consistently interacts with the skin to reduce and equalize skin impedance" [2]. Because of their unsatisfactory performance in long-duration experiments, conventional "wet" electrodes are not feasible for extended use. During long-term use increasing variations in resistance readings occur if the skin surface is damaged. Irritation as well as infection can result from the electrolytic paste [1]. Sadly enough, pastes can serve as sites for bacterial and fungal growth [7] as studies have shown increased aerobic and anaerobic bacteria at the attachment site [1]. Thus the attachment site becomes a prominent site for poisoning and/or contamination to occur.

Impedance

The desire to reproduce the time varying biological phenomena as a distortionless signal requires that current into the preamplifier be zero [1]. The input impedance of most biological preamplifiers is high [12] in order to avoid the loss of amplitude and distortion of the electrical waveform. Geddes recommends that the input impedance of the amplifier be 100 to 1000 times higher than the impedance of the electrode-subject circuit [13]. When the electrode-skin impedance magnitude is much smaller than that of the amplifier input impedance, distortion and noise effects on the biopotential reading are negligible [2].

Each type of electrode exhibits an impedance that depends on the nature of its design and the electrical double layer from which its electrical current (either actual or displacement) is derived [12]. Precaution must be taken, therefore, to permit as little current as possible through the interface so that a minimum of voltage loss and waveform distortion will be introduced by the electrode's impedance [13]. The series impedance of a given interface decreases with increasing current density per frequency. Geddes and Baker contend that a low impedance circuit can be obtained by a thin dielectric with a high dielectric constant or high capacitance [12].

10

Such a capacitance may be calculated from the relationship:

$$C = Kf^{-\alpha} \qquad (3.1)$$

where K is a constant that depends on the type of metal-
electrolyte junction, and α is a constant describing
the rate at which the capacitance decreases with
increasing frequency (ideally $\alpha = 5$).

Roughened surfaces, an increase in concentration of the electrolyte, and increase in temperature all increase the value of the series equivalent electrode-electrode capacitance [13]. If the two amplifier instruments are connected to skin impedances which have appreciable different values, the noise rejection capability of the amplifier system is seriously compromised [2]; however, it has been noted that impedance imbalance decreases with time [2,3,13]. In addition, Day and Geddes observed that the smaller the electrode, the higher the interface impedance [1,12]. Geddes states that electrode noise may be reduced if differences in electrode material are made as small as possible [13]. The overall solution to the impedance problem takes into account all of these factors. Most good biopotential systems are based on common mode rejection ratio or more aptly reported by Fraden et al. "common mode interference, detection, amplification, and compensation" [6].

Conventional Wet Electrodes

Various wet electrodes have been used reliably for quite some time. One of the oldest electrode designs is the suction electrode. This electrode employs a rubber cup that is easily and quickly applied, especially to a wet surface, but only for a short period of time because the negative pressure alters the capillary pressure gradient [6]. This electrode requires an electrolyte. The trend in clinics has been to use recessed electrodes with a conducting gel. The recessed electrode moves the metal disc a short distance away from the subject. This method results in movement-artifact free readings because the electrolyte absorbs the relative movement between the surface of the skin and the electrode. On the other hand, the electrode impedance is higher than direct contact electrodes.

Two promising concepts in electrode design and fabrication are the pressed pill and the disc [1]. The main design goals are a stable, reversible, low impedance electrode. The pressed pill electrode consists of metal-powder/metal salts that are combined under pressure. Often plant hydracolloids are included because they afford plasticity, adhesion, and texture. This technique also proved to be a good safety feature because the membrane protecting the electrode is homogeneous with the matrix and can be penetrated (scratched) or damaged. Hydrophillic colloid incorporated with silver/silver chloride was found to be relatively free from polarization effects and afforded extremely low potentials [1].

11

Geddes contends that the silver/silver chloride electrode is most suitable because of its low cell potential, stability, and longevity [1,12]. The silver/silver chloride electrodes are popular because they can be made electrically stable. The silver/silver chloride electrode has also been fabricated with a gelatin coat, and tests indicate that this process adds to the electrode's reversibility by keeping out protein and other poisoning molecules while being very compatible with human skin [1]. Nevertheless, wet electrodes are not without their disadvantage, as they all require an electrolyte which can be contaminated in a chemical environment. Silver/silver chloride is photosensitive, reacts with light, and the chloride coating can be degraded by abrasion [12].

Dry Electrode/Active Electrodes

Another type of electrode, introduced by the USAF School of Aerospace Medicine, is the anodized aluminum plate (2.5 x 2.5 cm) electrode or dry electrode. The anodized metal disc relies on capacitive coupling with the skin [3]. A major disadvantage of aluminum oxide is that it can be corroded by saline [8]. The Air Force has also developed lithium impregnated balsa wood electrodes. This electrode was designated as a dry electrode since no electrolyte was necessary for use. Its design requires that the intermolecular air spaces in the balsa wood are first emptied and then filled with lithium chloride solution [14]. Although this electrode shows promise, it will be disregarded because its very design includes an ease of contamination by chemicals in the environment.

An active electrode is an electrode packaged with its amplifier into one single unit, which neither uses an electrolyte nor requires skin preparation [5]. Presently, there are two types of active electrodes: insulated and dry [5,13]. Insulated electrodes contain "no metal-electrolyte interface at all". Theoretically, the only current is due to capacitor coupling [7,10,12]. One plate of this capacitor is the electrode itself while the other plate includes the insulating covering on the electrode and the dry outer layer of skin (stratum corneum) [10,13]. This insulating covering is usually a surface oxide film of the metal that has been grown on the electrode plate by vapor deposition [10]. Because no electrode-electrolyte interface is used, there are no artifacts from motion or electrode polarizaton [3]; however, "displacement on the skin will change the capacitive coupling and hence alter the charge distribution and potential" [13]. Whether this technique causes major problems has not yet been determined. On the other hand, the dry electrode incorporates the use of metallic or other conductive contact between the body and the input of the electrode amplifier [5]. Both of these electrodes are excellent prospects because: (1) there is no need for an electrolyte, (2) there is improved patient safety since little or no DC current is passed, (3) long-term application is possible, and (4) reduction of electrode area is feasible [5].

The capacitive electrode shows much promise in the noninvasive measurement of physiological signs, particularly the electrocardiogram. One must take a couple of points into consideration.

12

Since the output impedance of the electrode is very high, it is necessary to supply an impedance matching circuit in conjunction with the electrode to be used along with the usual clinical monitoring equipment [3]. Also, a field effect transistor (FET) or a metal-oxide semiconductor field effect transistor (MOSFET) is useful in cleaning up the signal from an insulated electrode [3]. These devices help prevent electrostatic puncture of the insulator. However, this extra precaution is not as necessary when an insulated power supply such as batteries is used [13]. Another means by which high impedance output may be compensated for is by putting ultrathin film of insulating materials having high dielectric constants and strength on the surface of the electrode [13].

A few feasible types of insulated electrodes are being employed today. A recent paper by Griffith et al. [7] delineates a lighter weight, more compact electrode configuration through the use of hybrid integrated-circuit technology. Their electrode consists of such a circuit adhered to a capacitor. The capacitor has been formed by "sputtering thin films of tantalum-pentoxide dielectric on a circular silicon substrate 0.176 cm in radius" [7]. However, if a larger substrate had been used, they could have used a more efficient impedance matching circuit. One drawback of this electrode is that there must be no gap between the subject and the capacitor of the electrode. Any misconnection creates a series capacitance that seriously affects results [5]. The capacitor is housed in a plastic disc that is attached to an electrode housing that contains a hybrid impedance matching circuit. The capacitor is linked directly into this circuit. This is particularly advantageous because this enables capacitors to be exchanged without changing the impedance matching circuit. In order to meet the ideal operational amplifier requirement of no significant DC offset at its output, the largest chip resistor, 100 MΩ (Mini-Systems, Inc.), was used in the buffer circuit [5,9]. The conductor circuit was printed onto a circular ceramic substrate (1.35 cm in diameter, 0.064 cm thick) with a conducting glaze fired on top. Then the operational amplifier and resistor chips were attached. The electrode was finally integrated to the input of the impedance matching circuitry. The ensemble was then placed in a National Aeronautics and Space Administration (NASA) plastic electrode housing [5]. Studies were done on the electrode's ability to function if dirty or damaged and showed no change in step response until the film "had been heavily scratched." The signal from the active electrode is superior and quite readable although a little noisy upon overall comparison with that of conventional wet electrodes. The main problem at present occurs when gross separation between the subject and the capacitor happens which causes capacitance changes [5].

Ko et al. [3] used a silicon substrate rather than a ceramic substrate. The insulting layer is thermally grown silicon dioxide instead of tantalum-peroxide. Their chip of N-type silicon (6 x 6 mm, 0.23 mm thick) incorporates a MOSFET in place of a FET. Results of their studies show that a thicker dielectric layer is not really necessary as the true dielectric layer is the thickness of the stratum corneum plus the thickness of the insulating film [3,13]. The silicon may be specially etched for a desired circuit; however, this technique is costly regardless of the superiority of design.

13

Problems To Overcome

The main problem appears to be perspiration or moisture-- the lack of it, the presence of it, the unknown amount of it. Sweat can corrode the insulating layer and/or change the impedance, etc. [12,13]. Chemical contamination could easily occur, as an instrument is used on one victim after another, if it is not waterproof. Therefore a thin, waterproof, insulating coating is suggested.

Electrode size should also be considered. The basic capacitance theory does relate size to actual capacitance which affects impedance. The smaller the electrode, the higher the interface impedance [12]. High input impedance amplifiers have made dry electrodes very feasible with records of equal quality to wet electrodes [1,3].

References

1. Day, J. L., and C. K. LaPinta. The Evolution of Long-term Systems for Electrocardiography on Manned Space Flight, pp. 351-355. *In* Biomedical Electrode Technology-Theory & Practice. Miller, H. A., and D. C. Harrison (Eds.). Academic Press, Inc., 1974.

2. Olson, W. H., D. R. Schemincke, and B. L. Henley. Time and Frequency Dependence of Disposable ECG Electrode-Skin Impedance. *Med Instrum* 13:269-272 (1979).

3. Ko, W. H., M. R. Neuman, R. N. Wolfson, and E. T. Ton. Insulated Active Electrodes. *IEEE Trans Ind Elec Control Instrum* 17:195-198 (1970).

4. Gove, P. B., (Ed.). Webster's Third New International Dictionary. Springfield, Mass.: G&C Merriam Co., 1976.

5. Ko, W. H., and J. Hynecek. Dry Electrodes and Electrode Amplifiers, pp. 169-181. *In* Biomedical Electrode Technology-Theory & Practice. Miller, H. A., and D. C. Harrison (Eds.). Academic Press, Inc., 1974.

6. Fraden, J., M. R. Neuman, and R. Rick. A Dry Electrode Monitoring System, pp. 36-39. Engineering Design Center and Francis Payne Bolton School of Nursing, Case Western Reserve University, Cleveland, 1979.

7. Griffith, M. E., W. M. Portnoy, and L. J. Stotts. Improve Capacitive Electrocardiogram Electrodes for Burn Applications. *Med Biol Eng & Comput* 641-646 (1979).

8. Ruggera, P. S. An EMC Test Procedure for an Electro-encephalograph Using Human Subjects and Simulated Electronic Patients. *IEE Internat Symp Electomag Compat* 200-205 (1980).

9. Johnson, D. E., and V. Jayokumar. Operational Amplifier Circuits: Design and Application. Englewood Cliffs, NJ: Prentice-Hall, Inc., 1982.

10. Webster, J. G. Medical Instrumentation, Application and Design. Boston: Houghton Mifflin Co., 1978.

11. Mackay, R., and J. Stuart. Biomedical Telemetry: Sensing and Transmitting Information from Animals and Man. New York: John Wiley & Sons, Inc., 1968.

12. Geddes, L. A., and L. E. Baker. Principles of Applied Biomedical Instrumentation. New York: Wiley-Interscience Publication, 1975.

13. Geddes, L. A. Electrodes and the Measurement of Bioelectric Events. New York: Wiley-Interscience Publication, 1972.

14. Salter, M. G. Fabrication of Lithium Chloride-Balso Wood Electrodes for Electrocardiographic Monitoring. USAF School of Aerospace Medicine, AFSC, Brooks Air Base, Tex, SAM-TR-69-51, Aug 1969.

CHAPTER 4

IMPEDANCE PLETHYSMOGRAPHY

Electrical bioimpedance plethysmography is a noninvasive technique by which small changes in tissue volume can be detected. The electrical impedance method is a safe noninvasive measurement technique for assessing the mechanical activity of the heart rather than the electrical activity, i.e., blood flow, cardiac output, pulse volume, stroke volume, etc. [3,4].

The basis for the impedance plethysmograph principle is the dissociation of biological tissues salts, into their corresponding positively charged cations and negatively charged anions [1]. Similar to the electrons in inorganic substances, the ions of biological tissues are responsible for the conduction of electricity. Thus, the conductance (G) of a current (I) through biological tissue depends on the number of charged ions in the tissue fluid volume [1]. Since the number of ions is fixed relative to the volume of fluid, it is theoretically possible to relate conductance to the total volume (V) of that tissue. Any change in conductance (δG) will reflect a change in volume (δV), or

$$\delta V/V = \delta G/G \qquad (4.1)$$

This relationship makes it practical to determine the impedance of the tissue by applying a small magnitude, high-frequency current across the tissue and sensing small variations of voltage with a pair of electrodes. The relationship then becomes,

$$\delta V/V = -\delta Z/Z \qquad (4.2)$$

As the volume of tissue changes due to pulsations of blood, the impedance of the tissue changes, thus, "biovolumes" can be measured in terms of electrical impedance of the tissue.

Impedance Plethysmograph Systems

For reasons of economy and ease of application, some early impedance plethysmograph systems use two electrodes. The same electrodes are used to apply the current and measure the voltage. This method causes several problems [6]:

(1) The current density is higher near the electrodes than elsewhere in the tissue. This causes the measured impedance, $Z=V/I$, to weight the impedance of the tissue more heavily at the electrode site than throughout the rest of the tissue.

(2) Pulsations of blood in the tissue cause changes in the skin-electrode impedance as well as changes in the desired tissue impedance. Since the skin-electrode impedance is in series with

17

the desired electrode impedance, it is impossible to separate the two and determine the actual tissue impedance.

To resolve these problems, a four-electrode impedance plethysmograph system is used. In the four-electrode system the excitation current flows through the two outermost electrodes. This results in a more uniform current density in the region sensed by the two inner electrodes. A tetrapolar electrode system is used to eliminate skin/electrode problems and establish a current field between the outer electrodes, or the chest [5]. The inner voltage sensing electrodes are placed as accurately as possible at the base of the neck and the level of the diaphragm [7], as shown in Figure 4.1.

The choice of frequency and current magnitude used for detecting bioimpedance or bioimpedance changes, is dictated by the prevention of harmful effects, i.e., stimulation of tissues or imparting excessive energy which is dissipated as heat [8]. Even low values of current through the thorax can stimulate sensory receptors and nerves which result in an unpleasant shock to the patient. With higher values of current, muscle tissue is stimulated and there is a potential danger of inducing ventricular fibrillation [8].

It has been shown that with increasing frequency, larger currents can be used [1,6,8]. The use of higher frequencies not only provides the protection to avoid tissue stimulation, but it permits the safe use of currents at magnitudes which could be lethal if the frequency were lower [8]. Several considerations suggest the use of a frequency of about 100 kHz [6]:

(1) It is desirable to use a current greater than 1 mA in order to achieve adequate SNR (signal-to-noise ratio). At low frequencies this current will cause an unpleasant shock to the patient. Since the current required for perception increases with frequency, frequencies above 20 kHz are used to avoid perception of the current.

(2) As the frequency is increased from low values up to 100 kHz, the skin-electrode impedance will decrease by a factor of about 100.

(3) If frequencies much higher than 100 kHz are used, then impedances of the stray capacitance will make design of the instrument difficult.

With these considerations in mind, most impedance plethysmograph systems are designed to have a constant 4 mA 100 kHz output current, which is what Kubicek et al. [9] used in their original impedance cardiograph design. Systems available today, as typified by the Minnesota Impedance Cardiograph, offer several important features [10]. Since biological tissues will not respond to current frequencies in excess of 10^5 cycles per second (hertz-Hz) unless 30 to 50 mA are applied [8]. The use of this frequency at 4 mA has a large margin of safety. A 4 mA 100 kHz stimulating current applied to the chest results in a 12 to 13 degree phase angle, which means that the capacitive reactance is about 1/4 of the impedance.

13
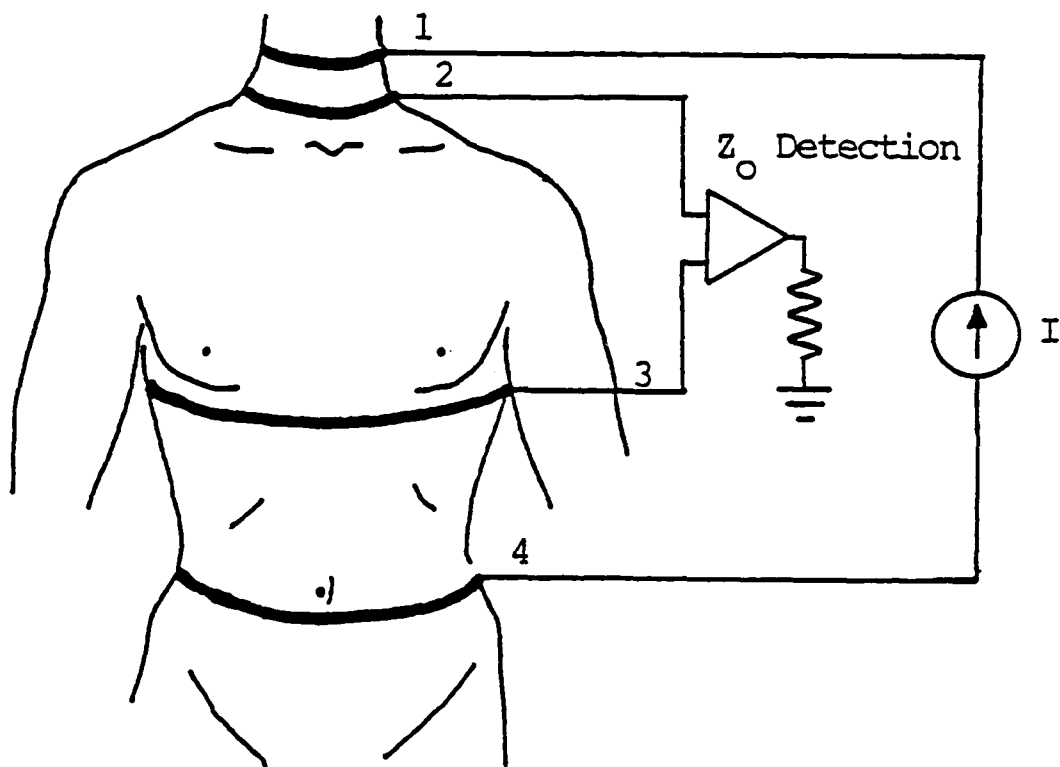
Figure 4.1. Four-electrode system for the indirect measurement of cardiac output or blood flow by means of electrical impedance.

At this frequency, there are no inductive reactance changes in biological tissue. A high output impedance (100K ohm) insures a constant current source and, along with the high input impedance (100K ohm), minimizes skin contact impedance to less than 0.004% [10].

Comparative Evaluations

In 1966, Kubicek et al. [7] introduced impedance cardiography as a noninvasive method for the measurement of cardiac output and stroke volume. The cardiac output can be calculated from the bioimpedance measurement with the following equation:

$$SV = R(L^2/Z_0^2)*t*((\delta Z/\delta t)_{max})$$ (4.3)

Where SV = Stroke Volume (ml),
R = Resistivity of the blood (ohm-cm),
(150 ohm-cm is normally used),
L = Mean distance (cm) between the two inner electrodes,
Z_0 = The basic impedance (ohm) between the two inner electrodes,
$(\delta Z/\delta t)_{max}$ = Maximum rate of change in impedance (ohm/s),
and t = Ventricular ejection times (s).

The ventricular ejection time is determined by measuring the time between the zero crossing of the first derivative just preceding the maximum negative peak $((\delta Z/\delta t)_{max})$ and the maximum positive peak at the time of the second heart sound (see Figure 4.2), or the end of t-wave of the ECG is determined by the first high-frequency component of the second heart sound in the absence of a definitive positive peak of $\delta Z/\delta t$ [7]. Since then several studies have compared measurement of cardiac output by the bioimpedance method to the dye dilution technique and to other methods. A study undertaken by Kubicek et al. involved simultaneous measurements by the two methods with the experimental subject at rest and while undergoing two levels of exercise on a bicycle.

Results of the study indicated that, on the average, the bioimpedance method provided the same physiological information concerning relative changes in cardiac output as the reference dye dilution technique [7]. This study also indicated that the reproducibility of single impedance observations of cardiac output is greater than for a similar value obtained by the dye dilution technique [7]. Other studies comparing the impedance method to the dye dilution technique confirm these results [4,11,12].

Some studies have reported consistently greater stroke volume when indirectly measured by impedance cardiography method than by dye dilution techniques [4]. In certain cases, the impedance method overestimates the stroke volume by about 30% [12].

20

ECG

PCG

S1   S2

$(\delta Z/\delta t)_{max}$

$\delta Z/\delta t$ ----- base line -----

1
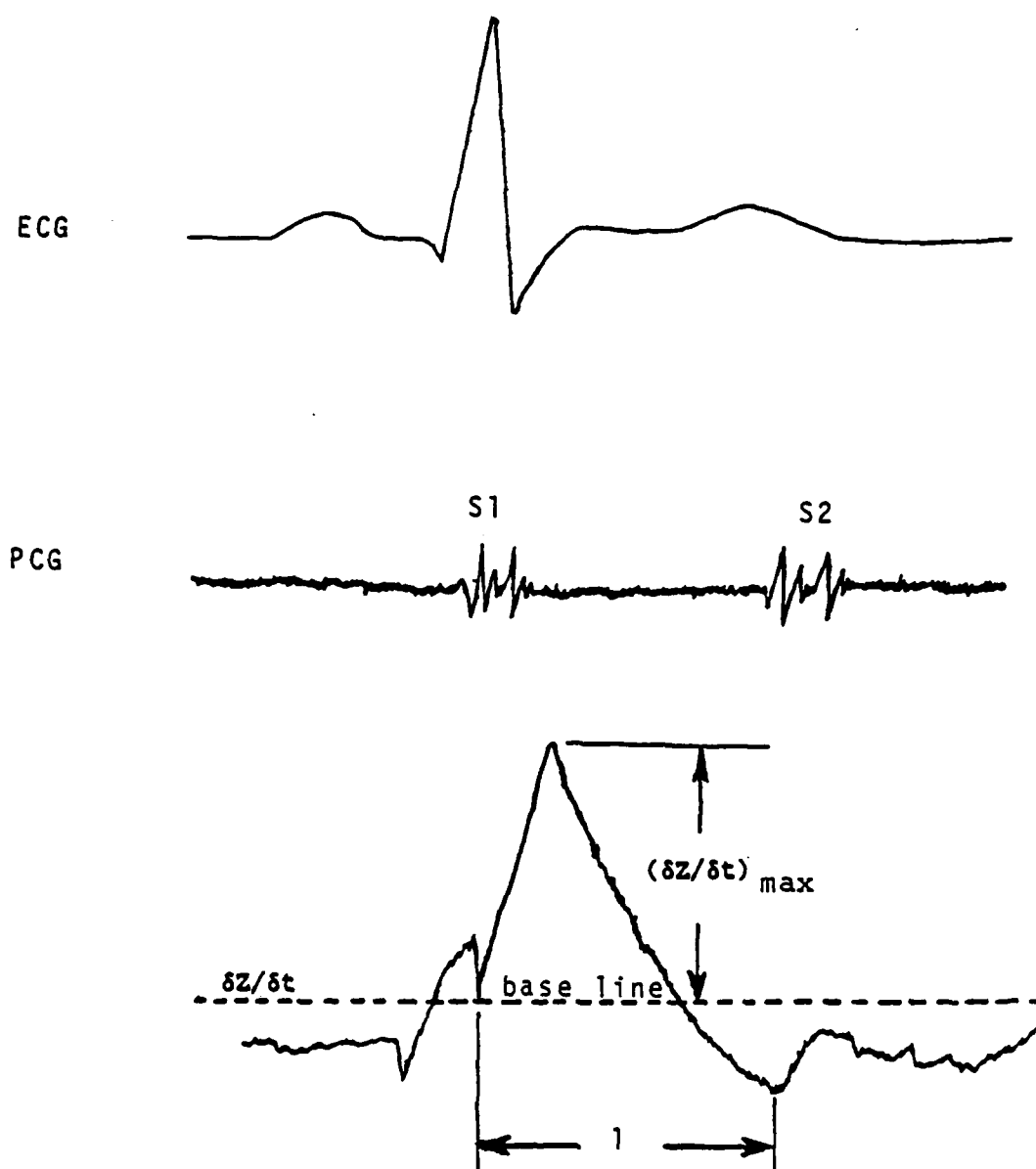
Figure 4.2. Record showing relationship between electrocardiogram (ECG), phono-cardiogram (PCG), and derivative of impedance ($\delta Z/\delta t$) during cardiac cycle.

The widest scatter between indicator dilution and impedance values was found in patients with heart disease [13]. This finding was especially true in the case of valvular incompetence [13,14]. If this is the case, the impedance method would be inaccurate for measuring stroke volume in these patients. In patients with aortic incompetence the impedance cardiac output was unrealistically high [13].

In summary, impedance plethysmography may be used to obtain a measure of stroke volume; however, it is not as accurate as other available methods. Although the bioimpedance method is noninvasive, it is not a passive measurement method since it requires that an excitation current be delivered to the subject. The use of four electrodes may not be a problem in the clinical environment, but it may present a major problem in the military field environment.

References

1. Van De Water, J. M., A. Philips, L. G. Thouin, L. S. Watanabe, and R. S. Lappen. Bioelectric Impedance. *Arch Surg* 102:541-547 (1971).

2. Nyboer, J. Electrorheometric Properties of Tissues and Fluids. *Ann NY Acad Sci* 170:410-420 (1970).

3. Geddes, L. A., and L. E. Baker. Principles of Applied Biomedical Instrumentation. New York: John Wiley and Sons, Inc., 1968.

4. Denniston, J. C., J. T. Maher, J. T. Reeves, J. C. Cruz, A. Cymerman, and R. F. Grover. Measurement of Cardiac Output by Electrical Impedance at Rest and During Exercise. *J Appl Physiol* 40:91-95 (1976).

5. Van De Water, J. M., B. E. Mount, J. R. Barela, R. Schuster, and F. S. Leacock. Monitoring the Chest with Impedance. *Chest* 65:597-603 (1973).

6. Webster, J. G. Medical Instrumentation. Boston: Houghton Mifflin Co., 1978.

7. Kubicek, W. G., J. N. Karnegis, R. P. Patterson, D. A. Witsol, and R. H. Mattson. Development and Evaluation of an Impedance Cardiac Output System. *Aerospace Med* 37:1208-1212 (1966).

8. Geddes, L. A., A. C. Baker, and T. W. Coulter. Hazards in the Use of Low Frequencies for the Measurement of Physiological Events by Impedance. *Med Biol Eng* 7:289-295 (1969).

9. Kubicek, W. G., R. P. Patterson, D. A. Witsoe, et al. The Impedance Cardiograph as a Noninvasive Means to Monitor Cardiac Function. *In* Development and Evaluation of an Impedance Cardiograph System to Measure Cardiac Output and Other Cardiac Parameters. Kubicek, W. G., (Ed.). Minneapolis: University of Minnesota Press, 1968.

10. Kubicek, W. G. Instruction Manual: Minnesota Impedance Cardiograph Model 303. Minneapolis: University of Minnesota Press, 1968.

11. Secher, N. J., A. Thomsen, and P. Arhsbo. Measurement of Rapid Changes in Cardiac Stroke Volume: An Evaluation of the Impedance Cardiography Method. *Acta Anaesth Scand* 21:353-358 (1977).

12. Judy, W. V., F. M. Langley, K. D. McCowen, et al. Comparative Evaluation of the Thoracicimpedance and Isotope Dilution Methods for Measuring Cardiac Output. *Aerospace Med* 40:532-535 (1969).

13. Harley, A., and J. C. Greenfield. Determination of Cardiac Output in Man by Means of Impedance Plethysmography. *Aerospace Med* 39:248-252 (1968).

14. Naggar, C. Z., D. B. Dobnik, A. P. Flessas, et al. Accuracy of Stroke Index as Determined by the Transthoracic Electrical Impedance Method. *Anaesthesiology* 42:201-205 (1975).

CHAPTER 5

ELECTRIC FIELDS

Another noninvasive system for biomedical monitoring and evaluation of cardiovascular function was first developed and described by William A. Shafer in the mid 1960s [1]. The system was described as a field-effect monitor. Shafer [2], Richardson [4], and Keefe et al. [5] reported detecting and recording extracorporeal electrical field changes originating from the human body by means of receptor antennas and high-impedance matching circuits.

Shafer's field-effect monitor consisted of a flat 6 x 8 in. (15.24 x 20.32 cm) rectangular copper plate which was backed by a slightly larger grounding screen. To obtain a high input impedance (800 megohm), signals from the antenna were input to a field-effect transistor. A cathode follower circuit was used to buffer the input from the lowpass filter stages. Shafer used a 30 Hz cutoff frequency [1]. In a later article, Shafer describes the system as an electric field distortion monitor with a pair of sensing antennas which were fine wires attached to the surface of a dielectric making a Faraday screen. This system sensed the difference in potential between the two antennas by means of a differential amplifier [3].

The system described by Richardson and Adams [4] is similar to Shafer's first system in that a single-ended amplifier with an input impedance of 10^{15} ohm was used. The sensing antenna consisted of two thin copper foil sheets pasted on an 8 in^2 (51.62 cm^2) piece of Bakelite dielectric. One piece of copper foil was grounded whereas the other piece of copper foil detected the electric field [4].

The system used by Keefe et al. [5] was developed by System Research Laboratories (SRL), Dayton, Ohio. This system consisted of whip antennas connected to battery-powered, high-impedance matching circuits. The output signals from the matching circuits were linearly amplified and bandpass filtered from 0.7 Hz to 30 Hz. Keefe et al. [5] and Richardson and Adams [4] used an aluminum screened room in their study while Shafer did not.

Theoretical Concepts

In his early works Shafer proposes two concepts on how the "electric field" that surrounded the body was affected or generated. His first concept was that the sensing antennas were measuring subtle changes in the field brought about by pulsations transmitted to the surface of the skin from underlying vessel networks. The second concept is that a field is generated by the body when blood is forced through the capillaries. Shafer discarded the first concept for the latter. Shafer contends "when a fluid is forced through a diaphragm or capillary, a potential drop is generated in the direction of flow". This phenomenon is referred to as "streaming potential" [2].

25

Richardson and Adams [4] disagreed with Shafer's "streaming potential" concept. In one set of experiments, occlusion of a subject's leg with a pressure cuff did not alter or diminish measurements about the leg. In a second set of experiments, measurements of the subjects' electric field were obtained before and after removal of excess (static) body charge by grounding the subjects. Grounding the subject diminished the field measurements to the point that the body's electric field became unmeasureable. Thus, Richardson and Adams proposed that the information contained in the body's electric field charges is net body charge and body proximity charge. Body proximity charges are caused by respiration and other body movements including the movement caused by heart action.

Keefe et al. [5] reported recording time-varying electric field signals which reflected both cardiac and respiratory activity from subjects in the supine position. Amplitudes of 0.1 to 7.5 mV were obtained with whip antennas about 12 in. (30.48 cm) from the body. The amplitude of the signals varied inversely with the square of the distance from the subject. Keefe et al. reported that in the instances where the antennas were located at the head and at the feet, the observed wave shape of the electric field measurements was similar in form and in phase with signals obtained by direct ballistocardiogram measurement. Keefe et al. discussed two hypotheses. One hypothesis is that the etiology of the observed extracorporeal electric field signals are the physical movement of the passively charged body surface. The second hypothesis is that the electric fields are generated by a repetitive electrical signal on the body from its own internal configuration. Against the first hypothesis and in contradiction with the results obtained by Richardson and Adams, Keefe et al. reported that when the subject was connected to ground, recordings of the signals showed little change. In addition, signals obtained from direct skin-contact electrodes have the same appearance to simultaneously recorded signals of the electric field from the body. Keefe et al. concluded that the field changes are not due to the electrical activity of heart. They favor a ballistogenically produced electric field with the exact cause remaining unknown.

To this date follow-on studies have not been conducted to determine the origin of the body's electrical field disturbances nor to determine the applicability to situations where noninvasive monitoring is necessary or desirable.

References

1. Shafer, W. A. Further Development of the Field Effect Monitor. *Aero Med Assoc Proc* 1:125-126 (1967).

2. Shafer, W. A. Non-contact Physiological Sensing, pp. 137-141. *Proc Natl Biomed Sci Instrum Symp*, 4th, Albuquerque, 1967.

3. Shafer, W. A. Telemetry on Man without Attached Sensors. *NY State J Med*, 2832-2837 (1967).

4. Richardson, P. C. and R. M. Adams. Electric-field Disturbances near the Human Body. *J Appl Physiol* 26:838-840 (1969).

5. Keefe, J. F., L. T. Rauterkus, M. J. Wolk, D. H. Brand, and H. J. Levine. Electrostatic Ballistogram: Analysis of Electrical Fields about the Human Body. *J Appl Physiol* 28:89-91 (1970).

CHAPTER 6

RESPIRATORY SOUNDS

Another family of noninvasive physiological measurement systems are the electro-mechanical devices which transform mechanical energy into electrical energy. A large number of medical instruments use strain gage transducers. Most recently self-generating piezoelectric transducers are being used in medical instruments. Some examples of these applications are:

(1) microphones for detection of sounds from the body,
    i.e., respiratory and cardiac,

(2) accelerometers for motion and tremor measurements, and

(3) ultrasonic measurements [35].

This chapter will discuss the use of microphones for detection of respiratory sounds and basic problems associated with the use of sounds as a means to diagnose the condition of the respiratory system.

Background

Laennec established the clinical relationship between respiratory sound and gross pulmonary pathology [21] and introduced auscultation of respiratory sounds by stethoscope [32] in the early 19th century. Since he established auscultation of respiratory sounds as a means of diagnosis of the lung's condition in 1819, auscultation in respiratory medicine has not undergone a great deal of development. This lack of advancement is due to (1) the confused usage of the subjective terminology, (2) the limitations of the instrumentation and the process of analysis of the sounds, (3) the incompleteness of understanding of the mechanism by which the sounds are generated, and (4) the lack of specificity of the location of the source of the sounds.

Confusion of Terminology

Physicians usually describe the quality of sounds heard by subjective adjectives meant to convey the idea of relative intensity and pitch used to detect pathology. The following words are often employed to describe respiratory sound heard through the chest wall: soft, whistling, rough, tearing, rolling, harsh, blowing, musical, scratchy, faint, moderately loud, loud, low pitched, moderately low pitched, moderately high pitched, and high pitched [5]. For adventitious respiratory sounds, words such as dry, wet, fine, coarse, etc. are often used to qualify rales, crepitations, wheezing, rhonchi, stridor [3]. None of these terms are defined in the language of acoustics, resulting in widely differing opinions as to their characteristics and significance. The diversity of these terms coupled with the nonuniformity of their usage in the medical

field creates difficulty in the use of respiratory sounds as an indicator of the respiratory system condition. Physicians not only differ in the way they interpret the meaning of terms, they also have different perceptions of the sound heard. This difference in perception is primarily due to the variations in human hearing ability and distortion induced by the detection instrument (stethoscope).

Limitations of Detection Instruments and Human Hearing

Although the stethoscope being used by physicians today is substantially different from the original version invented by Laennec, the underlying working principle remains the same. The entire range of heart and respiratory sounds is transmitted, but the frequency response is uneven. Some frequencies are amplified while others are attenuated [12]. In addition, selection of the chest piece to be used and the variation in pressure used in applying it to the chest wall affect the pitch of the sound heard. For a period of time there was a question as to which chest piece was best. It was decided that both the diaphragm and the bell were necessary for the auscultation of the heart. The difference in frequency transfer of the bell and diaphragm and the effect on frequency response of varying the application pressure can be demonstrated by the auscultation of heart sounds. Low pitched heart sounds are heard best with the bell resting lightly on the chest. On the other hand, firm pressure with the bell or diaphragm amplifies the higher frequencies and suppresses low pitched frequencies. Thus, the faint diastolic murmur of aortic reflux which is composed mainly of high frequencies and the mitral diastolic murmur which is composed mainly of low frequencies can be selectively heard.

Both the stethoscope and the ear have limitations in their use as instruments for the evaluation of respiratory sounds. Respiratory sounds have a wide spectrum. There is no significant concentration of energy in a particular frequency band except during wheezing. However, this frequency band will differ from one patient to another. In order to compare such relative frequency intensities within a particular sound spectrum, the measuring instrument must not contribute variations in intensity as does the conventional stethoscope. An additional complication in sound evaluation is the nonlinearity of the human auditory system. The ear recognizes very small differences in pitch, but its sensitivity to intensity variations decreases logarithmically as the intensity increases. In addition, the ear's perception of intensity falls off at both ends of the frequency spectrum [14]. The ear also has limitations in its ability to distinguish short sound bursts. A burst shorter than 3 ms will be heard only as a click irrespective of the frequency [16]. With the introduction of advanced electronic microphones, amplifiers, and filters, the human factor and instrumentation shortcomings can be easily overcome [10]. Electronic instruments can be designed to exhibit a flat frequency response over the entire range of respiratory sound spectrum. It is the lack of complete understanding of the mechanisms and sources from which respiratory sounds are generated, however, which still poses obstacles in the acceptance and advancement of using respiratory sounds as a major clinical tool in pulmonary medicine.

Mechanisms and Source of Respiratory Sounds Generation

The search for the sources of respiratory sounds and the mechanisms by which they are produced continued throughout the 19th century and up to the present time [2,4,5,13,15,18,20,24,25,34]. Bullar [2] did an experiment with exenterated lungs of a calf in which he enclosed the left lung in an air-tight, fluid-filled chamber with glass sides and left the right lung outside the thorax in a totally collapsed state. The two lungs were connected by the trachea, but were severed below the larynx. A bronchial breathing sound was heard over the right collapsed lung when inspiration was simulated in the left lung by lowering the pressure surrounding it in the artificial thorax. The trachea was then plugged and air was forced out of the left lung into the right lung. In this case a vesicular inspiratory murmur was heard over the right lung. Bullar also demonstrated that no sound could be heard without air flow despite fluctuations in lung volume and pressure. He concluded, therefore, that bronchial sounds were generated by air currents passing over the main bronchus of the outside lung, and the vesicular inspiratory sounds were generated when air passed from narrower to wider spaces inside the lungs.

In the early part of this century, Bushnell claimed that the sounds of expiration originated in the larynx and inspiratory sounds were generated partly in the larynx and partly in the alveoli [4]. He thought that the larynx was not only the principal origin of expiratory sounds, but also of inspiratory sounds. He attempted to prove that the alveoli had no part in sound generation. He suggested that the "vesicular sounds" which were heard over the chest wall were merely due to resonance in the thorax of the sounds originated in the larynx. His explanation of the inspiratory sounds which were heard over the chest wall of patients having had laryngectomy was that "other noises besides those produced in the larynx, if at all comparable to the latter, may contain sounds capable of exciting the chest resonance" [4]. Martini and Muller [23], on the other hand, believed that the branchial network of the lungs was responsible for the respiratory sounds generation. They demonstrated that each generation of bronchus up to the generation with inner caliber of 3 mm had their own specific frequency of vibration. During respiration the bronchi were set vibrating at their specific frequency and these vibrations acted on the lung tissues and on the chest wall. These vibrations were either weakened or strengthed according to the laws of the so-called forced vibrations, as first proved by O. Frank and quoted by Martini [24]. Martini argued strongly against the theory that the larynx was the origin of respiratory sounds. Based on Martini and Muller's observations [23], Fahr [13] used the analogy of labial instrument to explain the production of respiratory sounds. He also confirmed the finding of Martini and Muller that no bronchial sounds could be heard until consolidation of lung tissues extended from the periphery to the lung regions where bronchi with 3 mm inner caliber terminated.

As the knowledge of fluid dynamics increased, it was discovered that sound was generated by the turbulent flow of a fluid and that such phenomenon was observed in the human upper bronchial tree [8,19,33,36]. Forgacs et al. [15] performed an experiment in which asthmatic and chronic bronchitis patients were given a mixture of 79% helium and 21% oxygen.

31

They found that the respiratory sound intensity of the patient was lower than that measured while breathing normal air. Since it was known that a lower density fluid generates less turbulence under the same flow condition and that the helium-oxygen gas mixture used had a much lower density than air, Forgacs et al. concluded that respiratory sounds were generated in the turbulence zone of the bronchial tree. Based on the calculation of Reynolds numbers in the trachea and the first few generations of the bronchi by Pedley et al. [28], Forgacs et al. [15] deduced that air flow beyond segmental bronchi is laminar and hence air flow in the peripheral branches is silent. The term "vesicular sound" which suggests that sound is generated in the alveoli is a misnomer. Forgacs [16] recommended that this term be replaced with "normal breathing sounds."

Forgacs [16] also mentioned that in between the turbulence zone and the laminar zone there is an intermediate zone. In this intermediate zone, the laminar flow pattern is interrupted by whirlpools or vortices. The formation of vortices, also like turbulence, begins when the Reynolds number reaches a critical value. Above this number the rate of formation of vortices depends on flow rate alone. A hissing sound associated with the vortices changes into an "edge tone" of well-defined pitch when the rapid flowing gas stream hits a narrow wedge. The theory of vortex sound was first developed by Powell in 1964 [31]. But Forgacs [16] did not believe that musical respiratory sounds were generated by this mechanism. He believed that respiratory sounds heard through the chest wall were generated mainly in the turbulent zone, including the mouth up to the segmental bronchi with a minor contribution from the vortex zone in the more peripheral airways.

Hardin and Patterson [18], on the other hand, felt that turbulence played a minor role in the production of respiratory sounds which were produced primarily by vortices. They also suggested that the vortices induced frequency is directly related to flow rate within a range specific to each generation of bronchi. By using the mathematical equation they developed, they calculated the frequencies that would be generated by vortices for the 5th to 13th order of bronchi during forced expiration and inspiration. They claimed that the calculated result corresponded to the experimental result produced in a study of the effect of smoking on a 27-year-old adult. Also by way of mathematics, it was shown that a 19% constriction on all bronchi of the 6th order at a given flow rate produces a change in both frequency and sound intensity of the 5th and 6th orders of bronchi while these two parameters remain essentially unchanged in all other orders of bronchi. Hardin and Patterson believed that the spectrum of respiratory sounds could be used to detect changes in the state of the respiratory system. However, their proof that "vortices themselves produce the sound or that the spectral components of the respiratory sounds they analyzed came from the size of bronchi" was not satisfactory to Murphy [26].

Few experiments have been done solely to determine the source of generation of respiratory sounds. Researching the site from where respiratory sounds originated was almost always a by-product of research studying the mechanisms of respiratory sound production [2,13,15,18,23].

32

Only recently, Kraman [20] used a technique which he called "subtraction phonopneumography" to investigate the site of origin of "vesicular sounds." Lung sounds were recorded on a tape recorder simultaneously from two different areas of the chest. The two signals were played back with their amplitudes being equalized and then were added with and without phase inversion of one of them (i.e., subtraction and addition of the signals respectively). The resulting signals were displayed on different portion of screen of a storage oscilloscope. A ratio which he called "subtraction intensity index" (SII) was calculated based on the adjusted peak-to-peak amplitude of the resulting signals. Breath sounds which were generated from a single equidistant source from the two microphones would exhibit total cancellation at the subtraction display and hence would give a low SII; however, the result of the experiment was not conclusive. Several factors caused the uncertainty, such as multiple sources and different characteristics in sound transmission pathways. As Kraman [20] pointed out "the presumed presence of these factors that could eliminate cancellation precludes basing firm conclusions on the absence of cancellation."

From previous research on the mechanism of respiratory sound generation, one may conclude that respiratory sounds are generated by either turbulence or vortices, or perhaps by both of these phenomena within the tracheo-bronchial tree. Both phenomena occur when the Reynolds number of the air flow is greater than the critical value. The Reynold number is best applied to smooth and cylindrical pipes. The tracheo-bronchial tree is neither smooth nor perfectly cylindrical. There are factors which affect the pattern of air flow that are not included in the calculation of the Reynolds number. Thus the two explanations served as good preliminary models but are still not optimized for accurate prediction. The understanding of the mechanism of respiratory sound generation remains in its infancy.

Nevertheless, since Laennec's time it has been known that pulmonary pathology cause change in respiratory sound. It is not surprising that differences exist between normal and pathological respiratory sounds. Changes in the pulmonary system can be revealed by comparing pathological versus normal respiratory sounds. This is the approach of most research in respiratory sound recorded at the chest wall. There are problems with the analyses done on respiratory sound intensity recorded from the chest wall [1,7,9,11,22,27,29].

Problems with Sound Intensity Recorded from Chest Wall

Leblanc et al. [22] were the first group to study the correlation of respiratory sound intensity and distribution of pulmonary ventilation. They noticed that the intensity of respiratory sounds varied with lung volume, flow rate, body orientation, and site of recording. Ploysongsang et al. [29] extended Leblanc's experiment; they compensated for the transmission variation through the chest wall with the ratio of breath sound index (Ib) to sound transmission index (Tn). Comparing their measurement results with those obtained from Xenon-133 study, they concluded that uncompensated respiratory sounds cannot be used to assess

regional ventilation with certainty. On the other hand, the compensated respiratory sounds were much better indices of total regional ventilation. In further studies, they attempted to quantify ventilation of different lung regions by using the variation of respiratory sound intensity picked up from different parts of chest wall [30]. However, the variability in amplitude of the inspiratory sound heard on the chest wall was argued by O'Donnell and Kraman [27] and later followed by Dosani and Kraman [9] who stated that the variability of the amplitude is not due to distribution of ventilation nor chest wall thickness. These two studies showed that significant intersubject and intrasubject variations happen even with normal people without any diseases of the lung. They suggested that the site of production of the sound and its transmission path to the chest wall may be the factors affecting the intensity. Dosani and Kraman also point out that the chest wall thickness may not have a predominant effect on the intensity. From their results, it was shown that low or equal intensity at the lateral wall compares to positions near the spine where the thickness of the chest wall is greater.

Rationale for Trachea as Site of Respiratory Sound Detection

The variability of sound intensity as measured at the chest wall is due mainly to the variability of acoustic properties of the chest wall [1,7,11,17,29]. Research findings indicate that respiratory sounds measured at the trachea undergo very little filtering [7,11,17]. The location, as Charbonneau [7] points out, is more precise and less dependent on the subject's morphology. Furthermore, Druzgalski [11] reports that respiratory sound spectra obtained at the trachea correlate with that recorded over lobial regions.

Rationale for Experiment

Banaszak et al. [1] found a linear relationship between lung sound intensity of different frequency bands and peak flow rate by analog filtering techniques. Gavriely et al. [17] used and redrew Banasak's data and found an inverse, linear-relationship between log intensity and log frequency. These graphs clearly showed that the same frequency range existed for different flow rates. They also showed that the inspiratory sound amplitude spectrum and log amplitude spectrum of a wheezing patient had distinct additional peaks which differ from normal. They recorded flow rate but just used it as an indication for the initial digitalization point. Furthermore, Charbonneau et al. [7] reported that they can differentiate asthmatic patients from normal subjects by analyzing respiratory sounds picked up at the trachea at two different peak flow rates, 0.5 L/s and 1.0 L/s. Their results indicated that the mean inspiratory sound amplitude spectrum for a normal subject at the two peak flow rates has very similar shape [7]. Thus, it may be inferred that a frequency index, such as mean frequency of the power spectrum, may be used as a differentiating index between normal and pathological persons without reference to flow rate. Medically, respiratory sounds are accepted as more informative than radiological and some physiological tests concerning the

34

dynamic function of the respiratory system [6]. To date, no research has been conducted solely to establish the relationship between constant flow rate and frequency contents of the respiratory sounds as measured at the trachea. Only Charbonneau [7] examined several indices of respiratory spectrum with flow rate at peak value. Charbonneau's study does not examine constant flow.

Wing Chan Wong [37] for his master's thesis conducted experiments to determine the correlation between respiratory flow rate and the frequency spectrum of respiratory sounds as measured at the trachea in normal young male adults. Wong calculated three parameters from the power spectra of the respiratory sounds. These indices were:

(a) the mean frequency of the power spectrum (MPF), which corresponds to the first moment of the distribution about zero or the central tendency of the distribution,

(b) the frequency of the maximum power (peak power frequency--FP), which corresponds to the most frequent occurrence of an event or the mode of the distribution, and

(c) the highest frequency (FM) at which the power in the spectrum equals or is less than 10% of the maximum power, which corresponds to a rough estimate of signal bandwidth from DC to the frequency at which the power contents remains 10 db below the maximum power of the spectrum.

Results from the general linear model (GLM) multivariate analysis of variance (ANOVA) for unbalance data are shown in Table 6.1 for inspiration and expiration. From the table it can be inferred that it is highly unlikely that the means of the parameters MPF, FP, and FM at the various constant flow rates are equal. This means that the characterizing parameters are not constant during inspiration nor are they constant during expiration. Because the GLM ANOVA test for more than two means cannot resolve which mean is different from any other mean, both Duncan and Scheffe pairwise test were performed. The implication from the pairwise test results is that there may be a range of flow rates wherein the characteristic parameters may be constant. Therefore, regression analyses were performed over various ranges of respiratory flow. From inspection of the linear regression plots (example shown in Figure 6.1), a break appears to exist between 0.75 L/s and 1.00 L/s flow rates. The parameters MPF and FP were grouped by the Scheffe test from 0.75 L/s to 1.5 L/s; therefore, 0.75 L/s was selected as the break point. Tables 6.2 through 6.4 summarize the results of the regression analyses for the three characterizing parameters. The best estimates (intercept and slope) of the linear mode, Pearsen correlation coefficient (r), the r^2 value and the significant probability (PR > $|T|$) of the t-tests are given in these tables. The t-test is used to test the null hypothesis that the slope is zero:

$$H_0: \quad \beta_1 = 0 \tag{6.1}$$

35

TABLE 6.1. SUMMARY OF GLM RESULTS

Mode \ Parameter	Main effects		Interaction	r^2	C.V.
	Subject	Flow rate	Sub.*Flow		
Expiration					
MPF	0.0001	0.0001	0.0001	0.9060	6.05
FP	0.0001	0.0001	0.0001	0.5892	26.27
FM	0.0001	0.0001	0.0001	0.7401	8.84
Inspiration					
MPF	0.0001	0.0001	0.0001	0.9111	7.30
FP	0.0001	0.0001	0.0001	0.5525	34.78
FM	0.0001	0.0001	0.0001	0.8326	11.41

The value under an effect or interaction of a parameter is the PR>F value that the null hypothesis is true. r denotes coefficient of correlation. C.V. denotes cofficient of variance in percent. (C.V. is defined as the ratio of residual standard deviation to the mean of the dependent variable.)

36
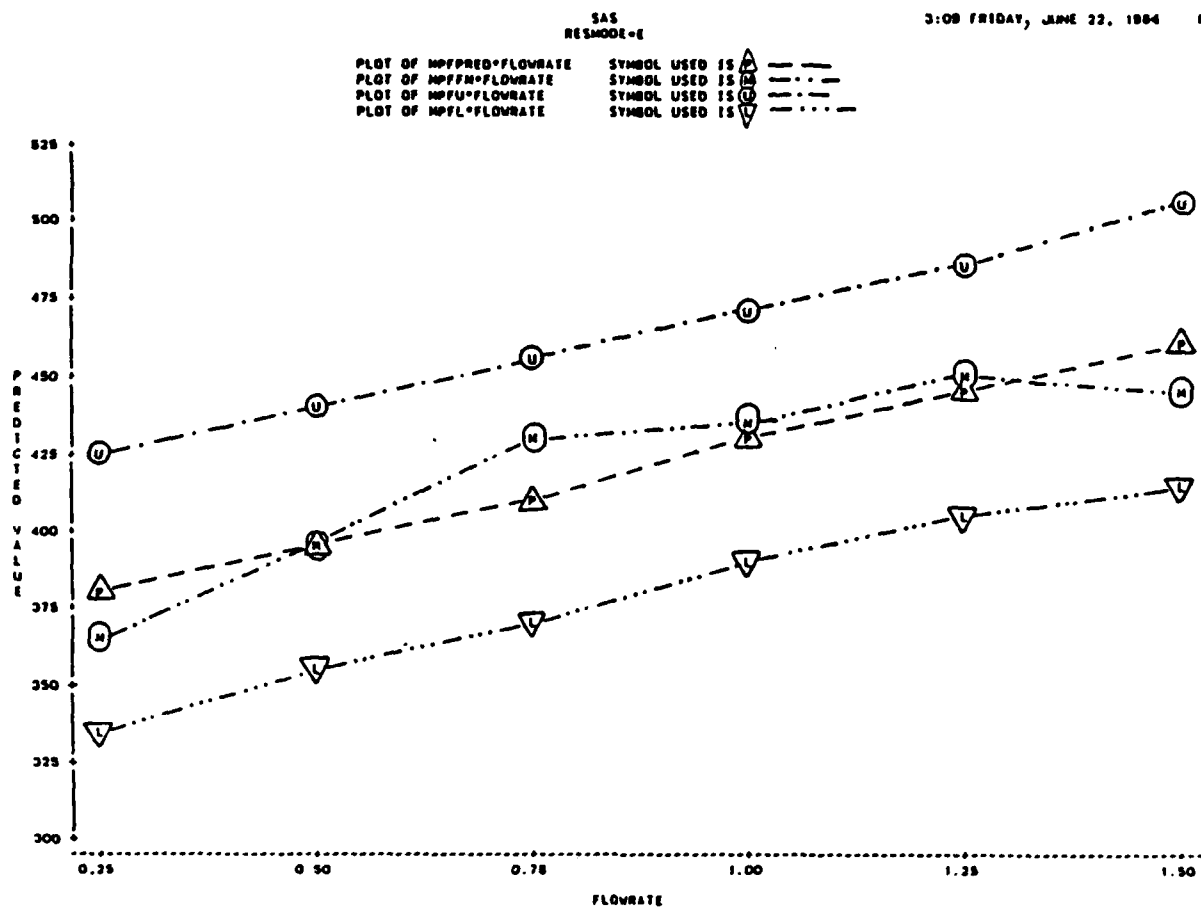
Figure 6.1. Plot of regression analysis result on between subject means of MPF of flow rates 0.25 - 1.5 L/s expiration.

TABLE 6.2. SUMMARY OF REGRESSION ANALYSIS OF PARAMETER MPF.

Resmode	Range	Intercept	Slope	r	r^2	Prob >|T|
E	.25-.75	335.9	121.66	0.9989	0.9978	0.0295
	.75-1.5	408.4	28.24	0.8610	0.7415	0.1389
	.25-1.5	363.3	65.30	0.9307	0.8662	0.0070
I	.25-.75	250.4	79.97	0.9870	0.9742	0.1026
	.75-1.5	276.5	49.37	0.9423	0.8879	0.0577
	.25-1.5	259.6	63.42	0.9760	0.9526	0.0009

For expiration (E) and inspiration (I), and flow rate ranges
0.25-0.75, 0.75-1.5 and 0.25-1.5 L/s.

TABLE 6.3. SUMMARY OF REGRESSION ANALYSIS OF PARAMETER FP.

Resmode	Range	Intercept	Slope	r	r^2	Prob >|T|
E	.25-.75	273.5	193.75	0.9992	0.9984	0.0257
	.75-1.5	406.0	32.50	0.6565	0.4310	0.3435
	.25-1.5	320.0	103.12	0.9010	0.8119	0.0142
I	.25-.75	161.9	107.23	0.7199	0.5183	0.4883
	.75-1.5	167.1	72.05	0.9567	0.9153	0.0433
	.25-1.5	179.3	64.05	0.8426	0.7100	0.0352

For expiration (E) and inspiration (I), and flow rate ranges
0.25-0.75, 0.75-1.5, and 0.25-1.5 L/s.

TABLE 6.4. SUMMARY OF REGRESSION ANALYSIS OF PARAMETER FM.

Resmode	Range	Intersept	Slope	r	r^2	Prob>|T|
E	.25-.75	580.1	157.93	0.9998	0.9997	0.0113
	.75-1.5	705.2	-14.78	0.3601	0.1297	0.6398
	.25-1.5	632.4	45.35	0.7057	0.4980	0.1172
I	.25-.75	453.2	145.37	0.9996	0.9993	0.0162
	.75-1.5	543.8	52.13	0.6187	0.3828	0.3813
	.25-1.5	478.3	105.70	0.9071	0.8226	0.0125

For expiration (E) and inspiration (I), and flow rate ranges
0.25-0.75, 0.75-1.5, and 0.25-1.5 L/s.

38

The conclusions reached by Wong were that the relationship between the spectra parameter (MPF, FP, FM) and flow rate increased from 0.25 L/s to 1.5 L/s [37]. This is in agreement with the finding reported by Forgacs [16] that the respiratory sound intensity was linearly related to respiratory flow rate within certain limits, up to a flow rate of approximately 60 L/min (1.0 L/s) at which point the relationship became nonlinear. Wong reports that the spectral parameters level off as the flow rate increases beyond 0.75 L/s during inspiration or expiration. Since the spectral estimators were not the same for inspiration as for expiration, additional information in terms of respiratory mode may be necessary in application of a discriminate function to separate a normal functioning respiratory system from an abnormally functioning system.

References

1. Banaszak, E. F., R. C. Kory and G. L. Snider. Phonopneumography. *Am Rev Resp Dis* 107:449-455 (1973).

2. Bullar, J. P. Experiments to determine the origin of respiratory sounds. *Proc Roy Soc London* 37:411-423 (1884).

3. Bunin, N. J. and R. G. Loudon. Lung sound terminology in case reports. *Chest* 76:690-692 (1979).

4. Bushnell, G. E. The mode of production of the so-called vesicular murmur of respiration. *JAMA* 77:2104-2106 (1921).

5. Cabot, R. C. and H. F. Dodge. Frequency characteristics of heart and respiratory sounds. *JAMA* 84:1793-1795 (1925).

6. Cegla, U. H. Some aspects of pneumosomography. *Prog Resp Res* 11:235-241 (1979).

7. Charbonneau, G., J. L. Racineux, M. Sudraud, and E. Tukchais. An accurate recording system and its use in respiratory sounds spectral analysis. *J Appl Physiol* 55:1120-1127 (1983).

8. Dekker, E. The transition between laminar and turbulence flow in the trachea. *J Appl Physiol* 16:1060-1064 (1961).

9. Dosani, R. and S. S. Kraman. Lung sound intensity variability in normal man. *Chest* 84:628-631 (1983).

10. Druzgalski, C. K., R. L. Donnerberg, and R. M. Campell. Techniques of recording respiratory sounds. *J Clin Eng* 5:321-330 (1980).

11. Druzgalski, C. Breath sounds in pulmonary diagnosis. *IEEE Frontiers of Eng in Health Care*; 383-385 (1981).

12. Ertel, P. Y., M. Lawrence, R. K. Brown and A. M. Stern. Stethoscope acoustics. *Circulation* 33:889 (1966).

13. Fahr, G. The acoustics of the bronchial respiratory sounds. *Arch Int Med* 39:286-302 (1927).

14. Fletcher, H. and W. A. Munson. Loudness, its definition, measurement and calculation. *J Acoust Soc Amer* 5:82-108 (1933).

15. Forgacs, P., A. R. Nathoo and H. D. Richardson. Breath sounds. *Thorax* 26:288-295 (1971).

16. Forgacs, P. *Lung Sounds*. London: Bailliere Tindall, 1978.

17. Gavriely, N., Y. Palti, and G. Alroy. Spectral characteristics of normal breath sounds. *J Appl Physiol* 50:307-314 (1981).

18. Hardin, J. C. and J. L. Patterson, Jr. Monitoring the state of the human airways by analysis of respiratory sound. *Acta Astronautica* 6:1137-1151 (1979).

19. Jaeger, M. J. and H. Matthys. Airway Dynamics, p 17. Springfield, ILL: Charles C Thomas Publishing Co., 1970.

20. Kraman, S. S. Determination of the site of production of respiratory sounds by subtraction phonopneumography. *Am Rev Respir Dis* 122:303-309 (1980).

21. Laennec,R. T. H. A Treatise on the Disease of the Chest and Mediate Auscultation, 1819. Translated from the French edition by John Forbes. New York: Samuel Wood and Sons, 1935.

22. Leblanc, P., P. T. Macklem, and R. D. Ross. Breath sounds and distribution of pulmonary ventilation. *Am Rev Resp Dis* 102:10-16 (1970).

23. Martini, P. and H. Muller. Studies on bronchial breathing. *Deutsche. Arch F Klin Med* 143:159-173 (1923).

24. Martini, P. The mechanism of production of respiratory sounds. *Arch Int Med* 32:313-322 (1923).

25. McKusick, V., J. T. Jenkins, and G. N. Webb. The acoustic basis of the chest examination. *Am Rev Respir Dis* 72:12-34 (1955).

26. Murphy, R. L. Auscultation of the lung: past lessons, future possibilities. *Thorax* 36:99-107 (1981).

27. O'Donnell, D. M. and S. S. Kraman. Vesicular lung sound amplitude mapping by automated flow-gated phonopneumography. *J Appl Physiol* 53:603-609 (1982).

28. Pedley,T. J.,P. C. Schroter, and M. F. Sudlow. The prediction of pressure drop and variation of resistance within the human bronchial airways. *Resp Physiol* 9:387 (1970).

29. Ploysongsang, Y., R. R. Martin, and W. R. D. Ross. Breath sounds and regional ventilation. *Am Rev Resp Dis* 116:187-199 (1978).

30. Ploysongsang, Y., P. T. Macklem and W. R. D. Ross. Distribution of regional ventilation measured by respiratory sounds. *Am Rev Respir Dis* 117:657-664 (1978).

31. Powell, A. Theory of vortex sound. *J Acoust Soc Am* 36:177-195 (1964).

32. Sakula, A. RTH Laennec 1781-1826 -- His life and work: a bicentenary appreciation. *Thorax* 36:81-90 (1981).

33. Schroter, R. C. and M. F. Sudlow. Flow patterns in models of the human bronchial airways. *Resp Physiol* 7:341 (1969).

34. Skoda, J. A Treatise on Auscultation and Percussion. English ed. London: Highly & Son, 1853.

35. Welkowitz, W. and S. Dentsch. Biomedical Instruments, Theory and design. New York: Academic Press, 1976.

36. West, J. B. and P. Hugh-Jones. Patterns of gas flow in the upper bronchial tree. *J Appl Physiol* 14:753-759 (1959).

37. Wong, W. C. Correlation of Respiratory Flow Rate with Frequency Spectrum of Respiratory Sound at Trachea of Normal Young Adults. Unpublished Master of Science Thesis, Texas A&M University, August 1984.

CHAPTER 7

PHONOCARDIOGRAPHY

Physicians use the acoustical stethoscope not only to examine a patient's respiratory sounds, but also to examine cardiac sounds for murmurs. Some clinics obtain phonocardiographs during medical examinations. Phonocardiography (PCG) is the graphic representation of the combined heart and great vessels sound. The vibrations that are produced within or about the heart or great vessels propagate outwards through the various tissues. These vibrations appear continuously on the surface of the body.

In the cardiovascular system, low-frequency (infrasonic) mechanical waves are produced and propagated to the skin surface in greater amplitude than the higher frequencies. Consequently, measurements at the skin contain infrasonic components of far greater magnitude than the audible sounds. The tremendous disparity in signal amplitude presents a technical problem in recording if the relative amplitudes of all waves are displayed. Recording systems with sufficient sensitivity to detect the low-amplitude, high-frequency sounds will be saturated by the large-amplitude, low-frequency events. Reducing the sensitivity of the recording system to accommodate the large amplitude of the low-frequency waves may result in loss or nondetection of the relatively small-amplitude, high-frequency sounds from the data. The infrasonic waves may be eliminated by filtering; then the instrument sensitivity may be increased to permit measurement and interpretation of the audible waves [1]. The use of electronic filtering may distort the signal. Distortion introduced by sharp band pass filters may obscure splitting of heart sounds making it impossible to discern where a heart sound ends and a murmur begins. The "ideal" set of filters cannot be optimized simultaneously for both heart sounds and murmurs. Van Vollenhoven et al. [1] suggest that the best compromise for obtaining the most information for clinical diagnosis is to use lower order high-pass filters which have cut-off frequencies in the low-frequency range and gradual slopes of attenuation.

Most PCGs have at least two filter settings. One range results in moderate filtering of low-frequency sounds, thereby reproducing more effectively low-frequency events. The second filter range setting results in greater filtering of low frequencies. It is designed to accentuate high-frequency events such as diastolic murmur of aortic insufficiency. American National Standards Institute (ANSI) recommends that the input signal be filtered with the standard B network for sound measurement. Webster [2] suggests that a solution to the problem of filtering is to pre-emphasize the heart sound frequencies by inserting a frequency-compensation network in the amplifier. The basic system for sound recording consists of a microphone, an amplifier, and an oscilloscope. The function of the microphone is to convert mechanical energy (sound vibrations) into electrical energy. There are many types of microphones, but the following two are the main types. The first is the crystal, or piezoelectric microphone. Certain crystalline materials generate electric energy when

43

subjected to the pressure changes of sonic vibrations. This electric energy occurs when pressures are applied to them in such a way as to deform the molecular lattice structure. Since the phenomenon is molecular, it is possible to obtain large electric signals from very small displacements. For this reason, low-frequency sound waves may be faithfully reproduced [3]. The second type is the dynamic, or electromagnetic microphone. In this apparatus, a diaphragm is connected to a movable coil, and the latter is located in a magnetic field. Sonic vibrations set the diaphragm into an oscillating motion, which in turn moves the coil back and forth in the magnetic field. This movement generates electrical energy in direct proportion to the displacement velocity of the coil; therefore, the strength of the electric signal is dependent on both the intensity and frequency of the vibrations. As a result, the system is less sensitive to lower frequencies than the piezoelectric system. On the other hand, its signals are easier to amplify for sound recording and less subject to the pickup of extraneous noise [1].

Microphones should have the general characteristic of being easily applied, comfortable to the patient and stable in contact with the chest wall. Microphones may make contact with the skin either through bell-shaped endings, which use air coupling between skin and sensing element, or by flat pieces, shaped like a diaphragm, which allow conduction through a solid material directly to the sensing element. Most researchers and clinicians prefer the bell-shaped microphone since it appears to reduce extraneous background noises. The microphones are usually held in place with an elastic strap or suction [1].

Travel states that there is little to be gained by attempting to standardize the amplification of sound waves, because of the variation in patient-to-patient from the contour of the chest and the sound intensity actually reaching the chest wall. It is better to adjust the gain of the instrument to demonstrate what the clinician is seeking. For best sound recording, it is generally desirable to increase the amplitude as much as possible, while maintaining a relatively smooth baseline [1].

Heart sounds are short-lived bursts (transients) of vibratory energy believed to be caused by sudden tension on valve leaflets and/or chordae tendineae [1]. In a normal PCG there are four heart sounds, but only two are used (Fig. 7.1). The first heart sound is composed of four components. The first component is composed of small, low-frequency initial vibrations, which coincide with the beginning of left-ventricular contraction. The initial vibrations are probably caused by muscular contraction during the earliest phase of ventricular systole. Atrial contraction may also contribute to this component. The second large, higher frequency vibrations, comprise the major component of the first heart sound and represent abrupt tension on the mitral valves as it finishes closing. This component begins 0.02 s after the first component. The third component is a second set of high-frequency vibrations which follows mitral closure by an average of 0.03 s. This component results from abrupt deceleration of blood as the mitral leaflets tense at the end of closure. Another theory suggests that this component may be due to initial injection into the great vessels. It is possible that both mechanisms may contribute to this
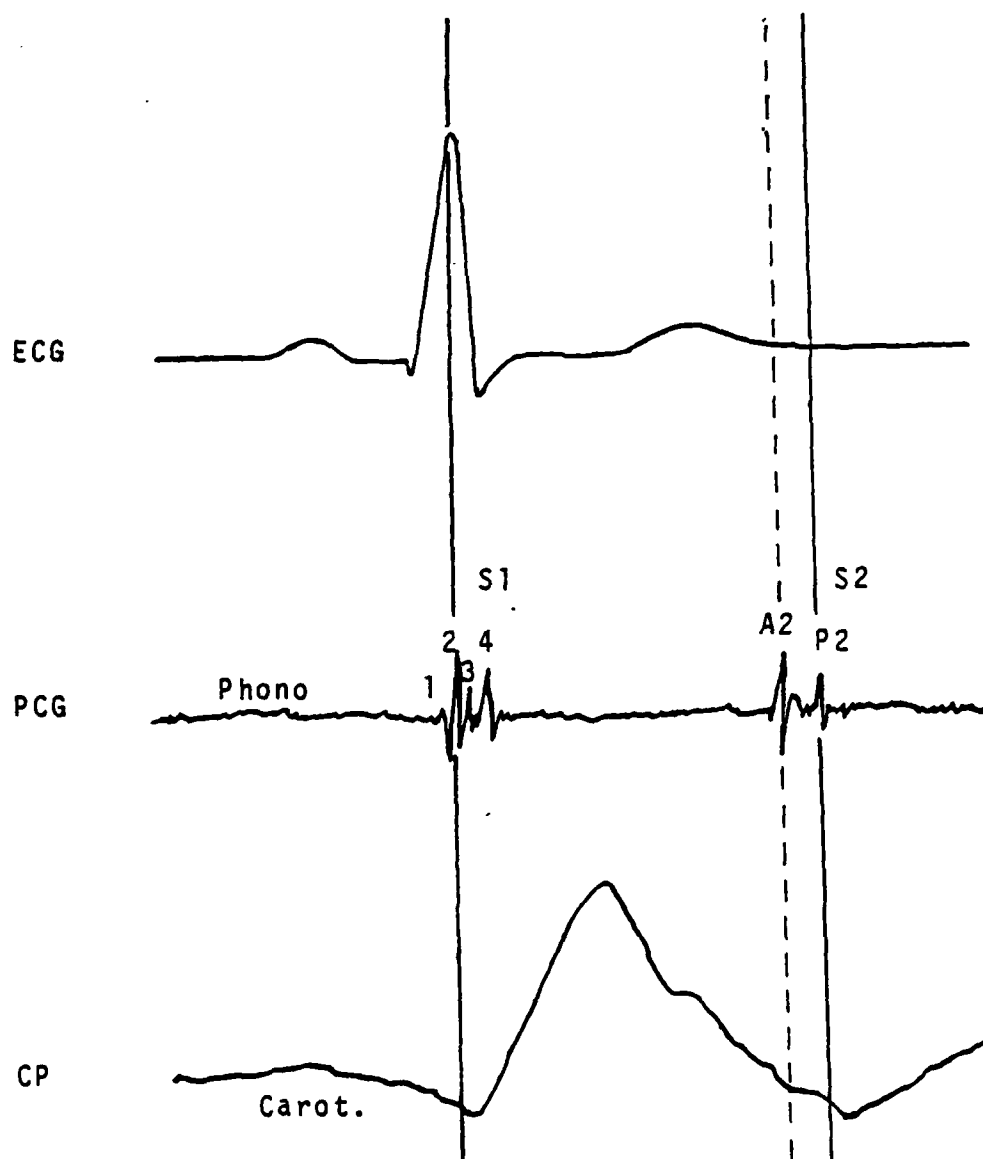
44

Figure 7.1. Heart sounds. Phonocardiogram (PCG) recorded in center channel with Electrocardiogram (ECG) (top tracing) and carotid artery pulse (bottom tracing). The first sound (S1) shows four major components labeled 1 through 4. The second sound (S2) is split into two components A2 and P2 which corresponds to aortic valve and pulmonary valve closure, respectively.

portion of the first heart sound. The fourth component consists of small, low-frequency vibrations which coincide with the acceleration of blood into the great vessels. The entire first sound lasts for an average of 0.1-0.12 s [1].

Aortic and pulmonary valve closures give rise to the second heart sound, presumably as a result of abrupt deceleration of blood as these valves tense at the end of their closure. Normally, the second heart sound is split into two separate components. The phenomenon reflects the fact that the aortic valve closes before the pulmonary valve. With quiet respiration the splitting interval varies in such a way that during expiration the sounds are superimposed in 90% of normal persons. The aortic sound is generally greater in amplitude than the pulmonary sound [1].

The third heart sound is a low-frequency transient (20-70 Hz) which is usually composed of 1 or 2 vibrations occurring during rapid ventricular filling of early diastole. The origin of this sound remains evasive. The most widely accepted theory is that the sound is produced by abrupt tension of the chordae tendineae and valve leaflets within the left ventricle as this chamber rapidly elongates in early diastole. However, recent studies show that this sound is still present even when the mitral and tricuspid valves and chordae have been removed. Thus, the third sound probably originates from within the left ventricular wall as it stops abruptly diastolic active and rapid elongation then begins to expand more passively and slowly in response to the incoming blood. The third heart sound occurs about 0.15 s after aortic closure. The duration of the third heart sound is 0.04-0.05 s [1].

The fourth heart sound is similar to the third heart sound in frequency and duration, although it tends to have a slightly lower frequency. It occurs at the time of atrial contraction immediately before ventricular systole. Because of its low-frequency the fourth heart sound is usually inaudible. However, it can be recorded easily by phonocardiography. The fourth heart sound is probably produced by vibrations within the ventricular walls as these chambers expand with the rapid inflow of blood produced by atrial contraction. The fourth sound begins approximately 0.14 s after the P wave of the ECG and lasts 0.04 s [1].

The PCG is useful in diagnosing problems within the heart. These problems range from murmurs to malfunctioning valves to diseases in the conduction system. Longhini et al. [4] presented a study that focused on spectrum analysis as a useful method of processing the cardiac sounds as recorded by PCG in order to obtain the frequency spectral distribution of normal heart sounds. Results from the study demonstrated that it was worthwhile to substitute Fast Fourier Transform (FFT) techniques for bandpass filtering. This is the first step necessary towards developing automatic analysis of the PCG.

46

References

1. Travel, M. E. Clinical Phonocardiography and External Pulse Recording. Chicago: Yearbook Medical Publishers, Inc., 1978.

2. Webster, J. G. Medical Instrumentation. Boston: Houghton Mifflin Co., 1978.

3. Geddes, L. A. and L. E. Baker. Principles of Applied Biomedical Instrumentation. New York: John Wiley and Sons, Inc., 1968.

4. Longhini, C., F. Portaluppi et al. The Fast Fourier Transform in the Analysis of the Normal Phonocardiography. *Jpn Heart J* 20:333-339 (1979).

47

CHAPTER 8

AUSCULTATORY METHOD OF INDIRECT MEASUREMENT OF BLOOD PRESSURE

The measurement of arterial blood pressure is an important indicator of vascular disease or physiological problems. Blood pressure is commonly used in clinical screening and in monitoring of acutely ill patients, because it reflects the effects of changes in cardiac output, peripheral vascular resistance, and other hemodynamic or physiological changes. The indirect measurement of blood pressure by a standard sphygmomanometer and stethoscope is not accurate when compared with direct intraarterial measurements. If the need is to establish whether a person's arterial blood pressure is in the normal range or not, then the accuracy of the measurement has limited consequences. But if the need is for accurate diagnosis of a murmur or serial observations during antihypertensive therapy, then the errors in indirect blood pressure measurements must be reduced or avoided [1]. The accuracy of arterial blood pressure measurements by the indirect auscultatory method obtained from normal subjects with normal circulatory status were found to be poor in some situations [2,3]. The accuracy of auscultatory method was found unacceptable in patients with abnormal blood pressure ranges as a result of shock [4].

Direct blood pressure measurements are generally obtained clinically from patients with an unstable cardiovascular system by inserting a 20-g catheter into a radial artery and recording the signals from a linear pressure transducer. The advantages of the direct or invasive method of measuring arterial blood pressure are:

       (1) permits continuous observation of blood pressure,

       (2) provides access to the arterial system for
           sampling blood, gases, electrolytes, and
           hematocrit/hemoglobin [5].

The disadvantages of direct measurement of intraarterial blood pressure are "technical problems of inserting the catheter, including air bubbles in the fluid-filled pressure lines, thrombus formation, ischemic damage, and cerebral embolization from irrigation of radial artery lines" [5].

The advantages of the indirect measurement methods of arterial blood pressure are improved patient safety, reduced risk of side effects, and ease of noninvasive measurement. The disadvantage of the indirect method is the accuracy of the measure.

The accuracy of indirect arterial blood pressure measurement by the auscultatory (Korotkoff) method is dependent on: (1) observer errors, i.e., observer bias, carelessness, inattention, influence by prior readings, (2) differences between observers, (3) errors because of the observed position and conditions under which the measurement is obtained, and (4) instrument error, i.e., incorrect size of cuff [1,7,8].

Equipment for Indirect Measurement of Blood Pressure

The mercury sphygmomanometer remains the standard instrument for measuring arterial blood pressure in medical practice. The sphygmomanometer consists of a compression bladder enclosed in an unyielding cuff, an inflating bulb or pump, a controllable exhaust valve, and a manometer. In addition a standard medical stethoscope is necessary to obtain the indirect measurement of blood pressure [1]. Geddes and Whistler [8] contend that the relationship of the width of the bladder in the cuff to the size of the member to which it is applied is the most important factor in the accuracy of the measure. In an effort to reduce the indirect measurement errors resulting from incorrect cuff size to no more than 5%, the American Heart Association (AHA) recommended that the cuff width should be 40% of the arm circumference. The arm circumference measurement is obtained at the midpoint of the arm, i.e., half the distance from the acromion to the olecranon [1]. An extract of the AHA recommended standard dimensions for blood pressure cuffs is given in Table 8.1. The bladder length recommended in Table 8.1 should cover 80% of the circumference of the arm. In summary, arm circumference is the basis for proper cuff and inflation bladder combination, not the age of the patient [1].

Manometers

The most commonly used manometers to register pressure are the gravity mercury manometer and the aneroid manometer. The mercury manometer consists of (1) mercury in a vertical tube and reservoir and (2) a calibrated linear vertical scale. Aneroid manometers make use of a metal bellows which elongates with applied pressure and mechanically transmits the movement to the indicator needle [1].

Determination of Blood Pressure

Suggested conditions for indirect measurement of arterial blood pressure are a quiet room at a comfortable temperature, no eating or smoking for 30 min before the measurement, no postural changes for 5 min before the reading and, finally, any factors which alter blood pressure should be recognized and avoided, i.e., anxiety, emotional turmoil, exertion, bladder distension, pain, etc. The deflated cuff should be placed 2.5 cm above the antecubital space with center of the bladder directly over the medial surface of the arm. The bell stethoscope is placed over the brachial artery in the antecubital space. Pressure is then increased by inflating the cuff to about 30 mmHg above the reading where the radial pulse disappears. The cuff is deflated at a rate of about 3 mmHg/s via the exhaust valve. Too rapid or too slow a deflation rate will result in measurement errors [1].

As the arterial pressure decreases, the Korotkoff sounds from the brachial artery become audible. The basic principle of blood pressure measurement is occlusion of the artery to prevent blood flow, as the occluding pressure is slowly released, blood is forced through the artery

in a turbulent flow condition. If the Reynolds number exceeds the critical value in the turbulent flow, noises or sounds will be produced by the turbulent blood flow. The characteristics of the sounds change as the pressure is released and the blood flow returns to near laminar flow.

The AHA describes the phases of the Korotkoff sounds as the pressure is decreased in the following manner [1].

Phase I: That period marked by the first appearance of faint, clear tapping sounds which gradually increase in intensity.

Phase II: The period during which a murmur or swishing quality is heard.

Phase III: The period during which sounds are crisper and increase in intensity.

Phase IV: The period marked by distinct, abrupt muffling of sound so that a soft, blowing quality is heard.

Phase V: The point at which sounds disappear.
When all sounds disappear, the cuff should be deflated rapidly and completely.

The systolic blood pressure valve is the level at which the initial tapping sound is heard, phase I. In adults, the best index of diastolic blood pressure is the value at which the onset of phase V or the Korotkoff sounds disappear. The accuracy of determining the diastolic pressure depends on the auditory acuity of the observer and the efficiency of the stethoscope [1].

In the last decade, numerous automatic noninvasive arterial blood pressure measuring systems were developed to eliminate errors resulting from the observer and to extend the range of measurement [7-12]. Silas et al. [7] evaluated the Dinamap 845 automated blood pressure recorder against a Hawksley random zero sphygmomanometer which was used as the standard. They did not use direct intraarterial pressure readings as a basis for comparison. Hunyor et al. [9] evaluated four automated devices, two manual models and the standard mercury sphygmomanometer against direct intraaterial blood pressure of the brachial artery to which the blood pressure cuff was applied. The findings suggested that all seven types of sphygmomanometers (automated or manual) were not accurate when compared with simultaneous direct readings. The subjects for this study were nine patients who were receiving various drug treatments for hypertension. Results of the differences in blood pressure readings between indirect and direct are given in Table 8.2. In all cases the indirect systolic blood pressure measurements were lower than the intraarterial systolic pressure. In all indirect diastolic blood pressure measurements, with the exception of the Cardy 8 system, the readings were higher than direct readings [9].

In summary, indirect blood pressure measurements whether taken manually or with an automated system are inaccurate when compared with direct intraarterial measurements. Edwards et al. [12] conclude that "even allowing for an unbiased approach of the observer and a perfectly still and rested subject, the results are no more satisfactory than those of a standard mercury-in-glass sphygmomanometer and stethoscope with moderate care. The sphygmomanometer has the advantage of cheapness and many years of user experience."

51

TABLE 8.1. RECOMMENDED BLADDER DIMENSIONS FOR BLOOD PRESSURE CUFF

(Extract, from AHA Committee Report 70- 019-B)

Arm Circumference (cm)	cuff/subject	Bladder width (cm)	Bladder length (cm)
17-26	small adult	11	17
24-32	adult	13	24
32-42	large adult	17	32

TABLE 8.2. COMPARISON OF THE DIFFERENCE BETWEEN INDIRECT MEASURE WITH DIRECT INTRAARTERIAL READINGS

(IDSBP-DSBP = difference)

System	Systolic $\pm$	SD	Diastolic $\pm$	SD
1. Accoson standard	-10	3.3	8	5.5
2. London School Hygiene Machine	-21	6.4	3	7.9
3. Hawklay Random Zero machine	-7	10.4	8	6.7
4. Kenz - 45	-14	7.7	10	11.0
5. Cardy 8	-11	7.3	-6	13.7
6. I-Health	-16	9.1	2	10.2
7. Arteriosonde 1217	-31	12.7	4	9.2

Data extracted from Table II of Hunyor et al. (9).

References

1. Kirkendall, W. M., M. Feinleib, E. D. Freis, and A. L. Mark. Recommendations for Human Blood Pressure Determination by Sphygmomanometers. Report of a subcommittee of the Postgraduate Education Committee, American Heart Association, 1980.

2. Ramsey, M. Noninvasive Automatic Determination of Mean Arterial Pressure. *Med Bio Eng & Comput* 17:11-18 (1979).

3. Collins, V. J., and F. Magora. Sphygmomanometry: The Indirect Measurement of Blood Pressure. *Anesth & Analg* 42:443-452 (1963).

4. Cohn, J. N. Blood Pressure Measurement and Shock. *JAMA* 199:118-122 (1967).

5. Paulus, D. A. Noninvasive Blood Pressure Measurement. *Med Instrum* 15:91-94 (1981).

6. Downs, J. B., et al. Hazards of Radial-Artery Catheterization. *Anesthesiol* 38:283-286 (1973).

7. Silas, J. H., A. T. Baker, and L. E. Ramsey. Clinical Evaluation of Dinamap 845 Automated Blood Pressure Recorder. *Br Heart J* 43:202-205 (1980).

8. Geddes, L. A., and S. J. Whistler. The Error in Indirect Blood Pressure Measurement with the Incorrect Size of Cuff. *Am Heart J* 96:1, 4-10 (1976).

9. Hunyor, S. N., J. M. Flynn, and C. Cochineas. Comparison of Performance of Various Sphygmomanometers with Intra-Arterial Blood Pressure Readings. *Br Med J* 2:159-162 (1978).

10. Polk, B. F., B. Rosner, R. Feudo, and M. Vandenburgh. An Evaluation of the Vita-Stat Automatic Blood Pressure Measuring Device. *Hypertension* 2:221-227 (1980).

11. Berkson, D. M., I. T. Whipple, L. Shireman, M. C. Brown, W. Raynor, and R. B. Shekell. Evaluation of an Automated Blood Pressure Measuring Device Intended for General Public Use. *Am J Publ Health* 69:473-479 (1979).

12. Edwards, R. C., R. Bannister, A. D. Goldbery, and E. B. Raftery. The Infrasound Blood Pressure Recorder: A Clinical Evaluation. *Lancet* 398-400 (1976).

CHAPTER 9

ULTRASOUND

High-frequency sounds called ultrasounds are used in clinical diagnosis of peripheral vascular diseases. The technique is noninvasive and nonioning. Nonioning means it does not require an ionic current to flow in the transduction of the phenomenon. Ultrasonic measurements present little risk to either patient or examiner. Literature indicates that there is no evidence of adverse biological effect from diagnostic ultrasonic equipments [1,2]. Advances in electronics and digital processing techniques in the past decade allowed sophisticated scanning and processing methods to be implemented in ultrasonic diagnostic systems. This advancement increased the use of ultrasound from solely midline detection in echoencephalography to valve motion and closure study in echocardiography; cysts, stone, and tumor detection in abdominal scanning; fetal examining in obstetrics; retina examination in ophthalmology; study of tissue lesions in the breast in gynecology; etc. The mechanical wave property of ultrasound systems may be used in biological studies where conventional radiological methods fail to delineate the interfaces of soft tissues. The relatively fast propagation speed coupled with the "hazard free" advantage of ultrasound have led to the development of real-time, two-dimensional imaging systems. These real-time systems rapidly proliferated into clinical settings and became well established in many medical specialties.

Since ultrasound is a mechanical wave, it obeys wave theory. When it travels through media, it will undergo reflection and refraction at the boundary. More than that, if the interface boundary moves, the reflected echo will exhibit Doppler shift. This property is being used to detect blood flow. Recent experiments have been published in which ultrasonic Doppler effects were used to determine blood pressure [3,4,5] and pulmonary hypertension [6]. Commercial products which use the Doppler method are available to evaluate peripheral arterial diseases [7].

It is the ability to detect flow and pressure by ultrasound noninvasively which seems most attractive in a chemical warfare application. Under the influence of toxic chemical, the cardiac output or the arterial pressure may fall to such a low value that without prompt treatment and compensation, the irreversible shock may take the victim's life. In theory, blood flow velocity obtained at the aorta using range-gated pulsed Doppler along with the aortic diameter obtained by regular pulse echo method can be used to calculate the blood flow or, more correctly, stroke volume. Then cardiac output can be calculated from the product of the stroke volume and heart rate. Unfortunately, there are technical problems, in determining the velocity precisely, that render the flow and cardiac output calculations inaccurate [8]. Furthermore, there is an even more fundamental problem when using an ultrasonic instrument in a chemical warfare situation; that is the coupling of the transducer and the body through the protective clothing or an air medium.

Theory of Operation

The ability of ultrasound to reveal subsurface structure is due to its mechanical wave properties. As the piezoelectric transducer vibrates under excitation, whatever medium is in contact with the transducer face is forced to undergo the same vibration. The energy emitted by the transducer is propagated as a pressure front. This pressure, P, causes particles ahead of it to displace from their resting position and appear to move with velocity, v.

The pressure P and the velocity v are related by the equation

$$P = \rho c v \tag{9.1}$$

where ρ is the density of the medium and c is the velocity of the ultrasound in the medium [9]. The velocity of sound, c, in the medium is governed by the medium's elastic property and density

$$c = \sqrt{(\xi/\rho)} \tag{9.2}$$

where ξ is elastic modulus [10].

The term P/v is called the acoustic characteristic impedance which may be expressed as

$$Z = P/v = \rho c \tag{9.3}$$

Table 9.1 lists the characteristic impedances of some common materials [11].

As the wave travels from one medium to another medium, there are no sudden discontinuities in either particle pressure or particle velocity. The two media remain in contact and both the particle pressure and velocity are continuous across the interface. These conditions are given by equations 9.4 and 9.5 as:

$$v_i\cos\theta_i - v_r\cos\theta_r = v_t\cos\theta_t \tag{9.4}$$

and $P_i + P_r = P_t$ $\qquad$ (9.5)

where v_i, v_r, v_t are incident, reflected and transmitted velocity,
$\qquad P_i, P_r, P_t$ are incident, reflected and transmitted pressure,
and $\qquad \theta_i, \theta_r, \theta_t$ are incident, reflected and transmitted angle as
$\qquad$ shown in Figure 9.1.

Rearranging equation 9.3 gives

$$v = P/Z \tag{9.6}$$

Expressing equation 9.4 in terms of P and Z results in equation 9.7.

$$(P_i/Z_1)\cos\theta_i - (P_r/Z_1)\cos\theta_r = (P_t/Z_2)\cos\theta_t \tag{9.7}$$

56

TABLE 9.1. CHARACTERISTIC IMPEDANCES OF SOME COMMON MATERIALS

Material		Characteristic impedance $\times 10^{-12}$ (kg $\cdot$ m^{-2}sec^{-1})
Non-Biological	Air at S.T.P.	0.0004
	Castor oil	1.43
	Water	1.48
	Polythene	1.84
	Aluminum	18.0
	Mercury	19.7
	Brass	38.0
Biological	Fat	1.38
	Brain	1.58
	Blood	1.61
	Human tissue, mean value	1.63
	Muscle	1.70
	Skull-bone	7.80
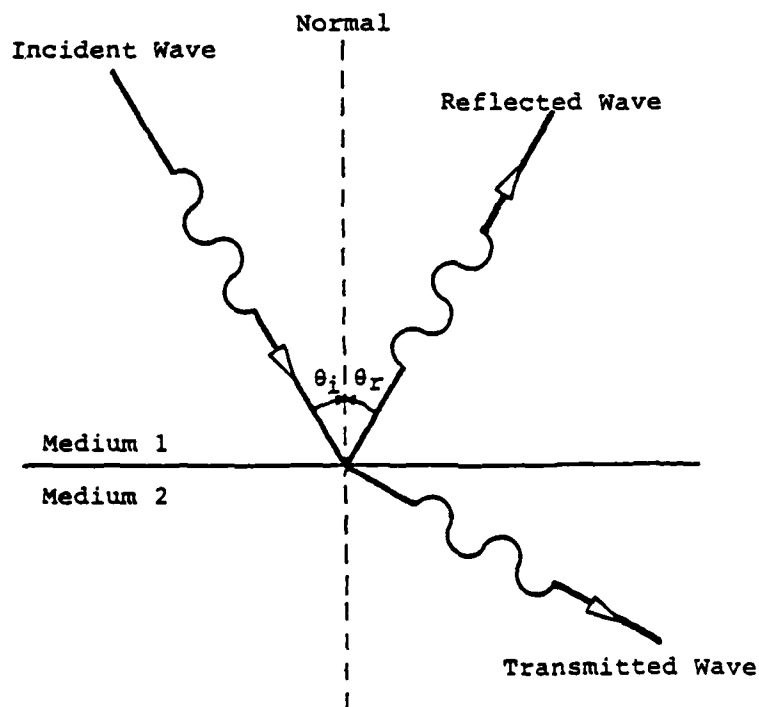
Figure 9.1. The relationships of incident, reflected, and transmitted ultra-sonic waves at an interface.

Since the wave obeys wave theorem, the incidence angle (θ_i) is equal to the reflected angle (θ_r).

$$\theta_i = \theta_r \tag{9.8}$$

The simultaneous solutions to equations 9.5 and 9.7 are given by

$$\frac{P_r}{P_i} = \frac{Z_2\cos\theta_i - Z_1\cos\theta_t}{Z_2\cos\theta_i + Z_1\cos\theta_t} \tag{9.9}$$

and

$$\frac{P_t}{P_i} = \frac{2Z_2\cos\theta_i}{Z_2\cos\theta_i + Z_1\cos\theta_t} \tag{9.10}$$

For ultrasonic imaging, θ_i and θ_t are assumed to be zero, hence equations 9.9 and 9.10 reduced to:

$$P_r/P_i = (Z_2 - Z_1)/(Z_2 + Z_1) \tag{9.11}$$

$$\text{and} \quad P_t/P_i = 2Z_2/(Z_2 + Z_1) \tag{9.12}$$

So if $Z_1 \gg Z_2$, P_r/P_i will be close to one and very little pressure is transmitted to medium 2. This is the case for any solid material interface with air, as shown in Table 9.1. This will happen if there is a thin layer of air in between the protective clothing and the skin.

Doppler Effect

If the assumption of good contact can be made by pressing on the clothing, there is another kind of technical problem to be solved when flow is to be measured correctly.

Ultrasound as a wave phenomenon will not only be reflected from a boundary, but it will also exhibit the Doppler effect if the reflective surface moves. The frequency shift is given by the expression

$$f_D = -2f\upsilon\cos\phi/c \tag{9.13}$$

where υ = absolute velocity of the reflective surface
along the direction of motion,
f = ultrasonic frequency,
c = ultrasonic velocity,
and ϕ = angle between the direction of motion and the axis
of travel of the sound beam.

The algebraic sign of f_D is positive if the movement is towards the transducer and negative if otherwise. This relationship holds true only if the transmitter also acts as receiver. In most cases, in order to cut down

58

Reflected sound beam

Transmitted sound
beam

α

θ

β

ν

Direction of flow
with magnitude ν

Figure 9.2. Angular relationship of flow to the transmitted and reflected
ultrasonic sound beam.

on cross talk, separate transmitter and receiver are used, then the situation becomes as shown in Figure 9.2. The frequency shift is then given by

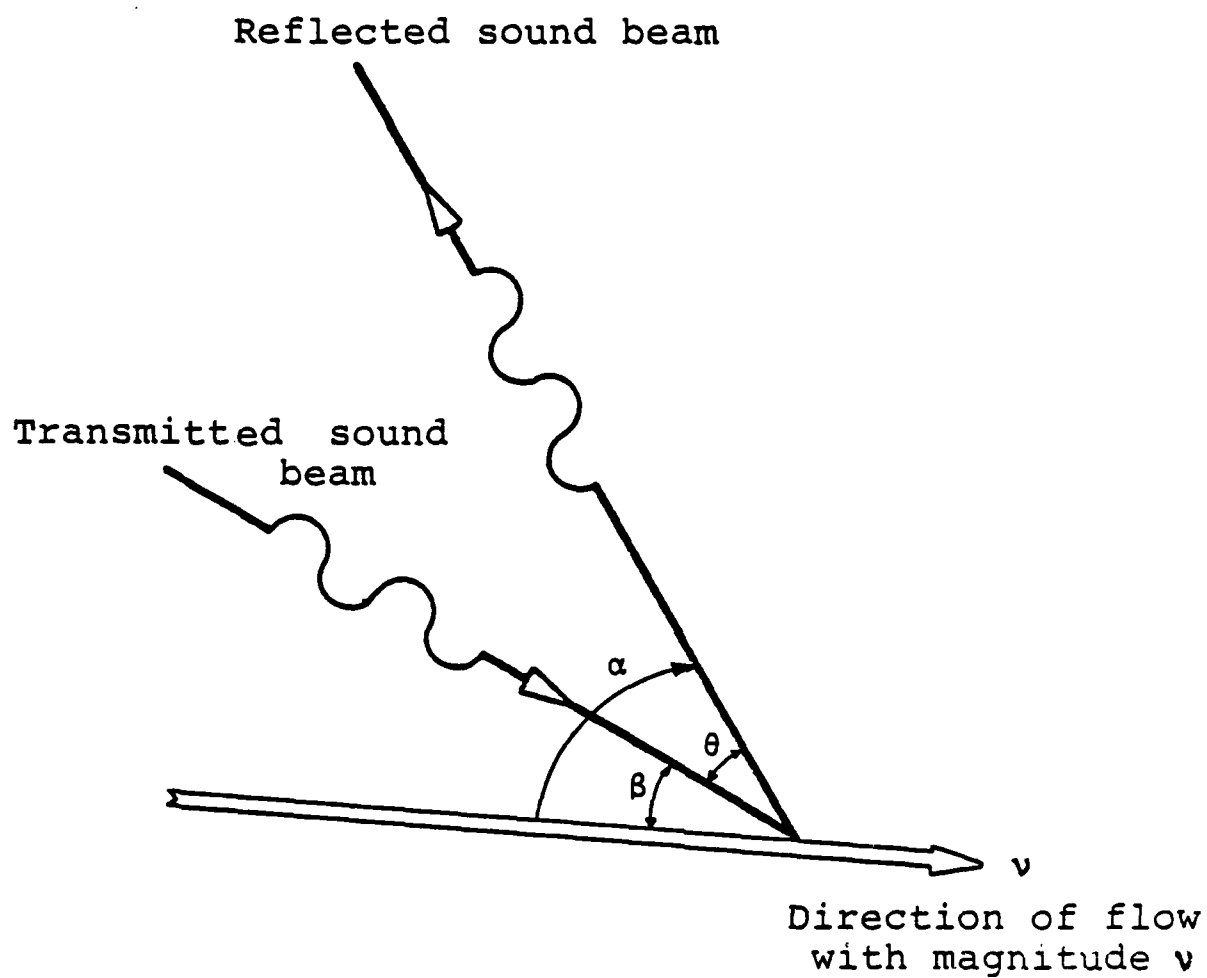$$f_D = ((c-v\cos\beta)/(c+v\cos\alpha) - 1)*f \qquad (9.14)$$

If $c \gg v$, which is always the case in biological systems, then

$$f_D = -(vf(\cos\alpha + \cos\beta))/c \qquad (9.15)$$

From the trigonometry identity $\cos(\alpha + \beta) = \cos\alpha\beta - \sin\alpha\beta$, equation 9.15 is rewritten as

$$f_D = -(2fv\cos((\alpha + \beta)/2)\cos((\alpha - \beta)/2))/c \qquad (9.16)$$

Comparing equation 9.16 with equation 9.13 shows that

$$\cos\phi = \cos((\alpha + \beta)/2)\cos((\alpha - \beta)/2) \qquad (9.17)$$

As Wells points out, the angle ϕ is always an unknown [12]. Hence, in the two transducers case, the two unknown angles, α & β compound the problem. There is no simple solution to this. Fahrbach [13] designed a probe which consisted of two Doppler flow probes inclined at right angles to each other. From the Doppler shifts measured by each probe, the angles can be calculated. Hence the velocity of blood flow can be found. Another system was designed by Hansen et al. [14]. The probe consisted of three transducers. Two act as transmitting transducers and the third one is the receiving transducer. The receiving transducer is placed in between the two transmitting transducers. Each transmitting transducer is excited by a slightly different frequency to produce a moving interference fringe pattern. The back-scattered signal is amplitude modulated and depends on the direction of the blood flow. This, by the first approximation, is independent of the angle of inclination of the beam to that of the direction of blood flow. The two systems seem to have solved the unknown angle problem provided that the blood vessel is located. Locating the blood vessel takes a skillful operator quite sometime to achieve, which is not desirable in an emergency situation.

In summary, Doppler ultrasound detects blood flow by the frequency shift of ultrasound reflected from moving blood (Doppler effect). The instrument emits a beam of ultrasound, with a frequency of 2 to 10 MHz, from a piezoelectric crystal in the tip of a hand-held probe. The ultrasound is transmitted into the tissues via an acoustic gel on the skin. Sound reflected from moving blood is shifted in frequency by an amount proportional to the blood flow velocity. The back-scattered ultrasound is received by a second crystal and the frequency shift is detected and amplified by the instrument.

Many commercial types of Doppler instruments are available, varying from small portable pocket-socket models to more sophisticated table-top instruments. Most detectors are continuous-wave devices which emit an ultrasound beam without interruption. Such devices are not range-specific;

that is, they will detect blood flow at any depth within the range of the instrument, up to several centimeters depending on the frequency of the instrument (the lower the frequency the greater the potential range of flow detection). Pulse-Doppler detectors transmit intermittent bursts of ultrasound which can be sampled for return signals at various times after transmission, permitting range resolution of detected flow at a given point from the transducer. Most Doppler detectors are not sensitive to the direction of the blood flow. Directional Doppler detectors are capable of determining whether the frequency of the backscattered sound is above or below the transmission frequency, permitting determination of flow toward or away from the Doppler probe. The output of Doppler instruments may be an audio signal (earphone or loudspeaker), an analogue tracing by means of a frequency-to-voltage convertor (zero-crossing detector), or a sound spectral analysis of the audio frequency spectrum. In addition, some instruments (continuous or pulsed) which incorporated a position-sensing arm between the Doppler probe and a storage oscilloscope permit imaging of accessible vascular segments, such as the carotid artery, by means of ultrasonic arteriography.

Applications

Doppler ultrasound may be used for the following three purposes:
    (1) blood velocity signal analysis,
    (2) determination of systolic blood pressure, and
    (3) vascular imaging.

Velocity signal analysis is used in the assessment of peripheral arterial, cerebrovascular, and venous disease. Systolic blood pressures permit semi-quantification of the presence, location and functional extent of peripheral arterial occlusive disease. Doppler ultrasonic imaging is most useful to detect arterial occlusive disease of the carotid bifurcation.

In summary, the Doppler ultrasonic velocity detector is the most versatile of all the available noninvasive diagnostic techniques to assess peripheral vascular diseases. The device may be as small as a large penlight, is portable, and may be used rapidly by an experienced technologist. The use of Doppler ultrasound in peripheral arterial disease appears as simple as measuring a standard blood pressure; however, the technique requires experience and attention to technical details. Cerebrovascular evaluation requires more experience and venous evaluation demands the greatest degree of skill and experience from the examiner. The technique requires some subjective interpretation of the character of flow velocity signals which are usually audibly interpreted by the observer. However, analogue tracings may be readily recorded for a permanent hardcopy record of the examination. With experience, a technologist may achieve approximately 95% accuracy in detecting peripheral arterial, cerebrovascular, or venous disease with this instrument. In general, the sensitivity of Doppler ultrasound to arterial and venous disease is restricted to those lesions which result in hemodynamically significant impairment to blood flow, 50% or greater reduction in diameter of the

vascular lumen. Thus, mild arterosclerotic plaques and small venous thrombi may be overlooked with this technique. With all its merits ultrasonic techniques may not be applicable in a chemical defense field environment for the following reasons:

(1) Line personnel as well as medical personnel will put on protective garments to prevent toxic agents from reaching the body. This precludes conventional medical methods of assessing the condition of a victim.

(2) In order that an ultrasonic device can perform its functions, a good acoustic coupling between the transducer and the body is mandatory. As shown by equation 9.10, if the acoustic characteristic impedance of a medium is much greater than the second medium, most of the acoustic energy will be reflected back. That leaves little, if any, energy to be transmitted through the air layer, hence, an acoustic shadow is formed behind the solid-air interface. This will be the case when the ultrasound travels through the garment and hits the air gap underneath layers of clothing or between transducer and skin. No information behind the air can be obtained.

(3) If some part of the body were exposed and a coupling gel used, then a good acoustic coupling might be achieved and blood flow could be measured. As discussed in the Doppler effect section, in order to measure flow, the angle of attack (ϕ) and the diameter of the vessel must be known to use the Fahrbach or Haneen method.

(4) In either case, a skillful, experienced operator is needed to locate the artery from which the flow is to be determined. If this is not done correctly, the error will be large and a wrong diagnosis will result.

Ultrasound is a very attractive diagnostic tool in the clinical environment where a good acoustic couple and proper orientation of probe can be achieved. But out in the field, with time and circumstance constraints, if good coupling and aiming cannot be achieved, ultrasound may not provide any useful information concerning the state of the patient.

62

References

1. Francis, J. F. Biological Effects of Ultrasound - A Review. *IEEE Proc* 67:604-619 (1979).

2. Pakmaker, P. L. Safety and Potential Hazards in the Current Applications of Ultrasound in Obstetrics and Gynecology. *Ultra In Med & Biol* 5:307-320 (1979).

3. Jarle, H. et al. An Ultrasound Doppler Technique for the Noninvasive Determination of Pressure Gradient in the Bjork-Shirley Mitral Valve. *Circulation* 59:436-442 (1979).

4. Dhanjoo, N. G. Noninvasive Cardiovascular Measurement, pp. 107-120. Miller, H. A., et al. (Eds.). Bellingham, Wash.: Society of Photo-Optical Instrumentation Engineerings 1978.

5. Anderson, D. Z., et al. Noninvasive Cardiovasive Cardiovascular Measurements, pp. 121-127. Miller, H. A., et al. (Eds.). Bellingham, Wash.: Society of Photo-Optical Instrumentation Engineerings 1978.

6. Stevenson, J. G. et al. Noninvasive Detection of Pulmonary-Hypertension in Patent Ductus Arteriosus by Pulsed Doppler Echocardiography. *Circulation* 60:355-359 (1979).

7. Milner, W. R. Hemodynamics, pp. 301-304. Baltimore: Williams and Wilkins Co., 1982.

8. Woodcock, J. P. Ultrasonics. Bristol: Adam Hilger Ltd., 1979.

9. Cracknell, A. P. Ultrasonics, p. 15. London: Alden Press, 1979.

10. Wells, P. N. T. Physical Principles of Ultrasonic Diagnosis. London: Academic Press, 1969.

11. Wells, P. N. T. Biomedical Ultrasonics. London: Academic Press, 1977.

12. Fahrbach, K. Ein Beitrag zur Blutgeschwindigkeitsmessung unter Anwendung des Doppler Effects. *Electromed* 15:26-31 (1970).

13. Hansen, P. L. et al. Clinical Blood Flow Measurement, pp. 28-32. Woodcock, J. P. (Ed.). London: Sector Publishing, 1976.

CHAPTER 10

PHOTOPLETHYSMOGRAPHY

The use of electromagnetic radiations from the body in the infrared spectrum of light energy provides a passive, noninvasive method of measuring and recording a subject's relative blood volume change. Changes in blood volume and the blood volume pulse may be measured by observation of the peripheral vascular bed. Historically, blood volume measurements of the body were performed by submerging the body (or body part) in water or in a tightly enclosed air container. These volume measurements and recordings are referred to as plethysmography.

Plethysmography is a simple method of recording blood volume changes. The photoplethysmograph instrumentation is not complicated and the transducer can be applied to many external parts of the body. It is important to note that a plethysmograph is capable only of recording relative changes in blood volume and their temporal relationships [1].

The photoplethysmographic method is based upon the large difference between the extinction coefficient of whole blood and that of tissue. The extinction coefficient is also referred to as the absorption coefficient.

$$L = L_o * 10^{-\epsilon_1 t - \epsilon x} \tag{10.1}$$

where: L_o = incident light, L = transmitted light, ϵ_1 and ϵ are extinction coefficients of whole blood and tissue in the infrared region, respectively; x and t are equivalent "thicknesses" of blood and tissue in centimeters, respectively [1]. Tissue is comparatively transparent to the red part of the visible spectrum, whereas blood absorbs most of the red light. Thus, the extinction coefficient of blood is much higher than that of tissue, especially in the near-infrared region of the spectrum (800-900 nM). Therefore, light in this spectral region undergoes variations in intensity as it passes through the tissue. The variations in intensity are indicative of changes in the amount of blood in the tissue, since lower intensity of infrared light transmitted implies a greater amount of blood present. Two basic methods of photoplethysmograph implementation are (1) measurement of the light transmitted through the tissue (transmitted mode), and (2) measurement of the light reflected from the tissue (reflective mode). In either method, it is standard to record an upward pen reflection as an increase in opacity [1].

The photoplethysmograph transducer consists of two distinct parts: a light source and a photodetector. The most commonly used light sources are small incandescent lamps, which cover the 700-900 nM band with sufficient intensity. The size and intensity of the lamp are limited by heat emission, which may alter the phenomena to be measured [1].

In spite of the great difference between the extinction coefficients of blood and tissue, only small fluctuations in light intensity result because the blood volume is only a small part of the total tissue volume. In turn,

the blood volume pulse is also a small part of the blood volume. An average finger has a tissue volume of 4.5 cm³, a blood volume of 100 mm³, and a blood volume pulse with an amplitude of 2.8% of the blood volume. Calculations made by Weinman [1] show that only 1% of the incident light in the infrared region will be transmitted by the finger phalanx, and that the blood volume pulse will have an amplitude of only 1% of the transmitted light. Thus, the photodetector must be sensitive enough in this spectral region to register the small amount of infrared light reaching it. In addition, the inherent noise level of the photodetector must be 50 to 100 times smaller than the signal intensity level. Two photocells meet these criteria: the photomultiplier (PM), and the photoconductive cell (PhC). Weinman suggests the use of the photoconductive cell since it is much smaller than the photomultiplier.

The behavior of the photoconductive cell is such that the conductance of the cell varies proportionally to the fluctuations in light reaching it. A circuit which makes use of this property is shown in Figure 10.1. An increase in incident light causes an increase in the photocell conductance, G_{ph}, and a resulting increase in the current, I_{ph}. Thus, the voltage (V) across the load resistor, R_L, is varied respectively [1].

The response time of the photoconductive cell is a function of the incident light intensity, i.e., long response time for low light intensities and shorter for higher intensities. Weinman suggests use of a time constant of 10 ms as sufficient for blood volume pulse measurements. For example, assume that the photoconductive cell behaves as a low-pass filter, then the cut-off (corner) frequency will be

$$f_c = 1/(2\pi T) = 16 \text{ Hz} \qquad (10.2)$$

where T is the filter response time constant at a pulse rate of 60 beats per minute (bpm). The high-frequency component of the blood volume pulse will be about 4 Hz, well within the good signal reproduction range of the photoconductive cell [1].

Another important consideration in selection of the photodetector is linearity of the detector. Photocell conductance is a nonlinear function of light intensity as given by equation 10.3.

$$G_{ph} = KL^\gamma \qquad (10.3)$$

where γ is a function of light intensity, L.

However, since the intensity fluctuations caused by blood volume or the blood volume pulse are so small, linearity may be assumed [1].

A high signal-to-noise ratio is also an important characteristic in the selection of a detector, since the lowest detectable signal is limited by the noise level of the photoconductive cell. The signal-to-noise ratio of the photoconductive cell is a function of conductance. At large conductances (high intensities of light) the signal-to-noise ratio is high and deteriorates as the conductance decreases. The conductance of a cell
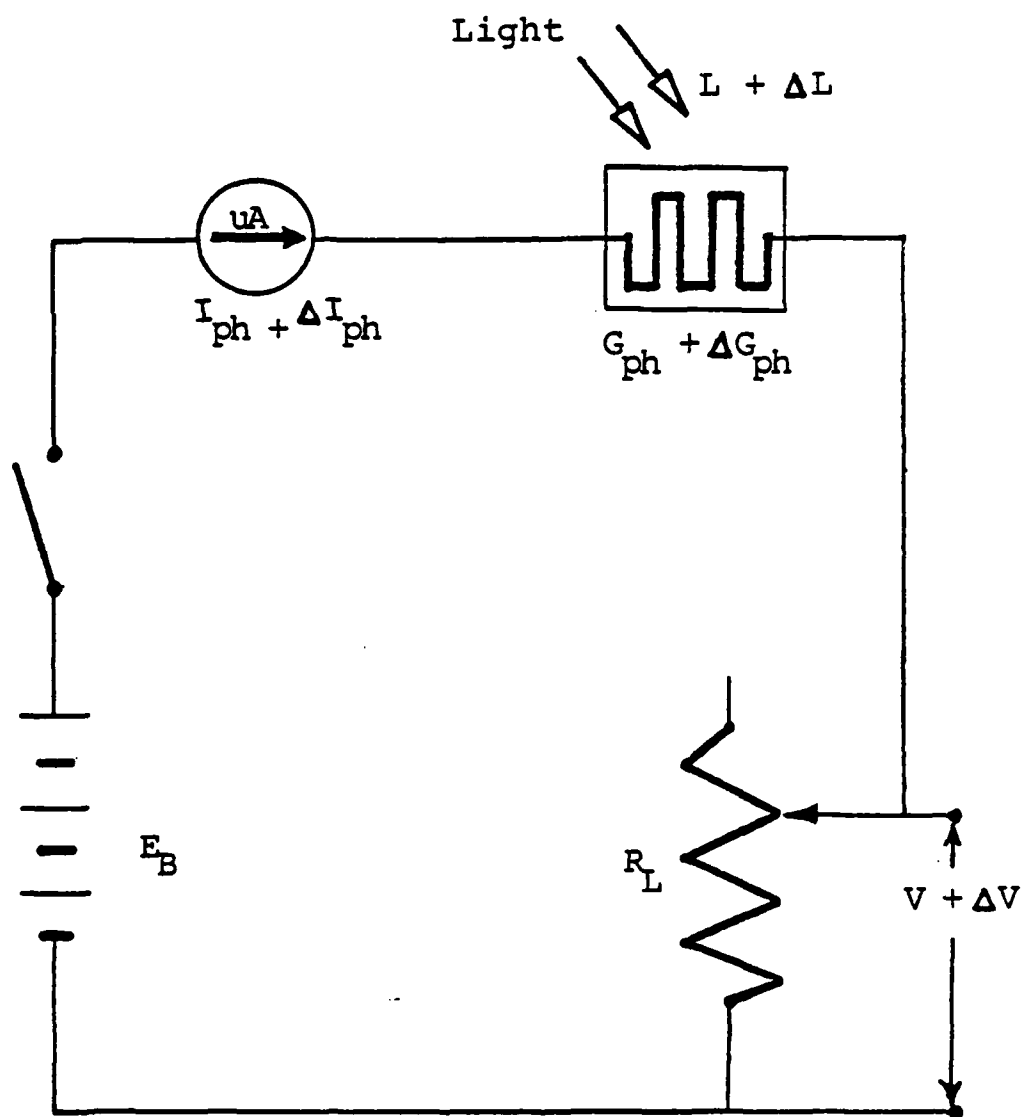
66

Figure 10.1. Circuit for the photoconductive cell.

is about 6.7 μmhos at typical photoplethysmographic intensities. The signal-to-noise ratio of a 903 Clairex cell is about 10,000 to 1.

The conductance of the photoconductance cell is not only a function of light intensity, but of light history. After application of the transducer, 5 to 10 min elapsed time is required to allow the effects of the exposure of the transducer to room lighting to diminish. A typical transducer may contain two light sources and a photocell. It may be used in either the transmitting or reflective mode. The transducers are usually small enough to be applied to a variety of locations. However, since the transducer must be held in place with a minimum amount of pressure to avoid signal distortion, it is very sensitive to motion artifacts. Thus, the subject must remain quite still during measurement recording [1].

An alternative to the system discussed so far is a recently developed LED-transistor plethysmograph. The LEDs spectral emission is 940 nM with a bandwidth of about 40 nM. The silicon photo-transistor used is sensitive to radiation only in this range [2]. This infrared system overcomes many problems associated with the miniature tungsten lamp/photocell systems, but presents other problems. The first of these is the question of how far the oxygen content of blood influences the measurement with the LED-transistor system. It is well known that the intensity of light transmitted through whole blood or reflected from it is a function of its oxygen saturation. If such is the case in photoplethysmography, no distinction could be made between light intensity changes caused by varying oxygen saturation and blood volume fluctuations. The oximetry of whole blood is based on the great difference between the distinction coefficients of saturated and reduced blood in the red region of the spectrum (650 nM). However, in the infrared region, the extinction coefficient is independent of blood oxygen content. By using infrared light, the influence of oxygen saturation of blood on photoplethysmographic records is removed [1].

Another disadvantage of the photocell is that its output is very temperature-dependent, whereas the phototransistor exhibits temperature drift of 4 mV/°C which is insignificant for most applications. Furthermore, the LED will not create as much heat as the miniature lamp. Test results indicted that the small amount of heat produced by the LED was either too small to be detected, or was dissipated too quickly to have any effect [2]. A further deficiency of the photocell which was mentioned earlier is dependence of the DC signal on light history. The photo-transistor tested in this respect showed remarkable stability under drastically changing light conditions, thus indicating that the output of the LED-transistor plethysmograph is independent of prior light exposure [2].

Spaiser [3] fabricated a functional LED-transistor infrared photoplethysmograph coupler. He found that its response was extremely stable and more consistent with the spectral response of blood volume pulse than previous systems. Spaiser estimated that such a system would take an experienced technician 10 h to construct at a total parts cost of about $150.

Photoplethysmographic signal processing involves simple amplification, with either DC or AC coupling. The blood volume pulse signal is obtained by AC coupling and amplification of the transducer signal. The close resemblance of the blood volume pulse to an arterial pressure wave has led to the belief that, if the blood volume pulse can be quantified, more information might be obtained from the signal. However, from Weinman's work it may be shown that absolute quantification of the blood volume pulse is not possible. Conductance of the photoconductive cell is given in equation 10.3, as $G_{ph} = KL^7$. From Figure 10.1, the conductance may also be expressed as

$$G_{ph} = I_{ph}/E_B \qquad (10.4)$$

where the current in the photocell may be written as

$$I_{ph} = KE_B L^7 \qquad (10.5)$$

or $\quad I_{ph} = aL^7$,where a is constant. $\qquad (10.6)$

Differentiating the photocell current I_{ph} with respect to the transmitted light results in equation 10.7.

$$\delta I_{ph} = a\gamma L^{7-1}\delta L \qquad (10.7)$$

Rewriting equation 10.7 yields

$$\delta I_{ph}/\delta L = a\gamma L^7/L \qquad (10.8)$$

Substituting equation 10.6 into equation 10.8 results in

$$\delta I_{ph}/\delta L = \gamma I_{ph}/L \qquad (10.9)$$

Then, rearranging equation 10.9 yields

$$\delta I_{ph}/(\gamma I_{ph}) = \delta L/L \qquad (10.10)$$

Recall equation 10.2 in the application of the Lambert-Beer law to circulating whole blood as

$$L = L_o * 10^{-\epsilon} 1^{t-\epsilon x} \qquad (10.11)$$

Differentiation of this equation with respect to the tissue thickness, x, yields,

$$\delta L = -\epsilon L_o(10^{-\epsilon} 1^{t-\epsilon x})(\text{Log}_e 10)\delta x \qquad (10.12)$$

Substituting equation 10.2 for transmitted light results in equation 10.13.

$$\delta L/\delta x = -\epsilon L(\text{Log}_e 10) \qquad (10.13)$$

Equation 10.13 may be rearranged as

$$\delta L/L = -\epsilon(\text{Log}_e 10)\delta x \qquad (10.14)$$

Equation 10.10 and 10.14 may be written as finite difference equations

$$\Delta L / L = \Delta I_{ph} / (\gamma I_{ph}) \tag{10.15}$$

$$\text{and} \quad \Delta L / L = -\epsilon (\text{Log}_e 10) \Delta x \tag{10.16}$$

$$\text{or} \quad \Delta L / L = b \Delta x \quad \text{, where } b \text{ is a constant.} \tag{10.17}$$

Then, combining equations 10.15 and 10.17 yields

$$b \Delta x = \Delta I_{ph} / (\gamma I_{ph}) \tag{10.18}$$

$$\text{or} \quad \Delta x = c \Delta I_{ph} / I_{ph} \quad \text{, where } c \text{ is a constant.} \tag{10.19}$$

From Figure 10.1,

$$\Delta I_{ph} = \Delta V / R_L \tag{10.20}$$

Equation 10.19 is written as

$$\Delta x = c \Delta V / (R_L I_{ph}) \tag{10.21}$$

where Δx is the change in the equivalent thickness of whole blood [1]. Thus, absolute quantification of Δx is not possible mostly because of unknown physical and physiological parameters that determine the constant c. However, relative quantification of the blood volume pulse can be obtained, and the blood volume pulse can be used to observe effects of various stimuli [1].

If the photocell transducer is DC coupled and amplified, the blood volume signal can be obtained. This signal is more difficult to analyze than the blood volume pulse. Changes in the blood volume measurement by photoplethysmography should indicate changes in the total volume of blood in the part of the body being measured. Weinman [1] demonstrated this finding during venous occlusion experiments. Occlusion of the brachial vein with a pressure cuff resulted in an upward baseline migration indicating an increasing blood volume in the finger. Similarly, vasodilation caused by placement of the hand into hot water resulted in a downward shift of the baseline. Thus, the information from the blood volume signal appeared related to vasomotion, and its effects on overall blood volume in the peripheral circulation.

With the information discussed so far, it would appear that photoplethysmography is a useful research tool in studying peripheral circulation. However, there remains a paucity of knowledge as to what factors actually contribute to the signals obtained. Hocherman and Palti [4] claim that there is very little correlation between the blood volume signal and actual blood volume. This conclusion was obtained from simultaneous recordings of photoplethysmographic and water plethysmographic measurements. They found that the general pattern remained the same for both signals, but that there was no constant relationship between the two. Sometimes, the discrepancy was so marked that the digital volume as

70

recorded by the water plethysmograph, and the opacity changes as recorded by the photoplethysmograph took opposite courses. From this data it is obvious that there is little direct correlation between the two measures. In other words, redistributing the blood in a finger causes a change in opacity that is not related to a volume change. If the suggestion is true, the reliability of the blood volume signal as a volume indicator is seriously impaired since local vasomotion is fairly unpredictable[4].

Because of the problems associated with three-dimensional orientation of blood within a vascular bed, D'Agrosa and Hertzman [5] developed a system which would enable photoplethysmography to be applied to a single vessel. The system consisted of a binocular microscope, with a photocell mounted in one of the eyepieces, and the other eyepiece left open to permit visual observation simultaneously. The light source was mounted on the microscope. A single artery of a frog's mesentery was isolated in the field-of-view. Simultaneous blood volume and blood volume pulse recordings were made during experiments that would produce known effects on the artery in question. In all experiments, it was noted that a reduction in flow (measured with an electromagnetic (EM) flowmeter) with no measurable change in vessel diameter was due to an increase in downstream resistance. The increased resistance was expected to increase pulsatile changes in the vessel wall, and thus increase the amplitude of the blood volume pulse. However, no pulsatile changes in the vessel walls were noted during visual observations. In fact, the amplitude of the blood volume pulse decreased. If the origin of the blood volume pulse were volumetric in nature, its amplitude should have increased with an increased outflow resistance. The results seem to indicate that opacity changes are not volumetric in origin, but seem to be more related to flow. It was observed that changes in flow create changes in the three-dimensional orientation of individual red blood cells within the vessel. This could account for opacity changes recorded with no change in vessel diameter. The implications are that more factors contribute to the blood volume pulse signal than were originally thought. The lack of information on the contribution of the orientation of erythrocytes to opacity prevents the blood volume pulse from being quantitatively related to flow [5]. There are differences of opinion as to which mode of measurement, transmitting or reflective, is best. Most locations on the body lend themselves to the reflective mode, since they are too thick to transmit light. Also, the reflective mode has the advantage of providing higher light intensities to be measured, yielding a better photocell time response and signal-to-noise ratio [1]. Uretzky and Palti [6] devised a system which permitted simultaneous display of both measurement modes when performed on the same finger. The results indicted that both modes were capable of reliably recording physiological events, and that the output waveforms were for the most part parallel. At times, drastic discrepancies occurred, but it was realized that variations in light intensity, as picked up by the photocell, originate principally in the vascular bed adjacent to the photocell. That is, the photocell on the dorsal side of the finger (transmitting mode) was fairly insensitive to changes occurring on the ventral side of the finger, and the ventral photocell (reflective mode) was insensitive to dorsal changes [6]. Generally, the transmitting mode is accepted as more accurate. The basis of its operation is quite simple: tissue is less opaque to near-infrared

71

radiation than whole blood and, consequently, less light reaches the sensor when the blood volume increases, and more light is transmitted when it decreases. Thus, light intensity is inversely related to blood volume, and the recording system is set up such that a positive pen deflection indicates less light or more blood [7].

Despite its advantages, the reflective mode is not as well understood. The reflective photoplethysmography technique is based upon sensing of the backscattered near-infrared light from the vascular tissue, and correlating the variations in reflected light intensity with blood volume changes of the tissue. The inverse relationship between reflected light intensity and blood volume pulse was reported by Weinman et al. [7]. They also reported the unexpected direct relationship between light intensity and blood volume, i.e., the more blood present, the more near-infrared radiation detected by the photosensor in the reflective mode. In simultaneous recordings the outputs for both modes were parallel and the inverse relationship was usually valid for both modes. However, in some instances Weinman et al. found a direct relationship in the reflective mode. Thus, they reported that reflective photoplethysmograms are a mixture of normal and inverted signals [7]. This suspicion is reinforced by the fact that the shape of the signal can be altered by moving the transducer. This change in transducer position reduces considerably the clinical value of reflection photoplethysmography in that a comparison of recordings obtained from the same patient at different times is not possible, because it cannot be ascertained whether a change in the waveform is due to physiological causes, or merely due to transducer position. In an attempt to understand the reason for these errors, Weinman et al. undertook a study of light reflection from a single artery. It was found that an artery embedded in tissue will be detected by the photocell as a signal consisting of the following components:

(1) backscattered light, emanating from the bulk of the tissue and attenuated by the interposed artery, and

(2) light reflected from the arterial wall proximal to the sensor.

Three possible cases of light intensity exist:

(1) the vessel will be detected as more light than the surrounding medium when the light reflected from the vessel wall predominates,

(2) as less light when light reflected from the tissue predominates, and

(3) the vessel is "invisible" to the sensor, if both elements of reflected light are equal.

Thus, the shape of the waveform depends upon the optical properties of tissues surrounding the vessel, as well as upon the position of the transducer. The inverse relationship therefore exists between light intensity and blood volume, because the tissue is usually responsible for the majority of the reflected light, and the presence of more blood serves

72

to decrease the amount of light reflected [7]. It is suggested that, since the majority of the light reflected by the tissues is due to the broad spectrum of light emitted by the miniature tungsten lamp, the use of an infrared light source would minimize this problem. The majority of the infrared light reflected will always be due to the red blood cells, and not to the tissue [2].

Another possible source of error in photoplethysmographic recordings that has been investigated is the effect of the hematocrit on opacity. As expected, it was found that an increased hematocrit caused an increase in opacity. It was concluded that a change in hematocrit of 28% or greater is sufficient to warrant taking it into account in the interpretation of the recordings. In one setting, however, any fluctuations in hematocrit can be considered to have a negligible effect on the photoplethysmogram [8].

Despite numerous potential sources of error, it is generally accepted that the blood volume and blood volume pulse signals are indicative of vasomotion within the peripheral vascular bed. Hence, photoplethysmography can be applied to the study of this area. Two specific applications are its use in diagnosing Raynaud's disease [9], and Vibration White Fingers (VWF) [10], a condition found among machinery or factory workers. Both conditions are caused by the body's overreacting to cold, and closing peripheral vessels sometimes to such a degree as to shut off the blood supply to the digits. It is important to be able to distinguish the two conditions from others with similar symptoms, because the usual treatment for Raynaud's or VWF is the severing of a sympathetic nerve. Photoplethysmography could be a useful clinical tool in this area. But, before the technique can be applied to other clinical and diagnostic areas, more widespread research in the infrared technology, greater error reduction, and quantification potential are necessary [2]. Also, a better optical model of tissue is required for an enhanced understanding of the principles involved [7].

References

1. Weinman, J. Photoplethysmography. A Manual of Psychophysiological Methods, pp. 187-217. Venables, P. H. and I. Martin (Eds). New York: John Wiley & Sons, Inc., 1967.

2. Tahmoush, A. J., J. R. Jennings, A. L. Lee, S. Camp and F. Weber. Characteristics of a Light Emitting Diode-- Transistor Photo-plethysmograph. *Psychophsiology* 13:357-362 (1976).

3. Spaiser, L. H. An Infrared Photoplethysmograph Coupler. *Psychophysiology* 14:75-77 (1977).

4. Hocherman, S. and Y. Palti. Correlation between Blood Volume and Opacity Changes in the Finger. *J Appl Physiol* 23:157-162 (1967).

5. D'Agrosa, L. S. and A. B. Hertzman. Opacity Pulse of Individual Minute Arteries. *J Appl Physiol* 23:613-620 (1967).

6. Uretzky, G. and Y. Palti. A Method for Comparing Transmitted and Reflected Light Photoelectric Plethysmography. *J Appl Physiol* 31:132-135 (1971).

7. Weinman, J., A. Hayat and G. Raviv. Reflection Photo-plethysmography of Arterial Blood Volume Pulses. *Med Biol Eng Comput* 15:22-31 (1977).

8. Ochoa, W. and I. Ohara. The Effect of Hematocrit on Photoelectric Plethysmogram. *Tohoku J Exp Med* 132:413-419 (1980).

9. Wouda, A. A. Raynaud's Phenomenon. *Acta Medica Scandinavica* 201:519-523 (1977).

10. Wasserman, D., W. Carlson, S. Sameuloff, W. Asburry and T. Doyle. A Versatile Simultaneous Multifinger Photocell Plethysmography System for Use in Clinical and Occupational Medicine. *Med Instrum* 13:232-234 (1979).

CHAPTER 11

MICROWAVE THERMOGRAPHY

Studies involving electromagnetic radiations from biological specimens and more recently live human tissues have grown rapidly in the last two decades [1,2]. The most recent flurry of biological research involves microwave energy. Three basic types of biological research involving microwave energy are absorption, generation, and scattering [1].

Most research efforts are directed at the absorption processes of various tissues when microwave energy is transmitted into the tissue and converted into heat [2]. These studies have shown that microwave thermography is possible. Since absorption studies usually require powerful microwave generators, the principal aim of these studies is to establish safety standards for therapeutic and diagnostic treatments of patients with medical microwave instruments [4].

In the area of microwave generation by living biological systems, very little work has been reported. These studies usually require sophisticated receiving units because of the low power of the generated waves [1]. Myers et al., [3] report using a microwave radiometer system to detect temperature gradients in live tissue. This technique, known as microwave thermography, involves detecting the intensity of the thermal radiation emitted by the body at microwave frequencies. The microwave intensity measurements correspond to temperatures. This information is plotted in two dimensions and used to locate abnormal heating or cooling spots of the body.

Detection of thermal patterns by microwave thermography depends upon two factors: thermal radiation by the body, and the partial transparency of the tissue to microwaves. It is well established that all objects including the body emit electromagnetic radiations resulting from collisions of accelerated electrical charges caused by internal thermal motion [2] and absorb electromagnetic radiations from their surrounding [3]. The intensity of emitted radiation is approximated by Rayleigh-Jeans equation

$$I(f,T) = e(f)*(2KTf^2)/C^2 \qquad (11.1)$$

where: K is Boltzmann's constant,
C is the speed of light,
T is the temperature of the object,
f is the microwave frequency,
and e(f) is dimensionless emissivity $\leq$ 1.

The emissivity depends upon the permittivities of the emitting and receiving media [2].

At normal human body temperature, the graph of specific intensity of black-body thermal radiation versus frequency has a maximum value about

75

3.0 x 10^{13} Hz or a wavelength (λ) about 10 μm. This frequency is in the infrared range. At the microwave frequency of 3.0 x 10^9 Hz (3.0 GHz or λ=10 cm) the electromagnetic radiation intensity emitted by the body is decreased by about 10^8 from its peak value. Thus expensive advanced, low-noise microwave radiometers are essential; however, the benefit of the measurement system is that at microwave frequencies the intensity is directly proportional to the temperature of the tissue. This direct relationship is what makes this technique viable.

The second factor, which deals with the transparency of tissue to microwaves, is also of great importance. The effective transparency of the body to microwaves depends upon frequency and the properties of the tissue. Studies have shown that absorption at specific frequency depends mainly upon the water content of the tissue, and that absorption increases with frequency. Thus, microwaves penetrate farthest in areas of low water content at low frequencies. However, if the frequency is too low, the penetration depth will possibly be much greater than the "hot" region under investigation, and the detected temperature variation will be reduced due to inclusion of an increased amount of "normal" tissue. Utilizing these facts, Myers et al. [3] selected an operating frequency of 3.3 x 10^9 Hz, giving a penetration depth of approximately 3 cm.

The experiments by Myers et al. used a radiometer operating at 3.3 GHz to measure the emitted radiation collected by three antennas. The antennas were open-ended, dielectric-filled waveguides, which were placed flush against the skin for maximum detection. Coaxial cable carried the signals from the antennas to the radiometer, and a strip-chart recorded the data. The results of the experiments conducted showed that subsurface temperature abnormalities can be detected by microwave thermography even when surface temperature measurements show no abnormality. One experiment detected a subsurface temperature rise in the thigh of a cat caused by focused ultrasound, whereas, surface temperature measurements did not detect the temperature change. Temperature rise due to muscular contraction was detected in a human study, from which the muscle primarily responsible for the action was distinguishable. Further experiments have detected cooling as well as heating [3].

Great potential for microwave thermography is evident in the possible clinical applications. The method can be used extensively in diagnosis, such as detection of breast cancer. Cooling of the facial tissue due to cerebrovascular blockage could be detected as well as heating due to inflammation caused by such things as an appendicitis. However, clinical studies and evaluation are still required as to the use of microwave thermography [3].

In other studies, Pedersen et al. [6,7] investigated the use of microwave radiation for pulmonary diagnosis. Their results indicated that the amplitude and phase of reflected microwave radiation is correlated with respiratory function. In addition, the ratio of lung tissue plus fluid to total lung volume is changed by pulmonary edema and emphysema.

76

These results stimulated studies by Lin [5] and Iskander et al. [8-12]. Iskander et al. conducted in vivo experiments on dogs and developed a numerical procedure to simulate and verify the sensitivity of the microwave method to quantify small changes in lung water content. Iskander et al. [11] reported a close correlation between changes in the phase of microwave transmission coefficient and the pulmonary arterial pressure. Experiments on isolated perfused lungs confirmed the sensitivity of the microwave method and revealed a correlation between the phase of the microwave transmission coefficient and the weight of the isolated lung [9]. Iskander et al. [8] reached the conclusion that "nonuniformities in water distributions in the aperture of the microwave transmitter, and location on the receiver significantly affect the microwave measurement."

Myers et al. [3] point out that the "resolution properties of any antenna depend upon the frequency, the antenna aperture dimensions, the source-aperture distance, and the dielectric properties of the medium being viewed." In most studies rectangular waveguide antennas in direct contact with the skin are used. Luedeke et al. [13] indicate that microwave radiometry measurements suffer from variable emissivity mismatch between the specimen under test and the receiving antenna. Finally, although the microwave measurements are affected by several factors other than changes in lung water contents, results are encouraging where it may be possible to develop a system and method suitable for clinical application.

The last classification of research involving microwave energy are studies into microwave scattering from biological tissue [1,5]. Griffin [1] states that about half of the microwave power incident on the surface of a subject is scattered. These scattered waves provide information on surface movement. The microwave reflection method of measuring surface movement of a subject has the advantages of not requiring any attachment or contact with the subject. The study of scattered or reflected waves requires the least elaborate microwave measuring equipment of the three types of microwave studies. The scatter study is less expensive and safer than other microwave studies because the equipment is a simpler generator and receiver system and the microwave power necessary for reflected waves of the human body is well below accepted standards.

Griffin used a microwave interferometer system based on the three-port circulator to detect small movements through the difference in phase between an input (incidence) reference wave and a reflected wave from the target area. A square-law detector was used in the interferometer to produce a DC output current given by the law of the cosine equation:

$$I = K(e_R^2 + e_S^2 + 2e_R e_S \cos\phi)/2 \qquad (11.2)$$

where: K is a proportionality constant,
e_R is the magnitude of the reference signal,
e_S is the magnitude of the reflected signal,
and ϕ is the phase difference between the reference and phase signals.

The e_S^2 term can be neglected for longitudinal movements that are small

77

compared to the distance between the test subject and the receiving antenna. The cosine term will cause an interference pattern in the detector output that decreases in amplitude with increasing separation of target and antenna. Small movements can be detected by placing the target between a maximum and an adjacent minimum in the interference pattern. The cosinusoidal interference pattern can be approximated by a straight line in this area. Movements of the target would be interpreted as a change in the detector output multiplied by a constant of proportionality. This constant of proportionality depends on the range and the slope of the line approximating the interference pattern at the operating point $\phi_0 = \pi/2$ or $3\pi/2$.

The straight line approximation places an upper limit to accurate motion detection. At one-tenth of the wavelength of the microwave, the straight line approximation is no longer valid. A nonlinear scale would allow for measurements beyond the cutoff. Two devices that could be used to study motion by the microwave method were discussed by Griffin [1]. One system which is easy to operate was the Magic Tee device. Another system, the three port circulator device, was 6 dB more accurate for the same power source, but it was more difficult to operate. Griffin claims useful measurements of the chest wall motion indicating the breath rate. Griffin also claims that movement of the foot while the knee was being supported by the other knee showed the heart rate. The suggestion was offered that the graph of the previous case could hold information of the reflex action of the subject, as well as the weight of the limb [1]. A simple microwave reflectometry device can be fabricated for about $15,000.

References

1. Griffin, D. W. Microwave Interferometers for Biological Studies. *Microwave J* 69-72 (1978).

2. Edrich, J. Centimeter-and-Millimeter-Wave Thermography:A Survey on Tumor Detection. *J Microwave Power* 14:95-108 (1979).

3. Myers, P. C., N. L. Sadowsky, and A. H. Barrett. Microwave Thermography: Principles, Methods and Clinical Applications. *J Microwave Power* 14:105-115 (1979).

4. USNC/URSI. Program and Abstracts 1976 Annual Meeting, pp. 1-158. Amherst, Mass, 1976.

5. Lin, J. C. Noninvasive Microwave Measurement of Respiration. *Proc IEEE* 63:1530 (1975).

6. Pedersen, P. C., C. C. Johnson, C. H. Durney, and D. C. Bragg. An Investigation of the Use of Microwave Radiation for Pulmonary Diagnostics. *IEEE Trans Biomed Eng* BME-23:410-412 (1976).

7. Pedersen, P. C., C. C. Johnson, C. H. Durney, and D. G. Bragg. Microwave Reflection and Transmission Measurements for Pulmonary Diagnosis and Monitoring. *IEEE Trans Biomed Eng* BME-25:40-48 (1978).

8. Iskander, M. F., R. Maimi, C. H. Durney, and D. G. Bragg. A Microwave Method for Measuring Changes in Lung Water Content: Numerical Simulation. *IEEE Trans Biomed Eng* BME-28:797-804 (1981).

9. Iskander, M. F., and C. H. Durney. Electromagnetic Techniques for Medical Diagnostics:A Review. *Proc IEEE* 68:121-132 (1980).

10. Iskander, M. F., and C. H. Durney. Electromagnetic Energy Coupler for Medical Applications. *Proc IEEE* 67:1463-1465 (1979).

11. Iskander, M. F. C. H. Durney, D. J. Shoff, and D. G. Bragg. Diagnosis of Pulmonary Edema by a Surgically Noninvasive Microwave Technique. *Radio Sci* 14:265-269 (1979).

12. Iskander, M. F., C. H. Durney, B. H. Ovard, and D. G. Bragg. Validation of Microwave Pulmonary Edema Detection by Isolated Lung and Phantom Measurements. *The 1979 Bioelectromag. Symp.* Seattle, 1979.

13. Luedeke, K. M., J. Koehler, and J. Kanzenbach. A New Radiation Balance Microwave Thermograph for Simultaneous and Independent Temperature and Emissivity Measurements. *J Microwave Power* 14:117-121 (1979).

CHAPTER 12

BIOMAGNETIC FIELDS

Biomagnetic fields are defined as "magnetic fields produced by electric currents associated with bioelectric activity or by magnetization of biological tissue" [1]. The concept of biomagnetism is not new, but until recently, the association of magnetism with biological processes was associated mainly with cults and quackery [2]. Oersted's experiments proved that a flow of electric current results in a corresponding magnetic field. Thus, the origins of small biomagnetic fields of the body are the resulting current dipoles of all excitable tissues, i.e., cardiac, muscles, nerves, and brain [3].

Measurements of biomagnetic fields began with the first reported recordings of the magnetocardiogram in 1963 by Baule and McFee [4]. Soon thereafter, Cohen reported recording the magnetic fields from the neural activity of the brain, the magnetoencephalogram [5]. But it was not until 1970 when Zimmerman fabricated the first SQUID magnetometer, that research in magnetic fields measurements and biomagnetism area stimulated significant scientific interest and growth [6].

Biomagnetic Field Theory

It is an established fact that the total magnetic field is the result of ion movement which constitutes a localized impressed current or a current dipole and the volume current which results from the potential gradients set up in tissue by the current dipole (impressed current) [7]. Thus Cuffin and Cohen [8] represent the total magnetic field, $\vec{H}$, as

$$\vec{H} = \vec{H}_d + \vec{H}_v \qquad (12.1)$$

where: the $^-$ denotes vector notation,
$\vec{H}_d$ is the magnetic field produced by the dipole current, and
$\vec{H}_v$ is the magnetic field produced by the volume current.

The calculation of the magnetic field produced by a current dipole within a sphere orients a right-hand coordinate system such that the Z-axis passes through the center of the dipole and the dipole lies in the Z-X plane. If the current dipole, $\vec{P}$, is not perpendicular to the Z-axis, it can be decomposed into its radial component along the Z-axis, $\vec{P}_z$, and its tangential component along the X-axis, $\vec{P}_x$ (Fig. 12.1).

Cuffen and Cohen [8] pointed out that the radially oriented dipole, $\vec{P}_z$, produces *no magnetic field* outside the sphere. In addition, Cohen and Hosaka indicate that the volume current represents the radial component which produces no magnetic field [7]. Thus, the magnetic field is produced by the tangential component of the current dipole, $\vec{P}_x$. The magnetic field
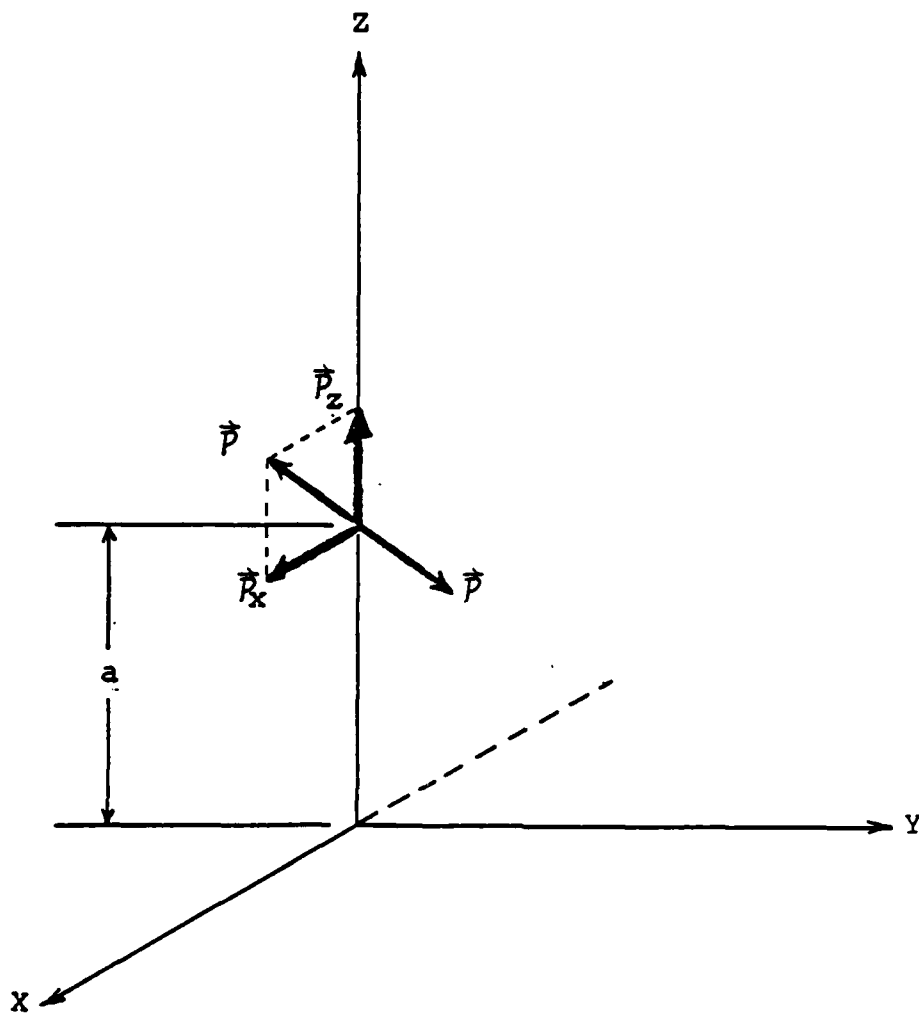
Figure 12.1. Coordinate axis, components of $\vec{P}$.

of a sphere resulting from the tangential current dipole is calculated from the curl of A divided by the permeability of the magnetic material [9].

$$\vec{H}_d = (\nabla \times \vec{A})/M \tag{12.2}$$

The vector magnetic potential, $\vec{A}$, as developed by Geselowitz, is as follows:

$$\vec{A} = \left(\iiint ((\mu \vec{J}^i/R)\delta v) - \mu\sigma \iint ((V/R)\delta\vec{s}) \right)/4\pi \tag{12.3}$$

where: $\vec{J}^i$ is the current dipole moment per unit volume of source current (current density), σ is the conductivity of the medium, V is the electric potential on the surface of the volume conductor, μ is the magnetic permeability of the media, δv is an element of volume, $\delta\vec{s}$ is a vector surface element, and R is the distance from an element δv or $\delta\vec{s}$ to the field point, p (Figs. 12.2 and 12.3).

The total magnetic field of equation 12.1 can be separated as

$$\vec{H} = \vec{H}_d + \vec{H}_v \tag{12.4}$$

where $\vec{H}_d = H_{dr}\hat{r} + H_{d\theta}\theta + H_{d\phi}\phi \tag{12.5}$

$$\vec{H}_v = 0 + H_{v\theta}\theta + H_{v\phi}\phi \tag{12.6}$$

or as the three vector components:

$$\vec{H}_r = \frac{a\sin\theta\sin\phi p_x}{4\pi r^3 \gamma^{3/2}} \tag{12.7}$$

$$\vec{H}_\theta = \frac{\sin\phi p_x}{4\pi r^2 \gamma^{3/2}} \left[\frac{\gamma\cos\theta}{\sin^2\theta} \left(\cos\theta - \frac{r}{a} + \frac{r\gamma^{1/2}}{a} \right) - \frac{a}{r}\left(\cos\theta - \frac{a}{r} \right) \right] \tag{12.8}$$

and

$$\vec{H}_\phi = \frac{\cos\phi p_x}{4\pi r_2 \gamma^{1/2}\sin^2\theta} \left[\frac{r}{a}\left(1 - \gamma^{1/2} \right) - \cos\theta \right] \tag{12.9}$$

These equations are in agreement with equation (22) on page 25 of Cuffen and Cohen [8]. For an indepth theoretical derivation of the magnetic field components of a magnetic field produced by a current dipole within a homogeneous sphere , the reader is referred to the works by Frank [10], Geselowitz [11,12], Cuffin and Cohen [8], and Lessard and Wu [13].

SQUID Magnetometer

Several types of magnetometers have been developed for measuring biomagnetic fields. The magnetometers varied from an ordinary induction
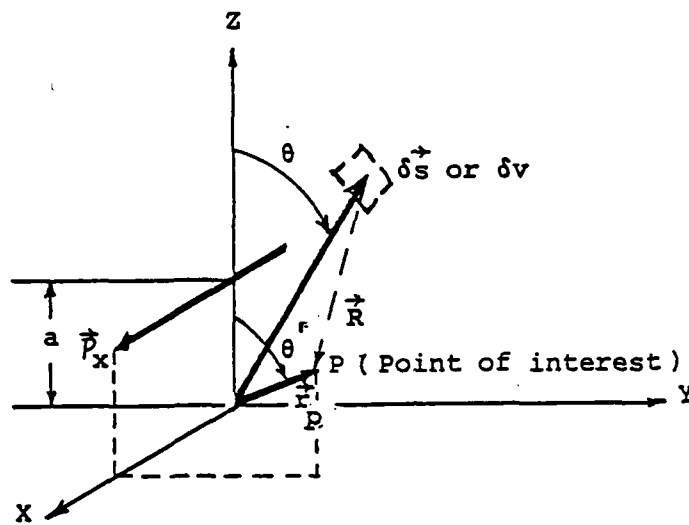
83

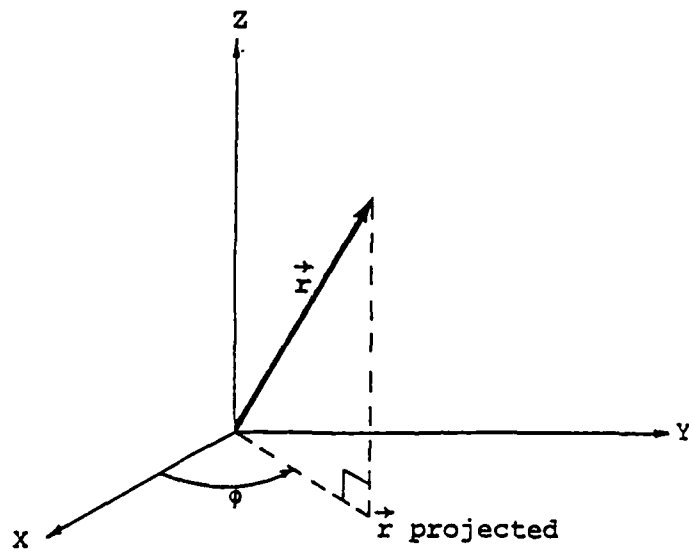Figure 12.2. Relationship of $\vec{r}$, $\vec{R}$, and $\vec{P}$.

Figure 12.3. Projection of $\vec{r}$ on X-Y plane.

84

coil of metal wire to low-noise, superconducting device of various coil configurations. Prior to the development of the Superconducting Quantum Interference Device (SQUID) by Zimmerman, biomagnetic measurements required elaborate magnetically shielded rooms [14-17]. However, in 1981, magnetocardiographic measurements in an unshielded, normally noisy environment were recorded by Barbanera et al. [18] with a 2nd derivative gradiometer coil configuration.

Detection of biomagnetic fields can be difficult, since the amplitude of the surrounding magnetic noise is greater than the amplitude of the signal from excitable tissues by many orders of magnitude. The steady magnetic field of the Earth is on the order of 1×10^{-4} Tesla (T), while the average amplitude of the magnetic fields of the heart is about 5×10^{-8} Tesla and of the brain is on the order of 10^{-12} Tesla. The higher order fields (Earth, urban noise, or other sections of the human body) are, for the most part, steady fields or regularly changing. A magnetometer or more precisely a gradiometer is not affected by steady fields.

The SQUID is a high-technology development of both the fields of cryogenics and of superconducting physics. The SQUID is based on the development of the Josephson effect found in superconductors. Superconductors are metals that have a surprisingly low resistance at extremely low temperatures ($<10°$ K). A Josephson junction consists of a 'sandwich' of a non-superconductor layer between two layers of superconducting metal. The DC-SQUID has two of the junctions in a ring, which is what forms the magnetometer. The critical current that flows around the ring is dependent on the magnetic flux that threads the ring. The SQUID can then be viewed as a sensor, or flux transformer, that has a voltage output, V, proportional to the current input. The device is basically a set of two coils, the detector coil, and the input coil (Fig. 12.4).

A magnetic field induces a current in the detector coil, which is transferred to the input coil. The input coil transduces the magnetic field to a voltage response. The following discussion, based on Williamson and Kaufman [19], describes the relationship of the two coils. The magnetic flux (ϕ_d) in the detector coil, produces a current in the input coil, I_i, in units of milliamperes, dependent on the combination of the inductances, L_d and L_i, which are in terms of microHenries.

$$\phi_d = (L_d + L_i)I_i \qquad (12.10)$$

$$\phi_d = N_d A_d B \qquad (12.11)$$

where N_d is the number of turns in the detector coil. A_d is the cross-sectional area of the coil (in square meters), and B is the magnetic induction. The current of the input coil can then be found to be:

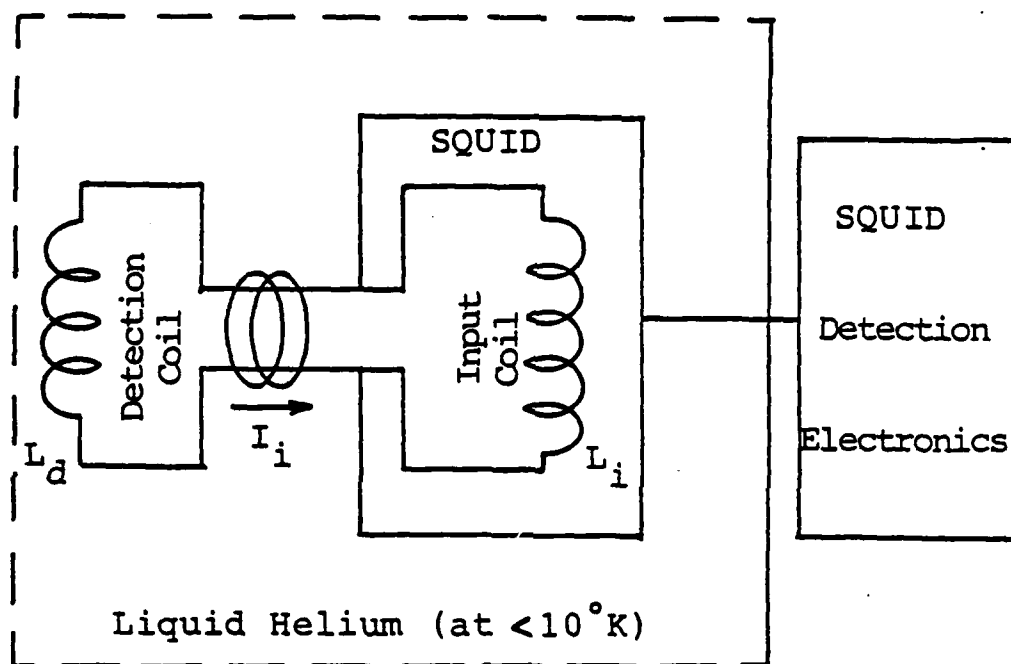$$I_i = \frac{N_d A_d B}{L_d + L_i} \qquad (12.12)$$

85

Figure 12.4. The DC-SQUID system illustration.

The detector inductance can be expressed [19] as:

$$L_d = \mu_o K_d N_d^2 A_d^{1/2} \tag{12.13}$$

where K_d is a dimensionless constant dependent on the geometry of the coil and is on the order of unity. To provide an optimal flux balance between the coils, the inductances on each arm must be equal ($L_d = L_i$). Substituting and rewriting equation 12.12:

$$I_i = \frac{A_d^{1/2} B}{2\mu_o K_d N_d} \tag{12.14}$$

From equation 12.14 it can be concluded that the input current is dependent on two main factors:

(1) the square root of the area of the coil ($A_d^{1/2}$) and
(2) the inverse of the number of input coils (N_d).

Since the field of a magnetic dipole is inversely proportional to the distance from the dipole to the sensor, a variety of different types of input coils can be designed. For steady and distant magnetic fields, the field detected by one coil can be almost offset by the field detected by a linked coil wound in the opposite direction. Using this principle, a gradiometer can be constructed using a series of linked coils wound in set orientations. In the second-order gradiometer (Fig. 12.5), the second spatial derivative of the field is the only part that is discernible. This result is possible by essentially having two gradiometers set opposite to each other, or in three sets of coils, having the first and third sets wound in the same sense, while the middle coil is wound in the opposite sense.

The DC-SQUID is illustrated in Figure 12.6. It consists of a superconducting loop with two weak links, or Josephson junctions, as described before. There is a DC bias voltage between the two junctions from a bias current of about twice the critical or bias current. The input inductor sets up a current through the SQUID loop that will increase the current at one junction and decrease it at the other. This nonlinear voltage change, as a result of the change of the current, is dependent on the period of the flux, ϕ_o. The voltage output is fed into a negative feedback loop, consisting of an AC modulation field inductively coupled to the SQUID, with the resulting voltage output returned by a phase locking detector/amplifier.

The SQUID can be used to measure low-level magnetic fields. The SQUID was used by Cohen [20] to measure the magnetoencephalogram (MEG), the magnetic fields generated by the brain. Williamson and Kaufman [19] give a comprehensive background into the instrumentation and theoretical aspects of the field of biomagnetism, within which neuromagnetism is discussed in detail. Further theoretical and practical aspects of the measurement of MEGs with the SQUID are explained in detail by Kaufman and Williamson [21] and by Reite and Zimmerman [22-24].
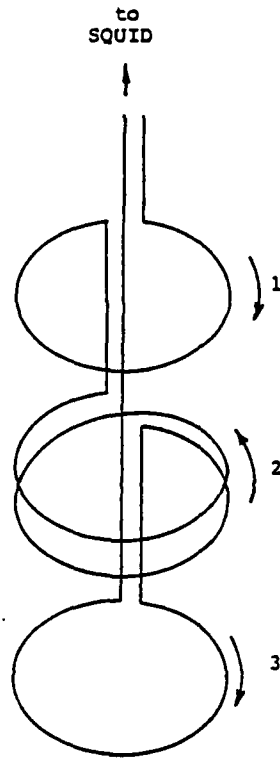
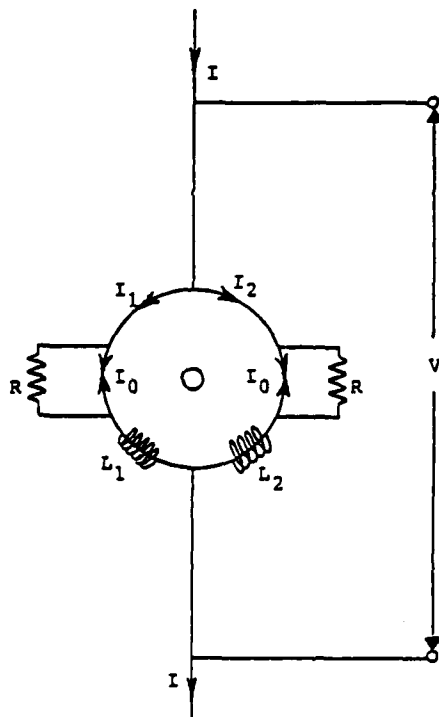Figure 12.5. A second-order gradiometer detection coil.

Figure 12.6. A schematic of the input coil and superconducting junctions of a DC-SQUID.

88

In summary, there have been numerous reports detailing the measurement and interpretation of magnetic fields of the heart (magnetocardiogram), brain (magnetoencephalogram), muscles (magnetomyogram), and lungs (magnetothoraciogram). The advantages of biomagnetic measurements are:

(1) magnetic measurements can be performed without having any attachments on the subject,
(2) very little briefing of the subject is required,
(3) use of the equipment is easy,
(4) the newer designs of the SQUID magnetometer require very little supporting hardware or maintenance, and
(5) the system will soon be portable.

The major problem with the magnetic measurements is that the signal-to-noise ratio is low. It is difficult to distinguish the very low-level biomagnetic signals from the surrounding environmental magnetic noise level.

References

1. Katila, T. Instrumentation for Biomedical Applications, pp. 3-31. *In* Biomagnetism. Erné, S. N., H. D. Hahlbohm, and H. Lübbig (Ed.). Berlin-New York: Walter de Gruyter and Co., 1981.

2. Freedman, A. P. Magnetic Significance of the Magnetic Activities of the Human Body, pp. 153-176. *In* Biomagnetism. Erné, S. N., H. D. Hahlbohm, and H. Lübbig (Ed.). Berlin-New York: Walter de Gruyter and Co., 1981.

3. Plonsey, R. Generation of Magnetic Fields by the Human Body (Theory), pp. 176-204. *In* Biomagnetism. Erné, S. N., H. D. Hahlbohm, and H. Lübbig (Ed.). Berlin-New York: Walter de Gruyter and Co., 1981.

4. Baule, G., and R. McFee. Detection of the Magnetic Field of the Heart. *J Appl Physics* 36:2066-2073 (1963).

5. Cohen, D. Magnetoencephalography: Evidence of Magnetic Fields Produced by Alpha Rhythm Currents. *Science* 161:784-786 (1968).

6. Zimmerman, J. E., P. Thiene, and J. T. Harding. Design and Operation of Stable RF Biased Superconducting Point Contact Devices, and a Note on the Properties of Perfectly Clean Metal Contacts. *J Appl Phys* 41:1572-1580 (1970).

7. Williamson, S. J., and L. Kaufman. Magnetic Fields of the Cerebral Cortex, pp. 353-402. *Biomagnetism Proceedings Third International Worshop on Biomagnetism* (1981).

8. Cuffin, B. N., and D. Cohen. Magnetic Fields of a Dipole in Special Volume Conductor Shapes. *IEEE Trans Biomed Eng* BME-24:327-331 (1977).

9. Hayt, W. H. Engineering Electromagnetics, pp. 191-196. New York:McGraw-Hill Co., Inc., 1958.

10. Frank, E. Electrical Potential Produced by Two Point Current Sources in Homogeneous Conducting Sphere. *J Appl Physics* 23:1225-1228 (1952).

11. Geselowitz, D. B. On the Magnetic Field Generated Outside an Inhomogeneous Volume Conductor by Internal Current Sources. *IEEE Trans Mag* MAG-6:346-347 (1970).

12. Grynazpan, F., and D. B. Geselowitz. Model Studies of the Magnetocardiogram. *J Biophys* 13:911-925 (1973).

13. Lessard, C. S., and H. Wu. Mathematical Validation of Forward and Reverse Magnetic Dipole Placement Problem. Unpublished paper for USAFAMRL contract No. 4919, 1983.

14. Kelhä, V. O. Construction and Performance of the Otaniemi Magnetically Shielded Room, pp. 33-50. *In* Biomagnetism. Erné, S. N., H. D. Hahlbohm, and H. Lübbig (Ed.). Berlin-New York: Walter de Gruyter and Co., 1981.

15. Cohen, A. A Shielded Facility for Low-Level Magnetic Measurements. *J Appl Phys* 38:1295-1296 (1967).

16. Mager, A. The Berlin Magnetically Shielded Room (BMSR) Section A: Design and Construction, pp. 51-78. *In* Biomagnetism. Erné, S. N., H. D. Hahlbohm, and H. Lübbig (Ed.). Berlin-New York: Walter de Gruyter and Co., 1981.

17. Erné, S. N., H. D. Hahlbohm, H. Scheer, and Z. Trontelj. The Berlin Magnetically Shielded Room (BMSR), Section B: Performances, pp. 79-106. *In* Biomagnetism. Erné, S. N., H. D. Hahlbohm, and H. Lübbig (Ed.). Berlin-New York: Walter de Gruyter and Co., 1981.

18. Barbanera, S., P. Carelli, R. Leoni, and G. L. Romani. Biomagnetic Measurements in Unshielded, Normally Noisy Environments, pp. 139-149. *In* Biomagnetism. Erné, S. N., H. D. Hahlbohm, and H. Lübbig (Ed.). Berlin-New York: Walter de Gruyter and Co., 1981.

19. Williamson, S. J., and L. Kaufman. Biomagnetism. *J. Magnetism & Magnetic Materials* 22:129-202 (1981).

20. Cohen, D. Magnetoencephalography: Detection of the Brain's Electrical Activity with a Superconducting Magnetometer. *Science* 175:664-666 (1972).

21. Kaufman, L., and S. Williamson. The Evoked Magnetic Field of the Human Brain. *Ann New York Acad Sci* 126:45-64 (1980).

22. Reite, M., and J. Zimmerman. Magnetic Phenomena of the Central Nervous System. *Ann Rev Biophys Bioeng* 7:167-188 (1978).

23. Reite, M., J. T. Zimmerman, and J. E. Zimmerman. Magnetic Auditory Evoked Fields: Interhemispheric Asymmetry. *Electroenceph Clin Neurophysiol* 51:388-392 (1981).

24. Reite, M., J. E. Zimmerman, J. Edrich, and J. Zimmerman. The Human Magnetoencephalogram: Some EEG and Related Correlations. *Electroenceph Clin Neurophysiol* 40:59-66 (1975).

CHAPTER 13

NUCLEAR MAGNETIC RESONANCE

This chapter addresses the basic theory of nuclear magnetism and nuclear magnetic resonance (NMR) essential to the understanding of a NMR blood flow measurement system. The four major aspects of NMR theory are (1) magnetization, (2) relaxation, (3) resonance, and (4) saturation. Magnetization depends upon the steady magnetic field to which the sample is subjected; relaxation governs the rapidity of the magnetization and demagnetization of the sample; resonance is essential in obtaining the responses from magnetized nuclei; and saturation is required in the measurement of flow rates [1].

The use of magnetic fields to study a number of atomic nuclei has lead to classification of various materials as diamagnetic, paramagnetic, ferromagnetic, and antiferromagnetic [1]. Diamagnetism is due to the magnetic moment caused by orbital electrons. The use of electron spin in biological systems is limited by the lack of biological substances having a net electron spin. Paramagnetism is due to a magnetic moment caused by a net electron spin and a nuclear spin. A number of biological substances are paramagnetic due to the nuclear spin. Hydrogen ion in the body is the most prominent element which has nuclear spin. Hydrogen atoms behave as spherical bodies with angular momentum and uniform charge distribution or as microscopic permanent magnets. In a magnetic-free field, nuclear paramagnetic substances exhibit no net magnetization because the microscopic nuclear magnets (spin axis) are randomly oriented [2]. When an external magnetic field, β, is applied, the nuclear paramagnetic atom dipoles realign either parallel or antiparallel to the direction of the magnetic field and a net magnetization is induced. The ratio of the number of dipoles parallel with the field (N(m+)) to the number of dipoles nonparallel to the field (N(m-)) is a function of the Boltzmann constant and the absolute temperature of the substance. This value can be expressed as:

$$N(m+)/N(m-) = \exp^{(2mH)/(kT)} \tag{13.1}$$

where: H is the external magnetic field strength,
k is the Boltzmann's constant,
T is temperature in °K, and
m is the magnetic moment equal to γ/I_m

I_m is the quantum number (which in the following derivation will be set equal to one-half) and γ is the non-zero spin angular momentum of the nuclei. This value, γ/I_m, is typically on the order of 0.001 to 0.0001 Bohr magnetons. Equation (13.1) can be rewritten as a proportionality of the total number of dipoles in the unit volume of the substance to the net difference between parallel and antiparallel nuclei. This value is expressed in equation (13.2) as:

93

$$\frac{N(m+) - N(m-)}{N(m+) + N(m-)} = \frac{\exp^{(2mH)/(kT)} - 1}{\exp^{(2mH)/(kT)} + 1}$$ (13.2)

Usually the term $(2mH)/(kT) \ll 1$ then the exponent terms can be approximated as $1 + (2mH)/(kT)$ by replacement of the exponent with the first two terms of the Maclaurin's Series expansion [2].

The total number of dipoles in the volume of a fluid can be denoted as N_o and the difference in the number of aligned nuclei can be expressed as the ratio of the nuclear magnetic force to the nuclear magnetic moment: M/m. Equation 13.2 is then rewritten as:

$$\frac{M/m}{N_o} = \frac{(1 + (2mH)/(kT)) - 1}{(1 + (2mH)/(kT)) + 1}$$ (13.3)

Solving equation 13.3 for M, the magnetic force of the nucleus, results in equation 13.4.

$$M = (m^2 N_o H)/(kT)$$ (13.4)

It should be noted that this derivation is restricted to a quantum number, I_m, of 1/2. A more general representation of the net nuclear magnetization is:

$$M = (N\gamma^2 h^2 I(I+1)H_o)/(3kT)$$ (13.5)

Equation 13.5 is a function relating the external magnetic field strength to the nuclear magnetic field strength [1]. Due to basic thermodynamic principles the energy released or absorbed on orientation of the nuclei when magnetized must have a sink or source. It is, in fact, emitted in the RF range at what is known as the Larmor frequency (w). the Larmor frequency is the relationship between the magnetogyric ratio (γ) to the external magnetic field (H) and can be expressed as $\omega = \gamma H$. Abragam [1] states that the total energy per unit time may be expressed, based on equation 13.1, as:

$$P = h\omega \left(\frac{h\omega_o}{kT}\right) \left(\frac{1}{2I + 1}\right) \left(\frac{\pi\omega_1}{2}\right) (\Sigma |(m|I|m-1)|^2 N f(\omega))$$

$$= 2\pi N \left(\frac{\omega\omega_o h^2}{kT}\right) \left(\frac{\gamma^2 h^2}{6}\right) I(I + 1) f(\omega)$$ (13.6)

where the only terms not previously defined are $f(w)$, the function of the frequency that is being emitted or absorbed, and h is Plank's constant divided by 2π. A change in the magnetic force M, measured indirectly, indicates a change in the magnetic moment, m, or in effect a change in the energy level of the nuclei [1]. The change in the magnetic force (M) can only occur as a change in the orientation of the nuclei with respect to the

94

imposed field, H. The energy that is emitted can then be measured by a radiofrequency (RF) receiver and is a direct measurement of the change in orientation.

The preceding discussion has involved only static unit volume of fluid. To measure flow, the fluid must have movement; therefore, a change in the magnetization with respect to time becomes necessary to measure. The following discussion will pursue this. The proportionality between the equilibrium magnetic force, M_o, and the applied magnetic field, H_o, in equation 13.5 may be simplified as:

$$M_o = X_o H_o \qquad\qquad\qquad (13.7)$$

where: $X_o = (N\gamma^2 h^2 I(I+1))/(3kT) \qquad\qquad (13.8)$

The factor X_o is called the static nuclear susceptibility or magnetic susceptibility. The change in magnetization for a moving system may be divided into two parts: (1) the polarization of the nuclei in the detector by the external magnetic field, and (2) the interaction of the nuclei with the resonance field. The first part can be derived directly from equation 13.6 as:

$$\delta M_z/\delta t = (X_o H_o - M_z)/T_1 \qquad\qquad (13.9)$$

where M_z is the initial or equilibrium net magnetization force that may or may not exist. The time factor, T_1, known as the relaxation time and is the time from aligned orientation to random orientation after removal of the external H field [3]. In the case of a completely isolated nucleus, i.e., the T_1 can be very high. The conclusion from this is that T_1 is very dependent on the density and interaction of the nucleus with the surrounding environment. The other determining factor in the change in magnetization involves the interaction of the nucleus with the resonance field at the RF wavelengths.

Flow of various fluids may be measured noninvasively by measuring how the electromagnetic force (EMF) generated as a conducting field within the fluid is affected by an external electromagnetic field. This method, though simple to implement and to interpret, is not useful for all fluids in all situations. For example, dielectric fluids may not be measured by this method due to the nonconductive properties of the fluids. The amplitude of the EMF also decreases squarely as the distance from the fluid increases, such that the sensor must be fairly close to the fluid being measured. External noise also affects the EMF flow transducer to a large degree; therefore isolation and shielding are necessary [4,6,8].

The nuclear magnetic resonance (NMR) flowmeter has no moving parts and is completely insensitive to spatial orientation of either the sensor or of the vessel. The information that is obtained from the sensor is in the form of a low RF electric signal that can be processed directly or digitized and transmitted for a distance to be interpreted. The signal can also be processed and used in control systems, such as in feedback loops. The sensor is easily calibrated and operates along a linear scale [5].

95

The method of measuring fluid flow using NMR has been applied to measuring blood flow in both animals and in man. The early methods were by inserting glass catheters into lumen of the vessel and the measurement sensor external to the body and the vessel. This method did not achieve the primary goal of a noninvasive measuring blood flow. The detection coil of this type of unit was tuned to 12 MHz and a modulation frequency of 1400 Hz. The resonance of the blood was observed at the same frequency. Though these first studies were percutaneous, their importance is in the information revealed concerning the nuclear properties of blood, especially the relaxation time, T [4].

Presently, two techniques are used in the measurement of fluid flow by NMR. The technique used to measure pulsatile flow is known as the "self-tag NMR method" and is necessary in determining arterial blood flow distributions. The technique used to measure steady flow is known as the "time-of-flight measurement" or the "active-tag NMR method" and is applied in the measurement of venous flow [2,4].

To determine the flow rate of a pulsatile fluid, a radio-frequency magnetic field which oscillates at the Larmor frequency is applied to the material perpendicularly to the direction of the static magnetic moment. This method causes randomization or the orientation of the microscopic magnetic moments contributing to the reduction of the net magnetism. When the fluid pulses, nonsaturated nuclei move into the detector coil and the NMR signal increases with the velocity of the liquid as the number of nonsaturated nuclei entering the detector increases. Conversely, as the velocity of the fluid decreases, the number of nonsaturated nuclei moving into the detector coil decreases proportionally. For example, during diastole, the magnetization is near zero because of the radio-frequency randomization of the individual magnetic moments of the nuclei and the low level of nuclei flowing into the detector; therefore, the NMR flowmeter output tends toward zero. However, during systole, the magnetized blood is located proximal to the detector coil and is passed through the detector coil during diastole. As a result, the peak-to-peak output voltage is directly related to the pulsatile component of flow where:

$$\Delta V = C_d A_t M \qquad\qquad (13.10)$$

where: C_d is the detector transfer constant,
A_t is the area of the lumen, and
M is the equivalent in the flow stream magnetization
as a function of pulsatility of velocity [5].

The active-tag method is used to determine the flow rate of a steady flow fluid such as venous blood. In the active-tag method a detector coil is placed downstream from a radiofrequency radiation coil which is periodically energized at the Larmor frequency. This causes demagnetization of a small bolus of fluid by saturation. The passage of the demagnetized bolus of fluid through the detector coil yields two parameters necessary in the determination of the flow rate: (1) T_d, the time from the tagging of the bolus to the time the tagged bolus reaches the detector, and (2) the tag signal amplitude, which is used to determine the volume of fluid [5].

The composition of blood is approximately 83% water and the balance consists of proteins, fats, and carbohydrates that comprise the erythrocytes, leukocytes, and thrombocytes. The hydrogen nucleus is of most interest in NMR because of the simplicity of its atomic structure. Thus, the T_1 of blood is best approximated by the relaxation time of hydrogen (water) as affected by the suspended particulate matter. Three phases of water are identified in blood: (1) bulk, or unbound water (98.4%) with a T_1 of 4.5 s, (2) hydrated to proteins (1.4%) with a T_1 of 0.016 s, and (3) within the particulate molecules (0.2%) with a T_1 of 54 μs. The composite relaxation time of blood is a combination of these three parts:

$$\frac{1}{T(net)} = \frac{f(a)}{T_1(a) + t(a)} + \frac{f(b)}{T_1(b) + t(b)} + \frac{f(c)}{T_1(c) + t(c)} \qquad (13.11)$$

where the f's are the fraction of water within the total blood volume and the t's are the residence times of the water in each of these states. The net value of the T_1 of blood is then calculated to be 0.07 s at low Larmor frequencies (<100 kHz) and approaching 0.4 s at the higher frequencies (>10 MHz) [4].

There are two major divisions of NMR blood flowmeters, the single coil regenerative design and the crossed coil design. The single coil, though simpler in concept, is much more difficult to design accurately and not nearly as efficient. The emitter time period of the device should be designed for high-frequency, low-amplitude emission. On the other hand, the receiver is best designed for low-frequency, high signal-to-noise response. A design that has only a single coil is a compromise at best, yet a two coil design is bulky and more expensive to build. The crossed coil design takes up little space (Fig. 13.1). This design is more stable throughout a range of frequencies as well as more sensitive than single coil variety. The transmitter excitation source may be designed to be frequency and amplitude stable, while the receiver can be designed for low noise. This allows the transmitter to be designed for high-frequency (>100 kHz) while the receiver can be designed to pick up low frequencies (<100 Hz). The coils are arranged orthogonally to eliminate the chance of crosstalk or mutual inductance.

Two types of crossed coil flowmeter design are the cylindrical crossed coil and the flat crossed coil designs. The cylindrical coil has two coils arranged at orthogonal angles around a 12.6 cm inner diameter fiberglass/epoxy tube (Fig. 13.1). This design was found to be adequate for measuring the blood flow of the upper limb of human adults and the legs of children. For accurate sensitivity, the magnetic field was constructed as large as possible, yet not too unwieldy. The magnet described was constructed of ceramic permanent magnet material, 58 cm wide, 36 cm high, 45 cm long, and produced a magnetic field of 750 Gauss. This system operated at 3.2 MHz. Studies have indicated that this system compares favorably to similar studies with electromagnetic (EM) blood flowmeters [5].
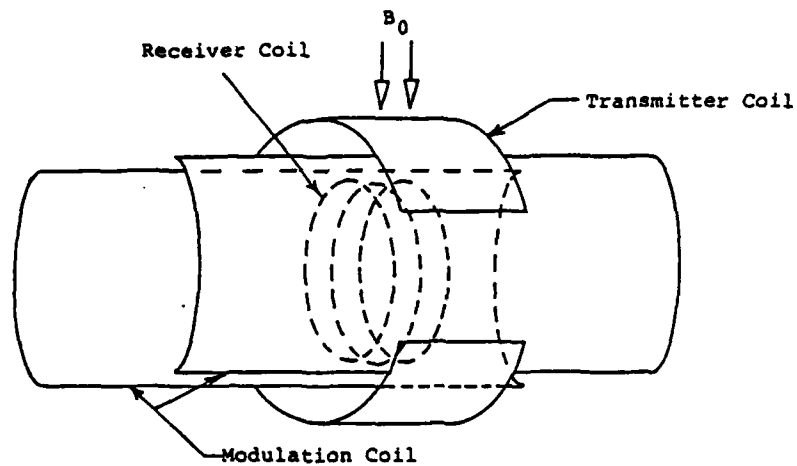
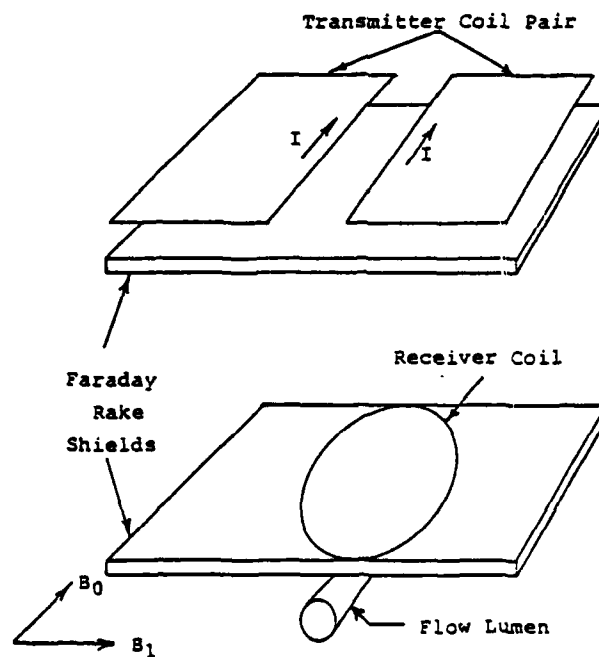Figure 13.1.   Arrangement of coils in cylindrical coil limb flowmeter.

Figure 13.2.   Flat coil detector.
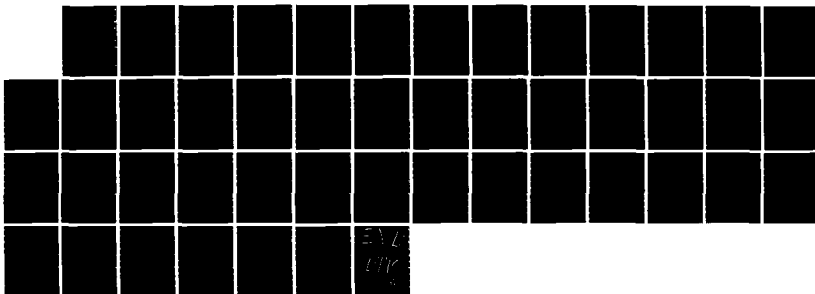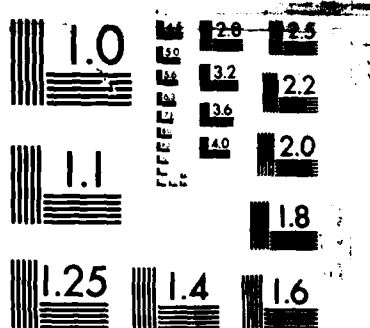
MICROCOPY RESOLUTION TEST CHART
NATIONAL BUREAU OF STANDARDS 1963 A

The second type of flowmeter, the flat crossed coil flowmeter, was designed to allow for the measurement of blood flow in the head and thorax (Fig. 13.2). The transmitter and receiver coils are mounted end-to-end in a planar fashion. A pair of rectangular transmitter coils mounted side-to-side produce concurrent currents in adjacent sides. A single receiver coil is mounted centrally below the transmitters. The magnetic field lines of the transmitter and receiver that intersect are orthogonal. This type of system is operated at 9 MHz, 21.4 MHz, and 75 MHz Larmor frequencies. The sensitivity of the system varies inversely to the spacing between the detector and the vessel due to the combined effects of the receiver coil sensitivity and the transmitter field level:

$$K(r) = A(c)/(\gamma^2 + \ell^2/4) \tag{13.12}$$

where A(c) is the area of the receiver coil, ℓ is the width of the receiver coil, γ is the spacing, and K(r) is the sensitivity of the system. This contrasts with the cylindrical crossed coil detector which has a fairly constant sensitivity throughout the length of the detector.

In summary, NMR blood flowmeters have been shown to be effective as a method for measuring the flow of blood in a convenient, noninvasive, and unobstructive manner. The methodology was shown to have no known side effects to the physiology of the body. Work being done currently in this facet of NMR research, as well as other facets (NMR imaging), is proving to be one of the foremost areas of future research in medical vital signs measurements, diagnostics, and imaging [10,11].

References

1.   Abragam, A. The Principle of Nuclear Magnetism. Oxford: Wrendon Press. 1961.

2.   Battocletti, J. H., A. Sances, Jr., S. J. Larson, S. M. Evans, R. E. Halbach, R. L. Bowman, and V. Kudravcev. A Review of Nuclear Magnetic Resonance Techniques Applied to Biological Systems, pp. 263-294. *In* Biological and Clinical Effects of Low Frequency Magnetic and Electric Field. Llaurado, J. G., A. Sances, Jr., and J. H. Battocletti (Eds.) Springfield: Charles C Thomas Publishing, 1974.

3.   Singer, J. R. Flow Rates Using Nuclear or Electron Paramagnetic Resonance Techniques with Applications to Biological and Chemical Processes. *J Appl Physics* 31:125-127 (1960).

4.   Battocletti, J. H., R. E. Halbach, S. X. Salles-Cunha, and A. Sances, Jr. The NMR Blood Flowmeter-- Theory and History. *Med Phys* 8:435-443 (1981).

5.   Halback, R. E., J. H. Battocletti, S. X. Salles-Cunha, and A. Sances, Jr. The NMR Blood Flowmeter-- Design. *Med Phys* 8:444-451 (1981).

6. Salles-Cunha, S. X., R. E. Halbach, J. H. Battocletti, and A. Sances, Jr. The NMR Blood Flowmeter— Applications. *Med Phys* 8:452-458 (1981).

7. Zhernovoi, A. E., and G. D. Latyshev. Nuclear Magnetic Resonance in Flowing Fluids. Consultants Bureau, 1965.

8. Battocletti, J. H., R. E. Halbach, A. Sances, Jr., S. L. Larson, R. L. Bowman, and V. Kudravcev. Flat Crossed-coil Detector for Blood Flow Measurement using Nuclear Magnetic Resonance. *Med Biol Eng & Comput* 183-191 (1979).

9. Halbach, R. E., J. H. Battocletti, A. Sances, Jr., S. J. Larson, R. L. Bowman, and V. Kudravcev. Blood Flow Detection Using the Flat Crossed-Coil Nuclear Magnetic Resonance Flowmeter. *IEEE Trans Biomed Eng* BME-28:40-42 (1981).

10. Hayes, C. E., T. A. Case, D. C. Ailion, A. H. Morris, A. Cutillo, C. W. Blackburn, C. H. Durney, and S. A. Johnson. Lung Water Quantitation by Nuclear Magnetic Resonance Imaging. *Science* 216:1313-1315 (1982).

11. Gross, S., and N. Zumbulyadis. Use of High Mixing Frequencies for RF Generation and Detection in a Multinuclear and Cross-Polarization Magic-Angle-Spinning NMR Spectrometer. *Rev Sci Instrum* 53:615-623 (1982).

CHAPTER 14

IMAGING SYSTEMS

The impact of technology upon clinical medicine is evident in many areas, but none more visible than the area of medical imaging. In less than 50 years, advances in instrumentation, detector fabrication, radionuclide production, and, most importantly, computer technology have made the field of medical imaging one of the fastest growing areas in medicine. Recent developments in other areas have brought out entirely new techniques for imaging such as ultrasonics, computer tomography, and nuclear magnetic resonance (NMR). One important factor deserving note is that transmission devices most often display anatomy whereas emission techniques can also display physiology, but with much lower resolution for the latter technique. This chapter will address the state-of-the-art in diagnostic radiography.

The science of radiology and nuclear medicine had its beginning in the late 1890s more by accident than by scientific method. In the fall of 1895, W. C. Roentgen, a German physicist, was conducting experiments on cathode rays in his laboratory. When he excited a low-pressure tube with high voltage, Roentgen noticed some crystals glowing on a nearby bench. Upon investigation, Roentgen found that the rays causing this phenomenon could pass through solid matter. Within a few days Roentgen took the first x-ray film of his wife's hand. Within weeks the news had spread around the scientific community and within months medical x-rays were being taken in many places around the world. The first documented electroradiographic process was demonstrated by S. P. Thomson in 1896. Thomson displayed a process called ionography to produce x-ray images using a mixture of charged lead and sulfur particles. The particles were attracted by the electrostatic field of a latent image formed on an ebonite disc. This technique was soon forgotten and replaced by the presently used method of xerography, using x-ray sensitive film to reproduce an x-ray image.

Nuclear medicine is the process of using radioactive materials (radioisotopes) to trace activities in the body (usually by injection of the material into the bloodstream). The history of nuclear medicine began in 1921 when Von Hevesy carried out the first biological radioactive tracer experiment. In 1927, Kotzareff produced one of the first images using radioisotopes, making an autoradiograph of the kidneys following intracardiac administration of a radium solution to animals. Later, artificially produced radionuclides and the introduction of charged-particle accelerators in the late 1930s made human studies possible. Recent developments in radiation detectors has decreased the necessary radiation dose to the patient enough to allow the practice of emission radiography to become an effective clinical tool.

A number of new imaging techniques have surfaced using the technological advances of the last 20 years. Ultrasound imaging is widely used on soft tissue studies or applications involving fetal visualization. Positron emission tomography, or PET scanning, uses opposing detector

arrays to collect data based on the annihilation of positron within the array field. Nuclear magnetic resonance (NMR was reviewed in previous chapter) is a technique used for years to analyze compositions of chemical samples. Recently, this technique has been applied to the medical field in order to visualize certain areas based on biochemical differences of tissues at the site. Proton scanning (a transmission technique) is analogous to standard x-ray transmission imaging except that heavier, positively charged particles (alpha particles, protons, deuterium) are used instead of x-rays. This technique allows for a lower exposure to the patient and better resolution for certain types of tissue types. Other variations in imaging technology are largely results of using these techniques but varying the methods of radiation delivery and collection, display, and especially processing.

All medical imaging techniques (except ultrasound) use some sort of ionizing radiation to gather information about tissue characteristics. Ionizing radiation (as opposed to nonionizing radiation) has the feature that the radiation ionizes the matter through which it travels (unlike infrared, radio, or light radiation). This radiation is produced either by instrumentation such as x-ray tubes (in transmission imaging) or by nature or man-made radioisotopes introduced into the body (emission imaging). Essentially three types of ionizing radiation exist for use in imaging systems:

(1) Beta rays are negatively charged electrons. Their velocity varies widely and may approach the speed of light. Their penetration depth depends on velocity, but is usually small.

(2) Alpha rays are positively charged helium nuclei that travel at less than 1/10 the speed of light. Their penetration is small.

(3) Gamma rays and x-rays are both electromagnetic waves that have a higher frequency than visible light. Penetration of these rays is relative to energy.

As shown in Figure 14.1, x-rays range from the ultraviolet frequency to almost 10^{20} Hz, with diagnostic medical x-rays in the frequency of about 10^{18} Hz. Gamma rays have a slighty higher range, surpassing 10^{20} Hz. Although x-rays and gamma-rays have essentially become synonymous in medical applications, x-rays are tube-generated for transmission radiography, while gamma radiation is produced by the decay of radioisotopes used in emission imaging.

It should be noted here that alpha, beta, and gamma radiations are primarily used in emission radiography, each produced by radioactive decay of radionuclides introduced into the body. Alpha rays have also been used for transmission imaging, but require a heavy particle accelerator, which makes this a cost-prohibitive procedure.

Another type of emission imaging technique involves the use of particles called positrons. A positron is a positively charged electron (antimatter) that is produced whenever a very high energy x-ray enters the

intense electric field of the nucleus. The result is emission of two particles: an electron and a positron. The positron is quickly annihilated and forms two photons of equal energy that travel in opposite directions. Although this process is of no use in transmission imaging because of the high energy required to produce the X-rays, positron emission scanning is a useful technique which will be discussed later, where detectors are arranged in opposing pairs to take advantage of the phenomenon of positron annihilation.

Ionizing radiation is biologically harmful and its dosage is cumulative. Excessive exposure can cause genetic mutations, can be carcinogenic, and can cause physical illness (radiation sickness), and even death. For these reasons, it is imperative that radiation dosage be kept to a minimum during each test.

In transmission radiography, dosage (or dose rate) is a measure of the energy of the applied radiation. X-ray energy is a function of frequency (E = hf) and is expressed in electron volts (eV). The applied radiation must be of high enough energy (frequency) to produce an effective image and of low enough energy to be biologically safe. Standard x-ray instruments characteristically produce a radiation energy from about 10 keV to 150 keV for normal applications, and up to 500 keV in special cases. In emission imaging, dosage is a function of the radiative decay of the radionuclide used (half life), radiation type, and washout (excretion or expulsion of the radionuclide). Since alpha and beta-rays have low penetration, their dosages would have to be greater to be detected externally.

The remainder of this chapter will focus primarily on the techniques, theory, and instrumentation involved in diagnostic transmission imaging, with brief mention of the instrumentation involved in emission scanning and specific emission scanning techniques.

Basically, production of x-ray beams used in diagnostic transmission radiology is achieved in two ways: the Bremsstrahlung quantum effect and by replacement of K-shell electrons in a nucleus. In the Bremsstrahlung effect, a fast electron approaches a target atom. If the electron passes close enough to the heavy, postively charged nucleus, it is deflected somewhat and loses energy in the process. This energy is emitted as an x-ray photon. The amount of x-ray radiation emitted in this manner depends on two factors: the mass of the target nucleus (more protons increase the attraction of electrons) and the velocity (energy) of the electrons (higher velocities increase the probability of penetration near the nucleus). A second means of x-ray generation occurs when a high energy electron strikes a K-electron in a target atom and knocks it out of its orbit and free of the atom. The vacancy is immediately filled by a higher-orbit electron and an x-ray photon is emitted in the process. The energy of this x-ray is characteristic of the target atom. So-called characteristic x-rays are of little use at the present; consequently, the Bremsstrahlung effect accounts for almost all x-ray generation used in medical imaging.

The device used to produce x-rays in this manner is the high-vacuum x-ray diode tube (Fig. 14.2). A cathode filament is heated on one side of a
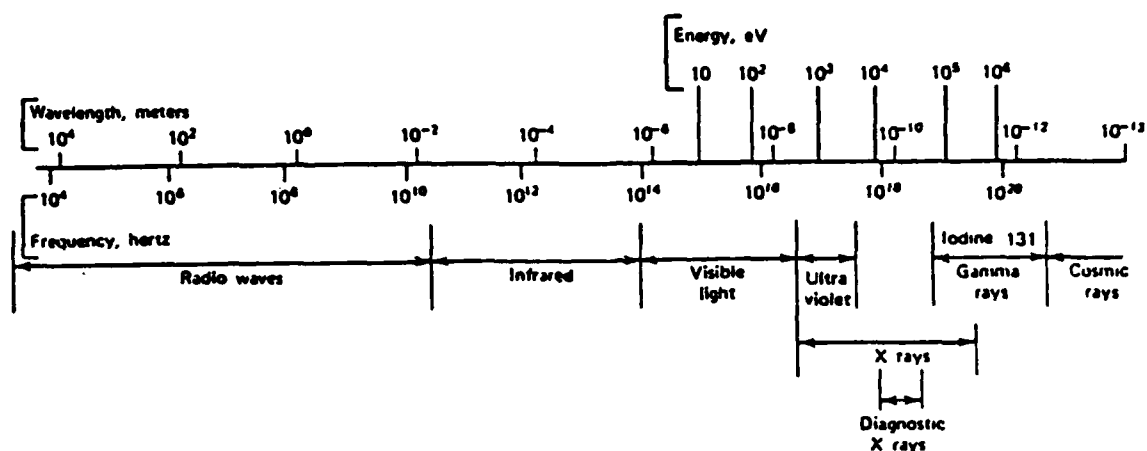
103

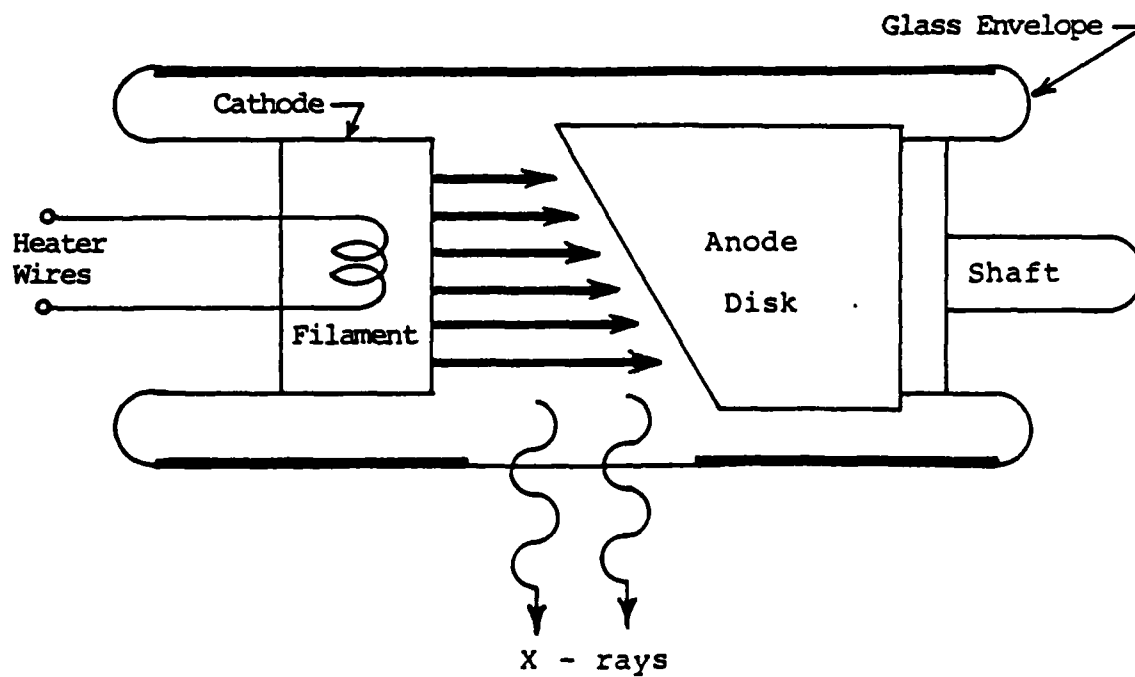Figure 14.1. Spectra of electromagnetic radiation.

Figure 14.2. High vacuum X-ray diode tube.

glass vacuum tube, providing a source of electrons ("boiling" them off). The electrons are accelerated toward the anode disk by a high voltage (from 10 kV to 150 kV), and x-rays are produced by the Bremsstrahlung effect at the disk surface. These x-rays are collimated (focused) to produce optimal contrast relative to the patient dose.

A typical block diagram of an x-ray machine is shown in Figure 14.3. Surprisingly simple, the instrument consists primarily of adjustable transformers and a rectifier supplying the necessary high voltage and current to the x-ray tube. DC voltage selection is achieved by switching between multiple taps on a line transformer and determines peak delivered radiation energy (which is analogous to penetration depth). A separate current selector determines the cathode filament current (heat) which regulates the amount of electrons "boiled off" to produce x-rays (analogous to x-ray quantity or exposure strength). A timing circuit is employed to control the exposure time as shown in Figure 14.3.

The anode disk is usually made of tungsten, because of its high atomic number which increases the Bremsstrahlung effect and high melting point. Since most electrons striking the anode do not produce x-rays, over 99% of the power generated is dissipated as heat. Because of this tremendous power, the anode in most machines is rotated from 3600 rpm up to 10,000 rpm in order to facilitate heat dissipation. Extensive safety features are built in to protect the users from excessive heat. Nevertheless, tube burnout is the most common cause of failure in these systems.

There are primarily three ways in which x-rays lose energy within the body (or within a detector). Since x-ray imaging is a measure of the attenuation of x-rays transmitted through the body, these effects can be used to control contrast or intensity of an image. The photoelectric effect occurs when an incoming x-ray photon transfers all of its energy to an electron which then escapes from the atom. The photoelectron then ionizes surrounding atoms for a short distance. This is primarily the phenomenon likely to occur in the intense electric field near the nucleus rather than in outer levels of the atom, and is more common in elements with a high atomic number (same as Bremsstrahlung effect). This characteristic causes the variation in attenuation between dense and loose tissue, or between heavy and light elements, that shows up on an x-ray image.

Another manner in which x-rays lose energy in the body is by photon collision with a loosely bound outer electron. The electron receives part of the energy of the x-ray photon, and the remainder is transferred to a Compton (scattered) photon, which then travels in a direction different from the original x-ray. The Compton effect is most pronounced in dense tissue consisting of light elements, or at high x-ray energy levels (greater than 100 keV) in all tissues.

The third phenomenon causing attenuation in the body is the pair production effect, or positron production. This effect occurs only at very high energy levels (greater than 1 MeV) which would be harmful to the body.
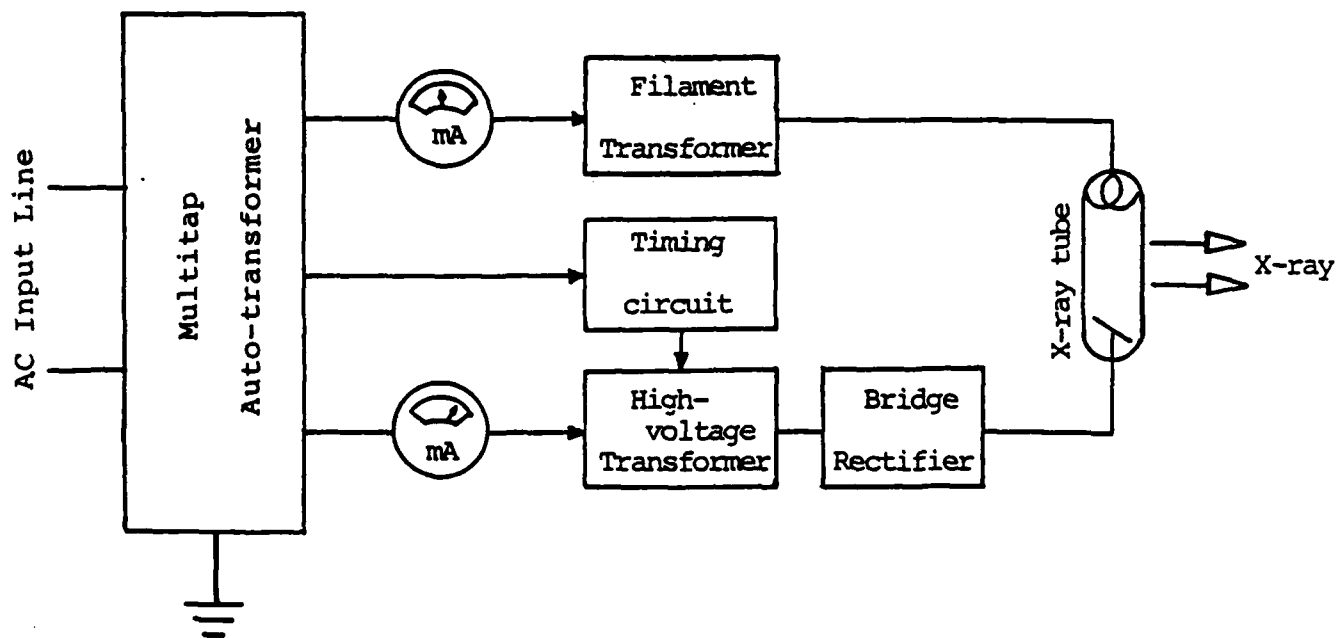
Figure 14.3. Block diagram of an X-ray machine.

Therefore, this phenomenon is of no use in transmission radiography, but does have some application in emission imaging.

With these effects in mind, optimum images can be produced by varying x-ray energy levels, exposure times, and field dimensions. For standard x-ray films, these parameters are determined subjectively by radiologists and technicians, producing a wide range of acceptable results for the physician to analyze. With the advent of modern computers and instrumentation, more quantitative control was gained through the use of digital image processing and photomultiplier techniques. These techniques are used in processes involving active detectors, rather than film, such as tomography, fluoroscopy, and emission radiography.

As stated before, ionizing radiation differs from nonionizing radiation in that it ionizes the gases through which it travels. This effect, along with those just discussed, is used in the construction of active detectors for both transmission and emission imaging systems. For use in techniques where a simple static x-ray film is not sufficient, these detectors are sensitive to a particular type of radiation and have several advantages over film such as real-time visualization, refresh capabilities, greater sensitivity, more precise orientation, and emission detection.

Basically two types of detectors are in use today: the scintillation crystal detector and the gas ionization chamber. Gas ionization tubes are primarily used for beta-ray detection (an emission phenomenon), while x-ray and gamma-ray detection is achieved using scintillation crystals. One of the most commonly used detectors is the Geiger-Mueller tube, a type of ionization chamber similar to the well-known Geiger counter.

The Geiger-Mueller tube operates by counting beta particles entering its chamber. Beta particles passing through the gas mixture in the tube cause ionization, and the electrons are collected by the anode and the positive ions by the cathode via a high potential of approximately 1 kV. Therefore, each beta particle causes a brief pulse of current. The total number of current pulses, electronically counted over a given period of time, indicate the radiation intensity falling on the mica window. This type of detector, and those related, are used in emission imaging techniques with beta-emitting radionuclides.

The scintillation crystal detector operates on the photoelectric effect principle. Certain materials (termed fluorescent) glow when struck by ionizing radiation. This so-called luminescence (as opposed to incandescence) is caused by ionizations evoked by the photoelectric effect at the crystal surface which cause energy emissions in the visible spectrum. The amount of light emitted is directly proportional to the energy and quantity of the incident radiation (as in the Bremsstrahlung effect). This principle may be used to detect any type of ionizing radiation, depending on the crystal material and device configuration, and it is the most widely used type of detector in medical imaging. Sodium iodide and zinc sulfide are the most common crystal materials, both being very sensitive to gamma and x-ray radiation.

The visible light emitted by the scintillation crystal detector is of very low ambient light intensity. Therefore, most detectors of this sort are paired with either a device called a photomultiplier or an image intensifier. When the crystal detects incident radiation, the resulting flashes are reflected onto the cathode of the photomultiplier tube. Dynodes multiply this signal up to 10 million times by a secondary emission process and produce an appreciable current pulse for each flash. These pulses are counted for the entire crystal surface and used to determine radiation intensity. The image intensifier tube acts as an accelerator for electrons emitted when light photons from the crystal detector strike a photocathode. The electrons may be accelerated to energies up to 25 keV and when focused on a small fluorescent screen, produce an image of the detected radiation. Note that the photomultiplier acts as a counter for the quantity of incident radiation while the image intensifier actually generates an effective real-time image (mainly used in fluoroscopy).

When detecting radiation transmitted through or emitted from the body, some scattering will occur and tend to blur the image. To obtain a satisfactory image (or count), a collimator is used to reduce the effect of scattering. A collimator acts as a type of lens used to exclude from the detector (or film) those photons which are not directly from the field of interest. A collimator used in x-ray film systems consists of a grid made up of lead strips slanted toward the transmission x-ray point source. Only x-rays traveling in a straight line from the point source pass through the grid onto the film, while the rest are absorbed by the lead. The principle of operation used in emission imaging is based on the same principle as the grid collimator. Collimators are not required in some techniques, such as positron emission tomography, because of unique detection methods. Generally collimators are needed for all transmission and most emission imaging.

Only in the last 20 years has medical imaging consisted of anything more than a standard static x-ray film. Better detectors and electronics, as well as practical radioisotope production, helped advance nuclear medicine and fluoroscopic techniques. But by far the single largest impact on medical imaging was caused by the advent of the modern computer. With the power and speed of the new computers, image processing became a new, effective means of reconstructing multi-dimensional views of the human anatomy and of physiological activity.

Essentially, four types of imaging systems are used clinically today (excluding conventional x-ray photography). Ultrasonic imaging will not be discussed in this chapter. The remaining three are transmission tomography, x-ray fluoroscopy, and nuclear medicine imaging. The first two are transmission techniques while nuclear medicine is considered an emission imaging technique. X-rays are produced as previously discussed and can be represented as a point source. With film placed behind the object to be x-rayed, an image is formed of composite bone, tissue, and air. These structures overlap and may be difficult to discern from one another. A subjective evaluation is performed by the radiologist, but structures which have roughly the same density are sometimes impossible to separate, such as tumors in soft tissue. However, this technique is still

effective for most needs, and remains the most common clinical imaging process used.

In the early 1930s, a process termed tomography was described which would help alleviate some of these imaging problems. If the film and x-ray point source were simultaneously moved in opposite directions within the same horizontal plane (with the patient in between), an image is produced which allows a new parameter to be controlled: depth. This technique is shown in Figure 14.4 and is explained as follows: If the rectangle abcd is a "slice" in the chest of a patient, for example, then the image of the rectangle ABCD can be constantly in focus only if the x-ray point source and the film are moved at precisely the same rate in the same plane as shown (that is, lines Oa, Ob, Oc, and Od always coincide with lines OA, OB, OC, and OD, respectively). If this is done, all other planes parallel to abcd will be blurred in the formed image. This phenomenon allows for selective control of the position of the rectangle abcd, or in more conventional terms, depth. Therefore, using the technique of tomography (in this case, longitudinal tomography), one can produce a two-dimensional representation (film) of a three-dimensional slice.

A process called axial, or transverse, tomography is depicted in Figure 14.5. The theory is essentially the same as in longitudinal tomography, but the slice (or abcd-plane) is in the transverse plane. A rotational rather than translational movement is used, with the patient and film being rotated in tandem as shown. These two procedures are an improvement over conventional x-rays, but still use x-ray film as the detector; therefore, these tomography techniques still depend much on the subjective determinations of exposure strength, time, and x-ray energy.

A new, more effective technique became possible with the advent of modern computers, with their processing power and speed. Instead of using film as the collection medium, computers were used to reconstruct images from information gathered by active detectors (scintillation or gas ionization). The process of computerized axial tomography (CAT), a transmission technique, began in 1972 when EMI Limited of England introduced the first CAT scanner. Perhaps no other medical device has received the publicity and rapid acceptance as the CAT scanner. Within 10 years, scanners used for both head and full body imaging have found homes in most every medical facility that could afford one.

The basic operating principles of the CAT scanner are diagrammed in Figure 14.6. A relatively high energy narrow x-ray beam (about 140 keV) is produced by an x-ray tube. This beam is scanned across the patient's body, and an opposing scintillation detector delivers information on tissue densities to a processing computer. The subject is rotated and a number of successive scans are taken. With this information, the computer reconstructs a transverse image of the slice in question using a series of image processing algorithms.

In the newer systems, the patient is placed between a twin set of x-ray emitters and an opposing pair of scintillation detectors. A scan is made in one direction at 160 separate points (80 for each detector) along the
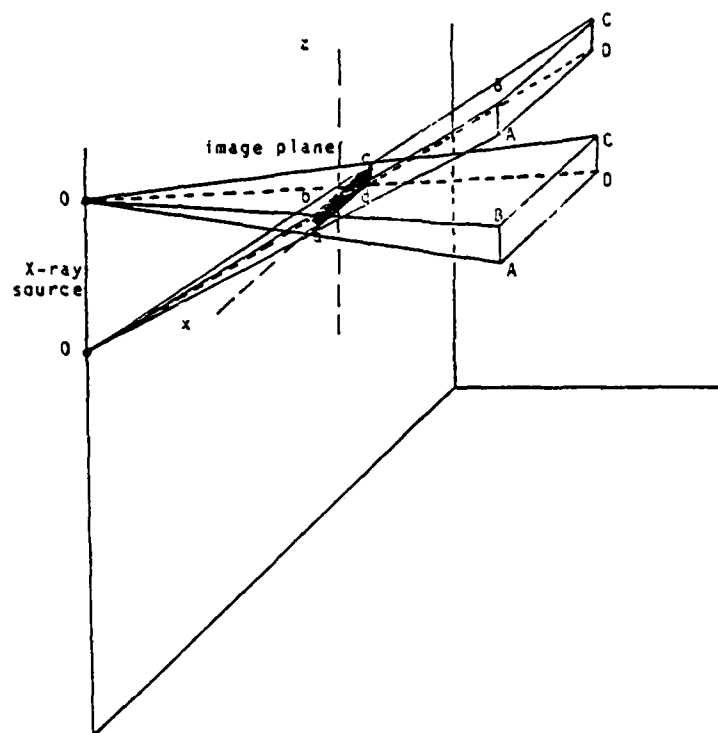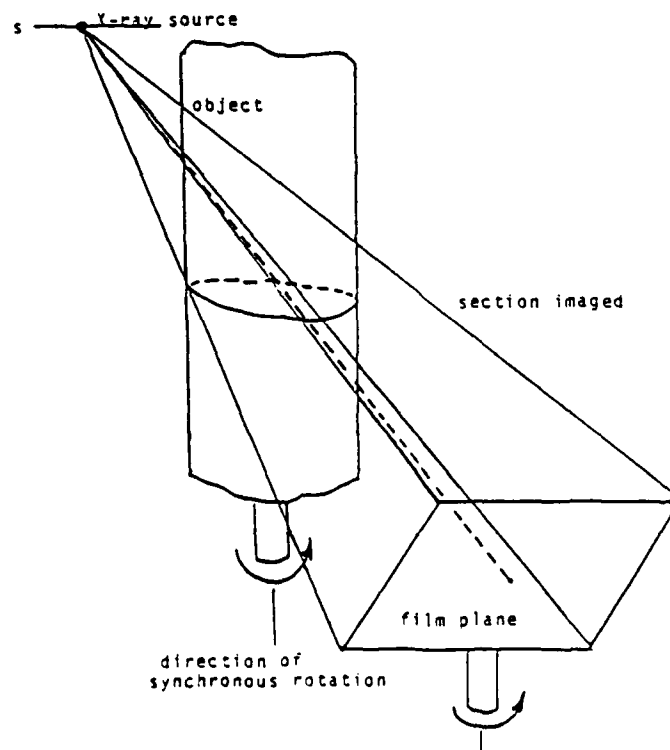
109

Figure 14.4. Longitudinal tomograph process.

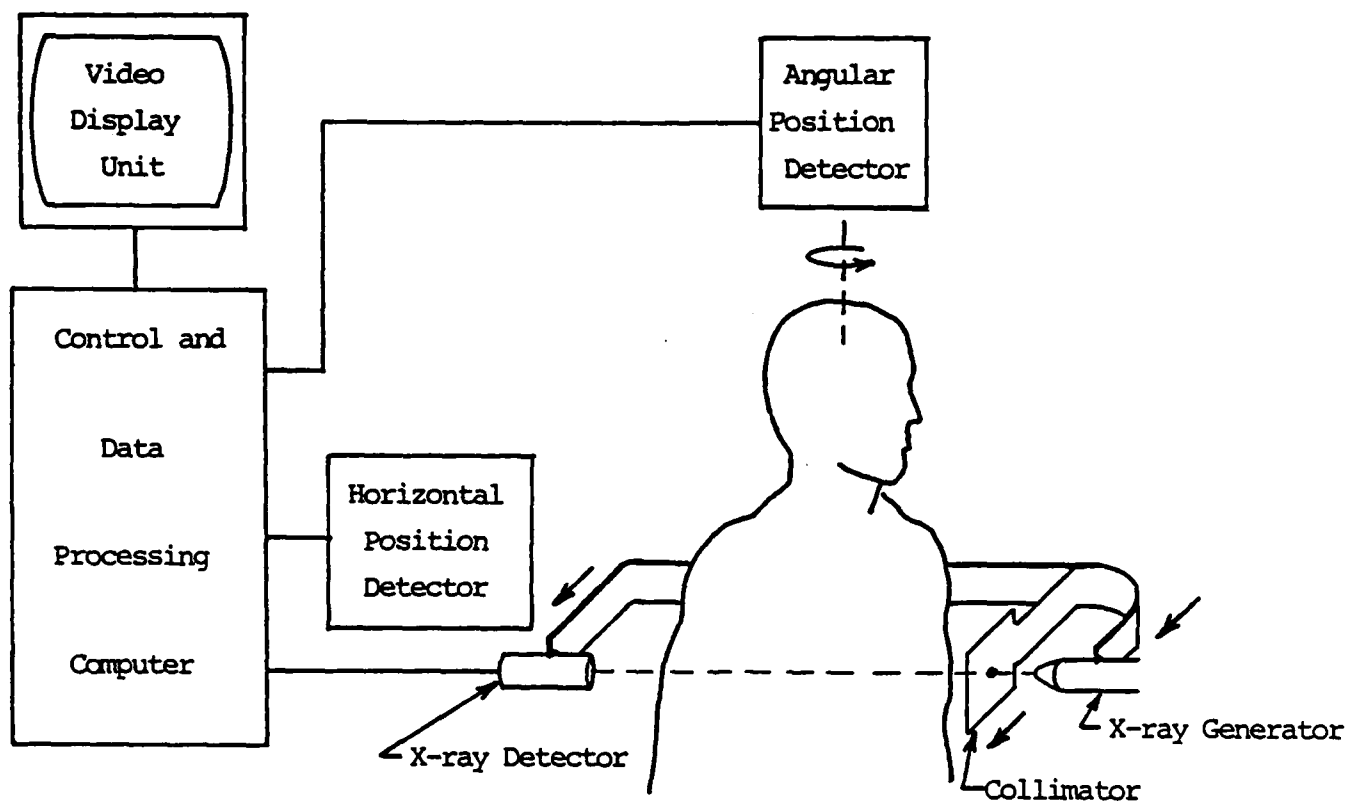Figure 14.5. Axial tomograph process.

Figure 14.6. Basic computerized axial tomography (CAT) scanner.

linear path. The entire system is then rotated 1° and another 160 point scan is taken. The process which takes about 4 min continues until a 180° rotation has been achieved. The computer analyzes the data received concerning densities in the slice and computes a reconstruction of the image. Output can be represented by a monochrome image (shades of grey corresponding to density), directly by numbers showing density, or by color coded images. Resolutions of 0.1% or better have been achieved on presently available systems.

One can understand why this technique was not practical until modern computers became available. A scan produces a 160 x 180 element image, or 28,800 pixels (picture elements). Processing arrays of this magnitude require great speed and storage capability, both of which have become available only recently. Images are computed by various algorithms such as the standard algebraic reconstruction technique (ART).

Many CAT scanners are now available from a number of manufacturers. While the general operational theory is the same for all of the scanners, differences in the gantry systems, radiation delivery and detection, reconstruction techniques, and display result in a wide range of performance.

The gantry is the motorized platform responsible for orienting and moving the emitter/detector pairs around the subject. Transmission and detection will vary depending on x-ray parameters and the type of detectors used. Computer operations controlling processing and display are very versatile and produce a variety of results.

A recently developed imaging system similar to a standard x-ray CAT scanner, at least in operaton, is the proton scanner developed at the Los Alamos Scientific Laboratory. Protons, and other heavy charged particles, deuterons, and tritons, interact with other atoms in a completely different manner than x-rays. X-ray detection in medical imaging is based on the difference between the quantity of x-rays entering a field and the quantity that exits the field (ΔN), where absorption and scattering account for the difference. The use of protons in medical imaging differs from that of x-rays by the fact that protons are charged whereas x-rays are not. In passage through matter, protons interact with many atoms losing a small amount of energy in each interaction, thus, a proton detector would measure the energy attenuation (ΔE) of the protons entering the field.

The advantages of this type of system are not readily apparent, especially if one considers the extremely high energy needed to accelerate the protons (about 200 MeV) compared to x-ray energies (about 100 keV). However, since essentially all the proton radiation passes through the field and can be processed (unlike x-rays), the radiation quantity is appreciably less than in x-ray systems, resulting in an overall improvement in dosage which is especially significant when the field (slice) is large. Several disadvantages do exist, however, which presently inhibit the widespread clinical use of this system. First, spatial resolution for most tissues is considerably less using proton scanning techniques (half as much), because of the small angular deflections caused by interactions with

the target atoms (Coulomb scattering). Also, this technique calls for the use of a charged-particle accelerator to produce the proton beam. At this time, such a dedicated accelerator costs about $7 million, a prohibitive amount considering the cost of about half a million dollars for a conventional CAT scanner. However, future advancements in accelerator design may reduce the cost to an affordable level, and proton scanners may then be considered a feasible addition to many medical institutions.

X-ray fluoroscopy is another transmission technique used extensively for medical imaging. A block diagram of a typical system is shown in Figure 14.7. Fluoroscopy is a technique used to visualize the dynamic activities of the body in vivo. X-rays are produced as in other procedures, but their energy is considerably lower due to an extensive exposure time needed for the real-time visualizaton. Since the x-rays are of very low intensity, a contrast medium is injected into the subject that allows the target organs to appear opaque to the x-rays. The detection system consists of a fluorescent crystal screen (scintillation type of detector) which gives a low intensity visualization of the real-time image, some type of image intensifier, and cameras to record and/or display the results. Presently, most systems use a video display and recording network that completely eliminates the use of photographic film. Transmission fluoroscopy is very useful in certain areas, such as visualizations of cardiac mechanics and joint function.

Nuclear medicine has come to be known as the study or practice of emission imaging. Basically, this differs from transmission imaging in that the source of radiation is internal and not directed; in other words, radiation is emitted from within the body, rather than transmitted through the body. The radiation, usually in the form of beta or gamma-rays, is detected and used to discriminate between normal or abnormal function of the large tissues.

Once a radionuclide is selected which will infiltrate the target area of the body and provide the necessary radiation (in decay) for detection, it is introduced into the body by injection, inhalation, or other means. A scintillation or a gas tube detector with photomultipliers is employed to pick up incident radiation emitted from the target area.

Two types of detection scanners are used in emission radiography. The system shown in Figure 14.8 is a rectilinear scanner imaging system. This type of system consists of a NaI crystal detector and a single photomultiplier tube together with a collimator as shown. The assembly is scanned across the field of interest in a rectilinear motion. Current pulses from the photomultiplier are amplified, discriminated, and recorded based on amplitude and quantity over time. A graph or contour map of radioactivity can then be drawn indicating the amount of radioactive isotope taken up by the target area. Compared to normals, improper amounts can indicate organ or circulatory malfunction.

The second type of scanner is a gamma camera or Anger camera. This device which acts as a stationary radiation detector consists of a large collimated NaI crystal and an array of photomultiplier tubes (usually 19
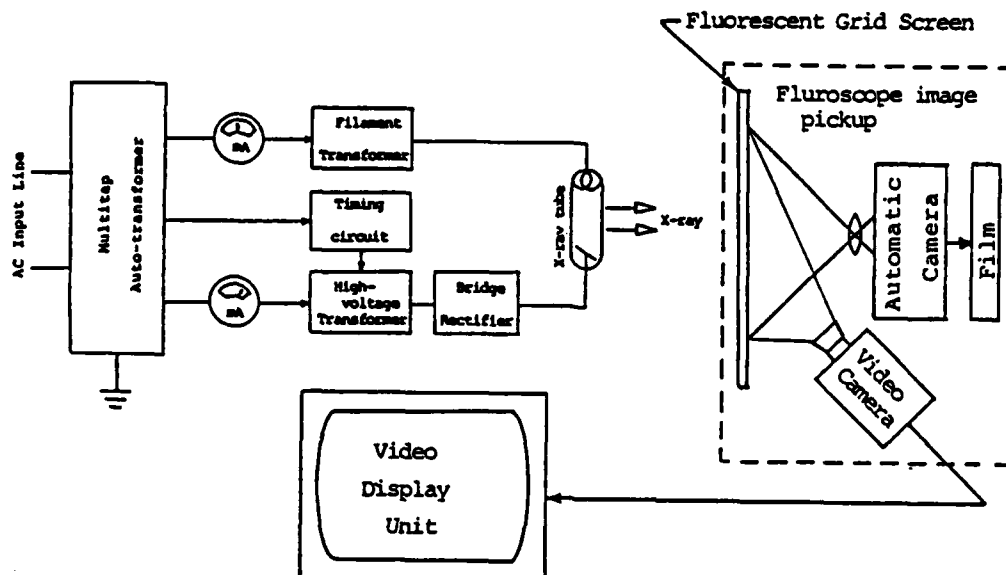
Figure 14.7.   Block diagram of an X-ray fluoroscopy imaging system.
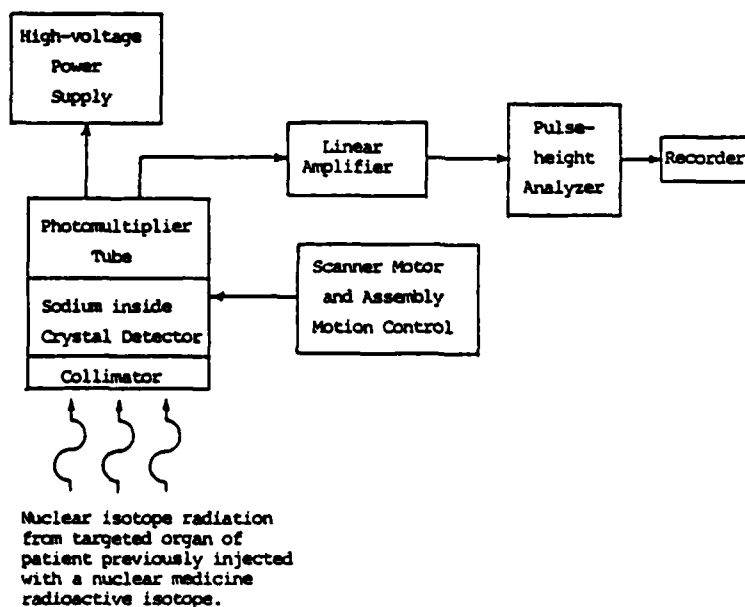

Figure 14.8.   Block diagram of a nuclear medicine, rectilinear-scanner, imaging
               system.

tubes) arranged symmetrically behind the crystal. Flashes caused by incident radiation are picked up by the tubes and a position analyzer determines the location of the source based on which tubes were activated. A pulse-height analyzer determines the validity and/or intensity of each flash, and together with position information an appropriate display is generated on an oscilloscope or similar media. This type of detector essentially acts as a simple radiation counter for relatively localized targets and static imaging.

A recently developed effective emission technique known as positron emission tomography, or PET scanning, is being used successfully in many medical institutions. The procedure differs from standard emission techniques in that positron emitting radionuclides are used as the radiation sources within the body. The use of these radionuclides offers several advantages over conventional emission techniques. First, positron annihilation detection results in high efficiency and high spatial resolution because of the absence of collimators. Since collimators usually absorb or block a large amount of radiation, their absence in PET scanning allows for a higher fraction of detected radiation which corresponds to greater efficiency and, subsequently, higher resolution. Second, because the total distance traveled by the two annihilation photons is constant for a given subject (body) thickness, their attenuation is independent of the source location when positioned between opposing detectors. This provides a more versatile imaging system which may aid in visualization of details of a radionuclide distribution. Finally, about half of all radionuclides are positron emitters, including the biologically useful elements ^{11}C, ^{13}N, and ^{15}O.

The positron emission techniques take advantage of a number of other imaging systems and have been proposed or developed using the same theoretical concepts described, but may vary in the process of radiation delivery, radiation collection, and/or data processing. These variations are too numerous to describe in any detail in this chapter.

In the near future, familiar processes of CAT scanning, fluoroscopy, and other transmission imaging procedures may be altered significantly by advances in accelerator technology or radiation physics. But present state-of-the-art techniques, such as those described in this chapter, will undoubtedly still be used in future hospital medical imaging systems. The use of imaging systems within a 2E level facility in a chemical defense application may be feasible at the present or near future, but not for the preliminary assessment of vital life signs in a field environment, i.e., away from a medical facility.

CHAPTER 15

DISCUSSION

In the event of hostile action in a toxic environment, military medical technicians need to identify and treat personnel exposed to toxic agents. A diagnostic instrument is required to assist technicians in performing preliminary triage. As a preface to the design of such a diagnostic device, this report reviewed current technologies which could be used to evaluate vital life signs of incapacitated military personnel. The development of a vital life signs detector must consider the limitations of personnel in a toxic environment, the greatest restriction being the protective garments which all personnel must wear and the need to avoid exposing incapacitated personnel to the contaminated environment. The garment is designed to encapsulate and prevent the outside toxic agent from reaching the service member, but, in addition, the garment also limits the accessibility to any body surfaces. Only the area of the throat underneath the protective hood, between the mask and jacket, can be exposed by lifting the front of the hood carefully. Ideally, the vital life signs detector should be noncontact, be noninvasive, and provide as many as possible of the physiological parameters required by emergency teams to assess the condition of incapacitated personnel. Noncontact implies that the measurement could be made from a standoff position without removing the protective garment. Noninvasive denotes that the measurement is taken inside the protective garment and in contact with the skin but not penetrating the epithelial layer of the epidermis. Invasive measurement techniques and systems were not included as part of this study.

Several noninvasive measurement systems and a few state-of-the-art noncontact technologies are available at the present time to assess vital signs, but their use may be restricted because of the stated special circumstances. Consequently, a quantitative methodology employing the concept of utility function seemed appropriate to assess the relative merits of the available methods or devices.

In obtaining a function, essential variables and their respective weights must be determined. In the utility function the variables are those factors necessary to evaluate by some figure of merit the most useful system or systems for vital life signs detection in a field environment. Hence, a limitation of the utility function analysis is that the outcome of the evaluation may not be the same for other applications, e.g., within the 2E level facility, in a medical evacuation aircraft, or a large well-equipped hospital. Another limitation is that the function is not unique, nor does it include all possible variables, e.g., maintainability, cost effectiveness, life-cycle costs.

A common sense approach was used in the selection of the factors. These include the need to evaluate the importance of what is being measured in the determination of vital life signs and how the measurement is obtained. Not as important is the need to evaluate how accurate the system may measure a vital sign, but how much exogenous noises may interfere with

the measurement. Physical size and power requirements were considered as necessary factors in the evaluation of any system considered for field use. The last two factors, skill and training, were included, because one of the constraints placed on the study by the U.S. Air Force contract representative was that the system must be used by young service personnel with little to no medical training. Hence, the various monitoring methods and instruments were evaluated on the basis of the following factors:

1. (10) method (noncontact, noninvasive, or invasive),
2. (10) usefulness of the measure to assessment of triage category or injury severity or physiological status,
3. (5) accuracy of measure,
4. (5) stability/repeatability of the measure,
5. (5) susceptibility to environmental noises or exogenous perturbations,
6. (5) weight/physical size,
7. (5) power requirement,
8. (5) skill level requirement to operate, and
9. (5) training requirement.

Factor Weights

Factor weights are the coefficients or multiplying factors by which the variables (factors) are multiplied. Magnitudes assigned to the factor weights are not unique. One method of obtaining the weights is to conduct a survey and have a large number of engineers or specialists in the area assign values based on some guides and criteria. Surveys require an extended period of time to collect and analyze. The alternative method is to survey a small sample which was the case in this study. A small sample may be tested against a population if the population were known. There is no guarantee that the results from a small sample will represent the results from the large sample. How dependable and reliable the final results of the study will be depends on how well the selection of factors and assignments of weights describe or represent the usefulness of the criteria for the specified conditions. As stated previously, a common sense approach was used to select the factors and assign an order of importance. All possible factors were not included, since evaluation of some factors from literature was not possible, e.g., maintainability, life-cycle cost, etc.

The next step is to select a scale for the factor weights. The scale from 5 to 0 in three discrete levels was selected to represent the most desirable (5), acceptable (3 or 2), or unacceptable (1 or 0). The scale was doubled for the most important factors, i.e., method and usefulness of measure. Thus, the factors were given weights based on their relative importance. The first factor, method, is weighted 10 points with the three following degrees and points:

1. Noncontact -- 10 points.
2. Noninvasive without media -- 5 points.
3. Noninvasive with media (i.e., gel) -- 0 point.

It is reasonable to assign a higher factor weight value to a system which could measure any of the primary vital signs at a distance from the subject without having to make contact with the subject than a system which could make the same measurement but would require skin contact. Noncontact, in this case, is external to the protective suit (without skin contact) which is most desirable. Whereas, a system which obtains the measurement noninvasively (doesn't penetrate the skin) without requiring a medium is acceptable, any system which requires a medium to obtain the measurement is not acceptable, since the medium may be susceptible to chemical contamination.

The second factor, usefulness of the measure, has three degrees for which 10 points are assigned to the measures of primary vital signs as discussed in chapter 2, i.e., respiration, cardiac (ECG), heart rate, and blood pressure. Five points are assigned to those measures which are not primary vital signs but may contribute to assessment of triage category, i.e., temperature, blood flow, heart sounds. Those measures which are not in the above two categories are assessed 1 point, i.e., electroencephalograph (EEG), volume measures, images. (Dynamic images of heart or respiratory function or mathematically processed images can provide heart rate, ejection fraction, respiratory rate, etc.)

The next set of factors, accuracy and repeatability, are system measurements. Accuracy is defined as deviation of the measurement from the true value. Accuracy is normally expressed in percent by the following expression:

$$\% \text{ accuracy} = \frac{\text{Actual measurement} - \text{True value}}{\text{True value}} \times 100\% \qquad (15.1)$$

The third factor, accuracy, is weighted 5 points and the 3° of accuracy are:

    (a) 5% or better -- 5 points,
    (b) between 5 and 10% -- 3 points, and
    (c) greater than 10% -- 1 point.

The fourth factor, stability/repeatability, is weighted 5 points with three degrees. System is stable if the output value remains within 5% of its proportional constant input value and is repeatable within 5% of previous measures, 5 points are assessed. Three points are assessed if the system is between 5% and 10%. If the measurement is not repeatable, then 0 point is given.

The fifth factor, susceptibility to exogenous noises, is weighted 5 points with three degrees. If the signal is not susceptible to external noises and the measure may be obtained with good signal-to-noise ratio, 5 points are assigned. Systems susceptible to noises which reduced the signal-to-noise ratio by a factor of two are assessed 2 points. Systems where the measure cannot be obtained without averaging techniques because of signal-to-noise ratios less than one are assessed 0 point.

The next two factors, weight and power requirement, are constrained for systems which are to be used prior to reaching a 2E level facility. The system must be carried by one man in a field environment where 120V 60 Hz outlets are not readily available. The sixth factor, weight of the system, is weighted 5 points with three degrees. Portable systems weighing less than 15 lb including power source are assessed 5 points. Portable systems weighing less than 25 lb without power source are assessed 2 points. Systems over 35 lb are not considered easily portable in a field environment; therefore, they are assessed zero point. The seventh factor, power required by the system, also is weighted 5 points with three degrees. Self-contained battery power packs weighing under 10 lb are assessed 5 points. Units requiring 110V single phase and less than 1 kVA of power are assessed 2 points. Systems requiring 110V or 220V three-phase or more than 1 kVA of power are given 0 point.

As stated earlier in this chapter, the last two factors, skill and training, are constraints imposed on the measurement system, i.e., the system is to be used by personnel with little or no medical training. The two factors, skill level and training requirement, each are assessed 5 points with three degrees as follows:

        (a) little to none -- 5 points,
        (b) some to moderate -- 2 points, and
        (c) high to extensive -- 0 point.

Evaluation of Dry Electrodes

In evaluating candidate systems the relative merit and/or utility value of each system is calculated from consideration of all factors in the model:

$$Y_n = \Sigma a_{ij} x_i \qquad\qquad\qquad (15.2)$$

where: x_i is the ith factor,
       a_{ij} is the weight of the ith factor
          with j degrees, and
       Y_n is the utility value of the nth system.

Since the factors are descriptors, the $a_{ij} x_i$ is not a product, but rather a designation of points which are summed to yield a utility value. For example, in the examination of a dry active electrode system to measure the electrocardiac signal or heart rate, the utility value is the sum of the following factor points: method (x_1) is assessed 5 points because skin contact is required without gel. Ten points are given for usefulness (x_2), since ECG/heart rate are considered a primary vital life sign. Accuracy (x_3) and repeatability (x_4) of the measures are assessed 5 points each, because most systems are well within 3%. Dry electrodes are moderately susceptible (x_5) to electric field perturbations but usually not enough to mask the large ECG signal when measured across the chest. This may not be the case when the measurement is taken at the throat where the ECG signal appears to be attenuated by a factor of at least 100. Two points are

120

assessed to the factor susceptibility to noise (x_5), although this is not supported by experimental results. With the current micro-electronic technology, a low power consumption, light-weight, analog and digital hybrid system could be fabricated. Thus, weight (x_6) and power (x_7) requirements are each assessed 5 points. Since little skill (x_8) or training (x_9) would be required to obtain the heart rate measurement in a field environment, both factors are assessed 5 points. The equation for utility value of dry electrodes systems becomes:

$$Y_{\text{dry electrode/HR}} = 5x_1 + 10x_2 + 5x_3 + 5x_4 + 2x_5 + 5x_6 +$$

$$5x_7 + 5x_8 + 5x_9 \qquad (15.3)$$

$$= 47 \text{ points.}$$

A system which uses dry active electrodes and amplifiers to obtain ECG signal does not require new technology involving high risks, but there is a risk in trying to obtain the electrical signals of the heart from the area of the throat. The risk is moderate and could be reduced when more research is done. Therefore, development in this area should be supported with full research funding.

Wet Electrode System

A system of wet electrodes (requires conductive gel as media for ionization) with amplifiers to obtain the ECG signal is evaluated as a control value for the utility. The resulting value is:

$$Y_{\text{wet electrode/HR}} = 0x_1 + 10x_2 + 5x_3 + 5x_4 + 2x_5 + 5x_6 +$$

$$5x_7 + 2x_8 + 2x_9 \qquad (15.4)$$

$$= 36 \text{ points.}$$

The factors x_1 (method), x_8 (skill level), and x_9 (training requirement) are reduced for the following reasons. The method (x_1) requires a gel which is not desirable because of the susceptibility to toxic contamination and increased risk to personnel. Zero point is assessed for method. Since skin preparation and electrode contact requirements are more stringent for good signals with low impedance amplifiers, greater training and skill level are required. Two points are assessed to each factor, x_8 and x_9.

Impedance Measurement System

Systems typified by the Minnesota Impedance Cardiograph require electrode contact with the skin. Most systems use a tape electrode without gel, although some systems use four disk electrodes with gel. Five points are assessed for the factor, method (x_1). Usefulness of the measure, x_2, is given 5 points, since cardiac output or stroke volume are not primary vital life signs. The accuracy of cardiac output or blood volume

121

measurements by impedance method generally exceeds 10%; therefore, 1 point is assessed for accuracy (x_3). Reproducibility of cardiac output by impedance measurement is better than by dye dilution method, thus 5 points are given for reproducibility of the measure (x_4). The impedance measurement is moderately susceptible to noise, so 2 points are assessed for factor x_5. These systems are small and portable so weight (x_6) is assessed 5 points. Two points are given to the power requirement factor (x_7), because these systems require 110V AC source. The impedance method requires a high level of skill and training; thus no points are assessed factors x_8 and x_9. In summary, the utility value of the impedance method is:

$$Y_{impedance} = 5x_1 + 5x_2 + 1x_3 + 5x_4 + 2x_5 + 5x_6 +$$

$$2x_7 + 0x_8 + 0x_9 \qquad (15.5)$$

$$= 27 \text{ points.}$$

Electric Field Measurement System

Time-varying signals of the extracorporeal electric field similar in form and shape to direct ballisto-cardiogram measurements were obtained by Keefe et al. [1] with whip antennas about 12 in. (30.48 cm) from the body. The electric field signals reflected both respiratory and cardiac activity from subjects in the supine position. This system provides a noncontact method of possibly assessing two primary vital life signs; therefore, factor x_1 (method) is given 10 points and factor x_2 (usefulness of measure) is given 10 points. Exactly how respiratory information may be separated from the cardiac information should be a subject for future study. Since neither accuracy of the system (x_3) nor repeatability (x_4) is discussed in any of the articles, 1 point is assessed to each factor.

An electric field is a vector which may be defined as the electric force on a charge divided by the size of the charge. By Coulomb's Law for a point charge q, the equation is expressed as:

$$\vec{E} = q\vec{r}/(4\pi\epsilon_0 r^2) \qquad (15.6)$$

where $\vec{r}$ is the unit vector from the charge to the point of interest, q is the charge in coulombs, and ϵ_0 is the permeability of free space. In summary, the electric field vector is a function of charge and distance, hence, other exogenous electric fields will result in system noise. Without shielding from other electric fields or a differential mode of signal acquisition the system would be very susceptible to noise; therefore, 0 point is assessed to factor x_5, susceptibility to noise. A bioelectric field measurement system can be fabricated as a small portable battery-operated system; therefore weight, x_6, and power, x_7, factors are each assessed 5 points. Skill level, x_8, and training, x_9, required to operate the system could be minimal, thus, 5 points are assigned to each factor. The total utility value of the bioelectric field measuring device is:

$$Y_{electc\ field} = 10x_1 + 10x_2 + 1x_3 + 1x_4 + 0x_5 + 5x_6 +$$

$$5x_7 + 5x_8 + 5x_9 \qquad\qquad (15.7)$$

$$= 42 \text{ points.}$$

Electromechanical Measurements -- Sounds

The use of microphones to detect sounds from the body, i.e., respiratory and cardiac, is a noninvasive method of obtaining two primary vital signs. Ten points are assessed to each of the factors, method (x_1) and usefulnes (x_2). Five points are assessed to all other factors with the exception of the factor x_5, susceptibility to environmental noises. The rationale is that the measures of respiratory and cardiac sounds are repeatable and most accurate in terms of frequency content of the signals when measured at the trachea. The electronic stethoscope uses miniature batteries and weighs less than 1 lb. Very little training and skills are required to use the stethoscope; however, noisy environments as in emergency rooms, will adversely affect the signal-to-noise ratio. Two points are assessed to factor x_5. The total utility value of the electronic stethoscope is:

$$Y_{stethoscope} = 10x_1 + 10x_2 + 5x_3 + 5x_4 + 2x_5 + 5x_6 +$$

$$5x_7 + 5x_8 + 5x_9 \qquad\qquad (15.8)$$

$$= 52 \text{ points.}$$

Ultrasonic Measurements

Ultrasound is a very attractive diagnostic tool in a clinical environment, but in a field environment good coupling and aiming cannot be achieved without a gel media and an examiner with the greatest degree of skill and experience in ultrasonic techniques. This results in assessment of 0 point for the factor, method (x_1), because a gel media is required. Five points are assessed to usefulness of the measures (x_2) blood flow, cardiac output, and stroke volume, since the measures are not primary vital signs used in triage categorization. Literature indicates that a very skilled and experienced technician can achieve about 5% accuracy, but most technicians are not highly experienced. An acceptable accuracy may be obtained by the average technician in ideal clinical or laboratory conditions. Therefore, 3 points are assessed to the factor, accuracy (x_3), for ultrasonic systems. The repeatability of the measurement (x_4) is assessed 5 points because the same technician repeating the measure can obtain repeatable results. The susceptibility to noise factor (x_5) is assessed 3 points because the system is susceptible to exogenous ultrasonic interference. Five points are assessed to the factor weight (x_6), since most ultrasonic systems are portable. The factor, power requirements (x_7), is assessed 2 points, since commercially available hospital ultrasonic systems use 110V AC power source. However, the system could be made

123

battery operated. The last two factors, skill level (x_8) to operate the ultrasonic system and the training required (x_9), are assessed 0 point because high skill level, extensive training, and experience are needed to obtain good accuracy and repetition in the measure. The total utility value for an ultrasonic system is:

$$Y_{ultrasonic} = 0x_1 + 5x_2 + 3x_3 + 5x_4 + 2x_5 + 5x_6 +$$

$$2x_7 + 0x_8 + 0x_9 \qquad (15.9)$$

$$= 22 \text{ points.}$$

Noninvasive Blood Pressure Measurements

The measurement of arterial blood pressure is an important vital sign, but with the constraints of maintaining the integrity of a protective garment this measurement becomes difficult. Evaluations of a standard sphygmomanometer and stethoscope or automated blood pressure measuring systems result in the following point assessment to the utility factors. Method (x_1) is assessed 5 points if the measurement could be taken; however, blood pressure measurements are not made through clothing. The bladder/cuff must be placed correctly to cover 80% of the circumference of the limb being used for the measurement. The stethoscope must be placed on the skin over the brachial artery. Clothing would attenuate the Korotkoff sounds. Usefulness of the measure (x_2) is given 10 points. Accuracy (x_3) and repeatability (x_4) are assessed 3 points each, even though the accuracy of the method is unacceptable in patients with abnormal blood pressure ranges as a result of shock. Experience has shown that the system is very susceptible to environmental noise as in an emergency room; therefore, 2 points are assessed to factor x_5. The system is portable with minimal power, so factors x_6, weight and x_7, power requirement are assessed 5 points. Training and skill level required to obtain accurate blood pressure readings are moderate, thus 2 points are given to factors x_8 and x_9. The total utility value for a sphygmomanometer/stethoscope unit to measure blood pressure by indirect auscultatory method is

$$Y_{BP} = 5x_1 + 10x_2 + 3x_3 + 3x_4 + 2x_5 + 5x_6 +$$

$$5x_7 + 2x_8 + 2x_9 \qquad (15.10)$$

$$= 37 \text{ points.}$$

With the restriction of exposing only a small area of the throat, blood pressure measurement by auscultatory method is not possible without modification of the protective garment; therefore, this method will not be included in the results.

Electromagnetic Infrared Measurement Systems

The electromagnetic radiations from the body in the infrared (IR) spectrum of light may be used to assess blood volume, blood pulse, and skin temperature. Evaluation of IR systems results in the following utility point assessment. Infrared photoplethysmography is a passive, noninvasive method of measuring a subject's relative blood volume change; therefore, the factors method (x_1) and usefulness (x_2) are assessed 5 points each. Accuracy (x_3) and repeatability (x_4) are given 3 points, since the area of the trachea increases difficulty of obtaining a good reliable measure. Photoplethysmography is susceptible to ambient background lighting; therefore, 2 points are assessed to factor x_5. Most photoplethysmographs are lightweight and can be powered with a battery, thus the factors weight, x_6, and power requirement, x_7, are given 5 points. The skill level to obtain measurements from the finger or the ear is minimal, but measurements at the trachea may require as much skill and training as an ultrasonic system. Thus, a mean value is selected for the factors skill (x_8) and training (x_9) which are assessed 2 points each. The total utility value of the IR measurement system is:

$$Y_{IR} = 5x_1 + 5x_2 + 3x_3 + 3x_4 + 2x_5 + 5x_6 +$$

$$5x_7 + 2x_8 + 2x_9 \qquad\qquad (15.11)$$

$$= 32 \text{ points.}$$

Microwave Measurement System

Microwave systems to measure electromagnetic radiations from the body are relatively new and still under study. Microwave measurements from the body are passive, noninvasive, and noncontact; therefore, 10 points are assessed for method (x_1). Because microwave systems are still being studied for various applications, only its usefulness in terms of core temperature measurement is considered as a useful secondary vital sign. Five points are assessed to usefulness (x_2). Accuracy of measurement (x_3) and repeatability (x_4) appear to suffer from emissivity mismatch between specimen under test and receiving antenna; therefore, 3 points are given to these factors. Susceptibility to external microwave or EMI noises is sufficient to decrease the signal-to-noise ratio below 1.0. To improve the signal-to-noise ratio elaborate, sophisticated, and costly ($15,000) receiving units must be used; therefore, factor x_5, susceptibility to noise, is given 0 point. Since the units can be fabricated so that they are portable, but may weigh over 15 lb and use 110V AC source, 2 points are assessed to each factor, x_6, weight, and x_7, power requirement. A high skill level and extensive training will be required for operation of a microwave system; therefore, the factors x_8 and x_9 are given 0 point. The total utility value of a microwave system to measure core temperature of the body is:

$$Y_{MN} = 10x_1 + 5x_2 + 3x_3 + 3x_4 + 0x_5 + 2x_6 +$$

$$2x_7 + 0x_8 + 0x_9 \qquad\qquad (15.12)$$

$$= 25 \text{ points.}$$

Magnetic Field Measurement Systems

Fabrication of the first Superconducting Quantum Interference Device (SQUID) in the 1970s spurred research in biomagnetic field measurements. The SQUID is the result of high-technology development in the fields of cryogenics and superconducting physics. The SQUID can measure the biomagnetic fields through clothing at a distance of several inches from the body; therefore, 10 points are assessed to the first factor, method (x_1). Magnetocardiograms were recorded by Barbanera et al. [2] from patients in an unshielded, normally noisy environment. Cardiac information, as well as rate measurements, may be obtained with a second derivative gradiometer coil configured SQUID. Ten points are given for usefulness of the measure, x_2. The SQUID may also be used to detect central nervous system (CNS) activity, i.e., magnetoencephalograms or magnetoevoked responses to visual or auditory stimuli. The accuracy (x_3) and repeatability (x_4) are similar to conventional electrical (electrode) systems; therefore, factors x_3 and x_4 are given 5 points each. The major problem with the magnetic measurements is that the signal-to-noise ratio is low and at times it may become difficult to distinguish the very low-level biomagnetic signal (magnetoencephalogram) from the surrounding environmental magnetic noise level. This may have been more of a problem before the 2nd derivative gradiometer coil configuration and before the DC SQUID. With these considerations in coil configuration, 2 points are assessed to factor x_5, susceptibility to noise. The sizes of SQUID magnetometers in use to date are very large and not portable, but a miniaturized state-of-the-art SQUID could be developed to be between 6 in. (15.24 cm) and 12 in. (30.48 cm) long, about 1 in. (2.54 cm) in diameter, self-contained with its own cyrogenic pump, and portable. This latest technological miniaturization of the SQUID system should be funded and feasibility studies started as early as possible into vital life signs detection, and other clinical or screening applications. The factor weight (x_6) is given 0 point even though the future looks very promising. Current systems use 110V AC source, so 2 points are assessed for power requirement (x_7). Future DC SQUID systems can be made battery operated. Skill level and training to operate the SQUID correctly should be moderate to minimal; therefore, each factor is given 2 points. Newer designs of the SQUID magnetometer will require little supporting hardware or maintenance, will be portable, and easy to use. The total utility value of a present day SQUID magnetometer is:

$$Y_{MCG(SQUID)} = 10x_1 + 10x_2 + 5x_3 + 5x_4 + 2x_5 + 0x_6 +$$

$$2x_7 + 2x_8 + 2x_9 \qquad\qquad (15.13)$$

$$= 38 \text{ points.}$$

The utility value of the future miniaturized 2nd derivative coil configured DC-SQUID gradiometer is:

$$Y_{DC-SQUID} = 10x_1 + 10x_2 + 5x_3 + 5x_4 + 5x_5 + 5x_6 +$$

$$5x_7 + 5x_8 + 5x_9 \qquad (15.14)$$

$$= 55 \text{ points.}$$

As impressive as this appears, however, it is a high-risk, high-technology, and high-cost system.

Nuclear Magnetic Resonance Measurement Systems

Nuclear magnetic resonance (NMR) devices have been used for blood flow measurements, but unlike the SQUID magnetometer a magnetizing coil must be used to align the spin axis of molecules. Evaluation of the NMR method and system to measure blood flow resulted in the following point assessment to the utility factors. The factor, method (x_1), is assessed 10 points since the measure can be obtained through the protective garment (noncontact). Blood flow is by previous definition a secondary vital sign, so 5 points are assessed the factor, usefulness (x_2). Since accuracy of blood flow by NMR method is acceptable (about 5%), 3 points are assessed the factor, accuracy (x_3). Likewise, the factor, repeatability (x_4), is acceptable, so 3 points are assessed. The amount of susceptibility to external fields is not described in the literature, but some may be expected. Therefore, a neutral position of acceptable is taken in assessment of 2 points to the factor, susceptibility (x_5). The systems described in the literature are not portable so the weight factor (x_6) is assessed 2 points. Zero point is assessed the factor, power requirement (x_7), since these systems usually require more than 1 kVA. The last two factors, skill level (x_8) and training requirement (x_9), are each assessed 0 point, since high skill level and extensive training are required to use the system with any accuracy. The utility value for a nuclear magnetic system to measure blood flow is:

$$Y_{NMR} = 10x_1 + 5x_2 + 3x_3 + 3x_4 + 2x_5 + 2x_6 +$$

$$0x_7 + 0x_8 + 0x_9 \qquad (15.15)$$

$$= 25 \text{ points.}$$

Imaging Systems

Imaging systems in general are very large systems requiring a large high-speed computer. The most common imaging system in use today is the X-ray film. In terms of vital life signs detection in a field environment, imaging systems have a low utility value. Most imaging systems are noncontact, although in nuclear medicine a radioactive material is usually injected into the bloodstream. Nevertheless, 10 points are assessed for

method (x_1). Usefulness (x_2) of images of vital life signs detection is
given 1 point. Imaging systems in general do not have a good resolution;
therefore, 3 points are assessed to the factors accuracy (x_3) and
repeatability (x_4). Two points are given for factor x_5, susceptibility to
noise, because the various systems have different signal-to-noise ratios.
Weight (x_6), power requirement (x_7), skill level (x_8), and training
requirements (x_9) are all assessed 0 point because most imaging systems are
large. A patient is usually placed within the field between emitter system
and sensor detection (receiving) system. Power requirement is large since
large amounts of energy are used by the emitter, receivers, and large high-
speed computer with array processors. Without a doubt, imaging systems are
the latest state-of-the-art technology in medicine which requires extensive
training in a computerized system. Similarly, the skill level requirement
may be greater than the skill level required of an X-ray technician. The
total utility value of current imaging systems for vital life signs
detection in a field environment is:

$$Y_{Imaging} = 10x_1 + 1x_2 + 3x_3 + 3x_4 + 2x_5 + 0x_6 +$$

$$0x_7 + 0x_8 + 0x_9 \qquad\qquad (15.16)$$

$$= 19 \text{ points.}$$

As rapidly as this area is growing, imaging systems of the future may be
altered significantly by advances in accelerator technology, radiation
physics, or solid state technology; therefore, the area of imaging should
be reviewed on a periodic basis.

Final results of the utility values of off-the-shelf and state-of-the-
art systems to obtain relative measures of vital life signs for field
determination of triage are given in Table 15.1. From the total value
points column, the most desirable systems to employ for a vital life signs
detector are: (a) electromechanical (phonographic) for respiratory and
cardiac action indications, (b) dry electrodes and preamplifiers for
electrocardiographic (ECG) signals, (c) bioelectric field device for
ballistographic indications of respiratory and cardiac activity, (d)
biomagnetic field device (SQUID) for magnetocardiographs (MCG) signals, and
(e) electromagnetic infrared detection systems for relative arterial pulse
and/or skin temperature measurements. The auscultatory method of blood
pressure measurement requires inflating a bladder around a part of the body
to occlude an artery. This measurement is not possible with current
protective garments unless the garments are modified to include a
bladder/piezoelectric detector; therefore, the utility value is not
acceptable, and the system is not recommended.

The most promising system may be a combination of an electronic
stethoscope (electromechanical phonogram) and dry electrode system. An
infrared detector may be added to the system, but its usefulness and
reliability may be questionable.

TABLE 15.1. RESULTS OF UTILITY FUNCTION EVALUATION

Measurement systems	Method x_1	Useful-ness x_2	Accuracy x_3	Repeat-ability x_4	Suscepti-bility to noise x_5	Weight x_6	Power x_7	Skill level x_8	Training requirement x_9	Total value point
1. Electrodes										
a. Dry	5	10	5	5	2	5	5	5	5	47
b. Wet	0	10	5	5	2	5	5	2	2	36
2. Impedance	5	5	1	5	2	5	2	0	0	27
3. Electric fields	10	10	1	1	0	5	5	5	5	42
4. Electro mechanical	10	10	5	5	2	5	5	5	5	53
5. Ultra-sonics	0	5	3	5	2	5	2	0	0	22
6. Auscultatory	5	10	3	3	2	5	5	2	2	37
7. Electomagnetics										
a. Infrared	5	5	3	3	2	5	5	2	2	32
b. Microwaves	10	5	3	3	0	2	2	0	0	25
8. Magnetic fields	10	10	5	5	2	0	2	2	2	38
9. Nuclear magnetic	10	5	3	3	2	2	0	0	0	25
10. Imaging	10	1	3	3	2	0	0	0	0	19

129

References

1. Keefe, J. F., L. T. Rauterkus, M. J. Wolk, D. H. Brand, and H. J. Levine. Electrostatic Ballistogram: Analysis of Electrical Fields about the Human Body. *J Appl Physiol* 28:89-91 (1970).

2. Barbanera, S., P. Carelli, R. Leoni, and G. L. Romani. Biomagnetic Measurements in Unshielded, Normally Noisy Environments, pp. 139-149. *In* Biomagnetism. Erné, S. N., H. D. Hahlbohm, and H. Lübbig (Ed.). Berlin-New York: Walter de Gruyter and Co. (1981).

CHAPTER 16

CONCLUSIONS AND RECOMMENDATIONS

The main purpose of this study was to evaluate current literature on noninvasive methods and instruments in order to provide recommendations on direction of technical development which could lead to a system or device for measuring vital life signs of incapacitated military personnel in a toxic field environment. Specifically, the first aim of the study was to determine the set of physiological parameters most likely to provide the vital signs necessary to assess the seriousness of a casualty. This method involves the concept of triage categorization of casualties according to a priority for further assessment and treatment. A survey of patients encompasses: (a) establishment of adequate airway; (b) checking the patient's breathing pattern; and (c) checking for presence of pulse, for heart rate, and relative pulse pressure strength. The physiological measures considered primary vital life signs during an emergency assessment in order of priority are: (1) respiration rate or respiratory sounds, (2) heart rate from the raw cardiac (ECG) signal or heart sounds, (3) blood pressure, and (4) core temperature. Responsiveness is not a physiological measure obtained with an instrument, so it was not considered.

The second specific aim of the study was to evaluate current noninvasive techniques and systems which could perform desired life signs detection in a field environment without violating the integrity of the protective garment. Table 15.1 in Chapter 15 summarizes the results of this evaluation. The most promising methods/systems in order of utility ranking are:

   (a) an electromechanical device such as an electronic stethoscope to
       measure respiratory and cardiac sounds;

   (b) a dry electrode/bioamplifier system to measure the electrocardiogrm
       (ECG);

   (c) an infrared device to measure arterial pulse and skin temperature;
       and

   (d) sphygmomanometer/stethoscope to measure blood pressure.

Since the area of the throat appears to be the only access to the body in a protective garment, a combination of electronic stethoscope plus dry electrodes may provide the essential information. A suggested breadboard system was fabricated and demonstrated. This system is described in a separate report, USAFSAM-TR-85-44-PT-2.

Infrared detection of the blood volume pulse can easily be obtained at the tip of the finger or ear lobes (which are inaccessible in a protective garment), but the application of infrared in the area of the throat to obtain carotid arterial blood pulse is very difficult and unreliable. Blood pressure measurement although highly desirable presents the problem

131

of inaccessibility of a limb to obtain the measurement. Only a bladder with pressure crystal built into the inner suit might result in reliable blood pressure measurements; therefore, this method is not recommended.

The last specific aim of the study was to recommend areas of technological development which may lead to the desired field system. The two most promising areas are given in order of payoff. Biomagnetic field measurements with a miniaturized, direct-current (DC), superconducting quantum interference device (SQUID) with a second derivative gradiometer coil configuration and a self contained cryogenic pump system offer the most advanced high-technology area for noncontact, through the protective garment measurements of the magnetocardiogram and possibly, magnetoencephalogram evoked responses from visual or auditory stimulations. Development of this system is considered the highest risk with highest payoff results.

The second new technology area is in the area of bioelectric field measurements with sensing antennas to measure variation in the electric field resulting from what appears to be body mechanical movement, e.g., respiration and cardiac, of the charged body surface. This technique is lower risk with lower payoff in utility results.

It is recommended that both of these technological areas be supported. The biomagnetic field area will cost considerably more than the bioelectric field area because of the high technology.

BIBLIOGRAPHY

Aaslid, R., and A. Brubakk. Accuracy of an ultrasound doppler servo method for noninvasive determination of instantaneous and mean arterial blood. *Circulation* 64:753-759 (1981).

Abernathy, M. R., J. A. Ronan, and D. T. Winsor. Diagnosis of coarctation of the aorta by infrared thermography. *Am Heart J* 82:731-741 (1971).

Alexander, H., M. L. Cohen, and L. Steinfeld. Criteria in the choice of an occluding cuff for the indirect measurement of blood pressure. *Med Biol Eng & Comput* 15:2-10 (1977).

Anderson, D. Z., M. O. Scully, and W. C. Speed. A new noninvasive technique for cardiac pressure measurement II: Scattering from encapsulated bubbles. *SPIE Seminar Proc* 167:121-127 (1978).

Anderson, M. Nuclear magnetic resonance imaging and neurology. *J Br Med* 284:1359-1360 (1982).

Anderson, R. E., A. G. Waltz, T. Yamaguchi, and R. D. Ostrom. Assessment of Cerebral Circulation (Cortical Blood Flow) with an Infrared Microscope. *Stroke* 1:100-103 (1970).

Aronen, H. J., H. T. Suoranta, and M. J. Taavitsainen. Thermography in deep venous thrombosis of the leg. *Am J Rad* 137:1179-1182 (1981).

Arthur, R. M., and D. B. Geselowitz. Effect of inhomogeneities on the apparent location and magnitude of a cardiac current dipole source. *IEEE Trans Biomed Eng* BME-17(2):141-146 (1970).

Baggs, J. W., and R. L. Amor. Thermographic screening for breast cancer in a gynecologic practice. *Ob & Gyn* 54:156-162 (1979).

Baker, L. E., T. W. Coulter, and J. D. Bourland. Simple versatile instrument for measuring impedance changes accompanying physiological events. *Med Biol Eng* 221-228 (1973).

Banaszak, E. F., R. C. Kory, and G. L. Snider. Phonopneumography. *Am Rev Respir Dis* 107:449-455 (1973).

Battocletti, J. H., R. E. Halbach, A. Sances, Jr., S. L. Larson, R. L. Bowman, and V. Kudravcev. Flat crossed-coil detector for blood flow measurement using nuclear magnetic resonance. *Med Biol Eng & Comput* 183-191 (1979).

Battocletti, J. H., R. E. Halbach, S. X. Salles-Cunha, and A. Sances. The NMR blood flowmeter-theory and history. *Med Phys* 8:435-443 (1981).

Battocletti, J. H., A. Sances, Jr., S. J. Larson, S. M. Evans, R. E.

Halbach, V. Kudravcev, and R. L. Bowman. A review of nuclear magnetic resonance techniques applied to biological systems, pp. 263-294. *In* Biological and Clinical Effects of Low Frequency Magnetic and Electric Field. Llaurado, J. G., A. Sances, Jr., and J. H. Battocletti (Eds.) Springfield: Charles C Thomas, Pub., 1974.

Bayevskiy, R. M., and I. I. Funtova. A contactless method for registering indices of the cardiovascular and respiratory systems. *Space Bio Med* 3:112-115 (1969).

Beyerl, D. Non-invasive measurement of blood oxygen levels. *Am J Med Tech* 48:355-359 (1982).

Borkat, F. R. Noninvasive monitoring of blood pressure—patient studies. *Proc San Diego Biomed Symp* 17:33-37 (1978).

Bronzino, J. D. Technology for Patient Care, pp. 103-155. Saint Louis: C. V. Mosby Co., 1977.

Brown, J. M., and J. J. Carr. Introduction to Biomedical Equipment Technology, pp. 367-384. New York: John Wiley & Sons, Inc. (1981).

Bunin, N. J., and R. G. Loudon. Lung sound terminology in case reports. *Chest* 76:690-692 (1979).

Cabot, R. C., and H. F. Dodge. Frequency characteristics of heart and lung sounds. *JAMA* 84:1793-1796 (1925).

Cacak, R. K., D. E. Winans, J. Edrich, and W. R. Hendee. Millimeter wavelength thermographic scanner. *Med Phys* 8:462-465 (1981).

Cameron, J. R., and J. G. Skofronick. Medical Physics, pp. 386-485. New York: John Wiley & Sons, Inc., 1978.

Carson, J., T. Rider, and D. Nash. A thermographic study of heat distribution during ultra-speed cavity preparation. *J Dent Res* 58:1681-1684 (1979).

Cegla, U. H. Some aspects of pneumosomography. *Prog Resp Res* 11:235-241 (1979).

Charbonneau, G., J. L. Racineux, M. Sudraud, and E. Tukchais. An accurate recording system and its use in respiratory sounds spectras analysis. *J Appl Physiol* 55:1120-1127 (1983).

Charbonneau, G., J. L. Racineux, M. Sudraud, and E. Tuchais. Digital processing techniques of respiratory sounds for objective assistance of asthma diagnosis. *IEEE CH1746-7* 736-738 (1982).

Chowdhury, S. K., and A. K. Majumder. Digital spectrum analysis of respiratory sound. *IEEE Trans Biomed Eng* 28:784-788 (1981).

Clark, R. P. Environmental physiology and thermography. *SPIE* 110:85-87 (1977).

Coleman, C. I. Effects of perturbing magnetic field on the performance of photoelectronic sensors. *Rev Sci Instrum* 53:735-748 (1982).

Colin, J., and J. Tiombal. Measurement of systolic timed intervals by electrical plethsmography--Validation with invasive and noninvasive methods. *Aviat Space Envir Med* 53:52-68 (1982).

Collins, A. J., and E. F. Ring. Measurement of inflammation in man and animals by radiometry. *Br J Pharmac* 44:145-152 (1972).

Cooper, J. A fast-response pyroelectric thermal detector. *J Sci Instrum* 39:197-202 (1962).

Cozen, H. J. Computer generated anesthesia record. *IEEE Symp Comput Appl Med Care 3rd Proc* 615-617 (1979).

Cromwell, L., E. A. Pfeiffer, and J. F. Weibell. Biomedical Instrumentation and Measurements, pp. 363-383. New Jersey: Prentice-Hall, Inc., 1980.

Cugell, D. W. Sounds of the lungs. *Chest* 73:311-312 (1978).

D'agrosa, L. S., and A. B. Hertzman. Opacity pulse of individual minute arteries. *J Appl Physiol* 23:613-620 (1967).

Day, J. L., and C. K. LaPinta. The evolution of long-term electrode systems for electrocardiography on manned space flight, pp. 351-375. *In* Biomedical Electrode Technology:Theory & Practice. Harry, A. M. (Ed.) New York: Academic Press, Inc., 1974.

Deland, F. H. Future direction of the specialty--Practical relevance to the clinical practice of nuclear medicine. *Clin Nucl Med* 6:131-135 (1981).

Demer, J. L., K. C. Mylrea, L. Adler, and W. R. Jewett. An esophageal multiprobe for temperature, electrocardiogram, and heart and respiratory sounds measurements. *IEEE Trans Biomed Eng* BME-25:377-382 (1978).

Deutsch, S., and W. Welkowitz. Biomedical Instruments:Theory and Design, pp. 189-207. New York: Academic Press, 1976.

Domizi, D. B., and R. H. Earle. On line pulmonary function analysis--program design. *Decus Proc* 19-22 (1970).

Dhupar, K. K., H. Baharestani, D. E. Bahr, and A. R. Kahn. A microprocessor-based ventricular function analyzer. *IEEE Frontiers Eng Health Care* 145-149 (1979).

Dosani, R., S. S. Kraman. Lung sound intensity variability in normal men. *Chest* 83:628-631 (1983).

Druzgalski, C. K., R. L. Donnerberg, and R. M. Campbell. Techniques of recording respiratory sounds. *J Clin Eng* 5:321-330 (1980).

Druzgalski, C. Breath sounds in pulmonary diagnosis. *IEEE Frontiers Eng Health Care* 383-383 (1981).

Earle, R. H., and P. H. Schlesinger. On line analysis of pulmonary function tests using a small digital computer (PDP-12). *Decus Proc* 23-28 (1970).

Engler, P. E., J. D. Cohn, and R. F. Thorsen. A non-invasive and non-contacting cardiopulmonary monitor. *30th ACEMB* 19:177 (1977).

Estrin, T., and R. Uzgalis. Computerized display of spatiotemporal EEG patterns. *IEEE Trans Biomed Eng* BME-16:192-196 (1969).

Fahr, G. The acoustics of the bronchial breath sounds. *Arch Int Med* 39:286-302 (1927).

Forgacs, P. The functional basis of pulmonary sounds. *Chest* 73:399-403 (1978).

Forgacs, P. Breath sounds. *Thorax* 26:288-295 (1971).

Forgacs, P. Lung sounds. *Brit J Dis Chest* 63:1-12 (1969).

Fraden, J., M. R. Neuman, and R. Rich. A dry electrode monitoring system. *IEEE Front Eng Health Care* 36-39 (1979).

Frazer, J. W., W. D. McDavid, and M. Millner. Diagnostic and therapeutic uses of radiofrequency fields. *Bull NY Acad Med* 55:1205-1215 (1979).

Funtova, I. Some problems in the method and technique of dielectrography. *Biomed Eng (USA)* 11:146-150 (1977).

Galbo, H., and P. E. Paulev. Cardiac function during rest and supine cycling examined with a new noninvasive technique (CED). *J Appl Physiol* 36:113-117 (1974).

Gavriely, N., Y. Palti, and G. Alroy,. Spectral characteristics of normal breath sounds. *J Appl Physiol* 50:307-314 (1981).

Geddes, L. A., L. E. Baker, and A. G. Moore. Optimum electrolytic chloriding of silver electrodes. *Med & Biol Eng* 7:49-56 (1969).

Ghista, D. N. Analyses for noninvasive monitoring of arterial blood pressure by (I) Phono-cuff-sphygmomanometry, for discrete measurements and (II) Arterial ultrasonic imaging, for continuous measurements. *SPIE Seminar Proc* 167:107-120 (1978).

Go, K. G. Physical methods for study of brain edema. *Advances Neurol* 28:1-8 (1980).

Grass, C., G. Marinone, G. C. Morandini, A. Pernice, and M. Puglisi. Normal and pathological respiratory sounds analyzed by means of a new phonopneumographic apparatus. *Respiration* 33:315-324 (1976).

Griffith, M. E., W. M. Portnoy, and L. J. Stotts. Improved capacitive electrocardiogram electrodes for burn applications. *Med Biol Eng & Comp* 17:641-646 (1979).

Gross, S., and N. Zumbulyadis. Use of high mixing frequencies for rf generation and detection in a multinuclear and cross-polarization magic-angle-spinning NMR spectrometer. *Rev Sci Instrum* 53:615-623 (1982).

Grossman, S. B., S. R. Hawkins, A. K. Gressle, R. P. Farley, and W. G. Opyd. Computer-aided facility for the rapid evaluation and optimization of IR image sensors. *SPIE* 225:109-115 (1980).

Grotberg, J. B., and S. H. Davis. Fluid-dynamic flapping of a collapsible channel--sound generation and flow limitation. *Biomechanics* 13:219-230 (1980).

Hackett, M. E. J., and H. P. Henderson. Infrared thermography in medicine. *SPIE* 110:74-77 (1977).

Halbach, R. E., J. H. Battocletti, S. X., Salles-Cunha, A. Sances, Jr. The NMR blood flowmeter--design. *Am Assoc Phys Med* 8:444-451 (1981).

Halbach, R. E., J. H. Battocletti, A. Sances, Jr., S. J. Larson, R. L. Bowman, V. Kudravcev. Blood flow detection using the flat crossed-coil nuclear magnetic resonance flowmeter. *IEEE Trans Biomed Eng* 28:40-42 (1981).

Hardin, J. C., J. L. Patterson, Jr. Monitoring the state of the human airways by analysis of respiratory sound. *Acta Astronautica* 6:1137-1151 (1979).

Hari, R., K. Kaila, T. Katila, T. Tuomisto, and T. Varpula. Interstimulus interval dependence of the auditory vertex response and its magnetic counterpart: implications for their neural generation. *Electroenceph & Clin Neurol* 54:561-569 (1982).

Hayes, C. E., T. A. Case, D. C. Ailion, A. H. Morris, A. Cutillo, C. W. Blackburn, C. H. Durney, and S. A. Johnson. Lung water quantitative by nuclear magnetic resonance imaging. *Science* 216:1313-1315 (1982).

Henahan, J. Thermography finds multitude of applications. *JAMA* 247:3296-3303 (1982).

Henderson, J. D. Solution of the quadrature field equations in the electromagnetic blood flowmeter. *Med & Biol Eng* 12:626-632 (1974).

Henderson, R. P., J. G. Webster, and D. K. Swanson. A thoracic electrical impedance camera, p. 322. *29th ACEMB* 1976.

Herman, G. T.(Ed.) Image Reconstruction from Projection, pp. 147-277. *In* Topics in Applied Physics. Herman, G. T.(Ed.) Berlin: Springer-Verlag, 1979.

Hill, D. W., and H. J. Lowe. The use of the electrical impedance technique for the monitoring of cardiac output and limb blood flow during anaesthesia. *Med & Biol Eng* 11:534-545 (1973).

Hine, G. J., and J. A. Sorenson. Instrumentation in Nuclear Medicine, pp. 2-383. New York: Academic Press, 1974.

Histand, M. B., R. A. Corace, and M. K. Wells. Ultrasound doppler and echo combined as a noninvasive blood flowmeter. *Biomed Sci Instrum* 17:73-78 (1981).

Hochberg, A. M. A Digital System for Low-dose Radiography. *In* Applications of Computers in Medicine. Schwartz, M. D.(Ed.) New York: IEEE Press 158-164 (1982).

Hocherman, S., and Y. Palti. Correlation between blood volume and opacity changes in the finger. *J Appl Physiol* 23:157-162 (1967).

Holen, J., S. Simonsen, and T. Froysaker. An ultrasound doppler technique for the noninvasive determination of the pressure gradient in the Bjork-Shiley mitral valve. *Circulation* 59:436-442 (1979).

Holloway, G. A. Jr., and D. Watkins. An electronic frequency shifting stethoscope for heart sounds. *J Bioeng* 2:59-64 (1978).

Hughes, J. R., J. Cohen, C. I. Mayman, M. L. Scholl, and D. E. Hendrix. Relationship of the magnetoencephalogram to abnormal activity in the electroencephalogram. *J Neurol* 217:79-93 (1977).

Jansen, B. H., J. R. Bourne, and J. W. Ward. Spectral decomposition of EEG intervals using Walsh and Fourier transforms. *IEEE 0018-9294* 6:837 (1981).

Jarvis, B. W., M. J. Nichols, T. E. Johnson, E. Alan, N. R. Hudson. A fundamental investigation of the composition of auditory evoked potentials. *IEEE Trans Biomed Eng* BME-30:43-49 (1983).

Jivet, J., and J. G. Webster. Errors in cuff blood pressure measurements for Korotkov and impedance plethysmography methods, p. 319. *29th ACEMB* 1976.

Johnson, W. K. The dynamic pneumocardiogram: an application of coherent signal processing to cardiovascular measurement. *IEEE Trans Biomed Eng* BME-28:471-475 (1981).

Kantrowitz, P. A review of non-invasive blood pressure measurement using a cuff, with particular respect to motion artifact. *Biomed Eng (Lond)* 8:480-481 (1973).

Kaufman, L., and S. J. Williamson. The evoked magnetic field of the human brain. *Ann NY Acad Sci* 340:45-65 (1980).

Kawakami, K., B. Watanabe, K. Ikeda, and M. Oshima. Capacitoplethysmography-plethysmography by capacitance change detection. *J Med Electron Biol Eng (Japan)* 15:410-415 (1977).

Keefe, J. F., L. T. Rauterkus, M. J. Wolk, D. H. Brand, and H. J. Levine. Electrostatic ballistogram: analysis of electrical fields about the human body. *J Appl Physiol* 28:89-91 (1970).

Klein, F. F., and D. A. Davis. The use of the time domain analyzed EEG in conjunction with cardiovascular parameters for monitoring anesthetic levels. *IEEE Trans Biomed Eng* BME-28:36-40 (1981).

Ko, W. H., M. R. Neuman, R. N. Wolfson, and E. T. Yon. Insulated active electrodes. *IEEE Trans Ind Elec Control Instrum* 17:195-198 (1970).

Kosonocky, W. F., H. G. Erhardt, G. Meray, V. Shallcross, and H. Elabd. Advances in platinum silicide Schottky-Barrier IR-CCD image sensors. *SPIE* 225:69-71 (1980).

Kraman, S. S. Determination of the site of production of respiratory sounds by subtraction phonopneumography. *Am Rev Resp Dis* 122:303-309 (1980).

Kudrow, L. Thermographic and doppler flow asymmetry in cluster headache. *Headache* 204-208 (1978).

Kurtev, N. G., Y. S. Inin, V. I. Khakhin, and Y. V. Khakhan. ATP-12M IR imaging system. *Meas Tech* 22:480-482 (1979).

Larson, L. E. An analysis of the intercorrelations among spectral amplitudes in the EEG: A generator study. *IEEE Trans Biomed Eng* BME-16:23-26 (1969).

Leblanc, P., P. T. Macklem, and R. D. Ross. Breath sounds and distribution of pulmonary ventilation. *Am Rev Resp Dis* 102:10-16 (1970).

Lee, K. M. Wall-less microwave cavity for optical detection of magnetic resonance. *Rev Sci Instrum* 53:702-704 (1982).

Lewis, R. W., and R. M. Harrison. Contact scrotal thermography. II. Use in the infertile male. *Fertile Steril* 34:259-263 (1980).

Lindstrom, K., L. Mauritzson, G. Benoni, P. Svedman, and S. Willner. Application of air-borne ultrasound to biomedical measurements. *Med Bio Eng & Comput* 20:393-400 (1982).

Malmivuo, J. A. V., and J. P. Wikswo, Jr. A new practical lead system for vector magnetocardiography. *IEEE Proceedings* 809-811 (1977).

Manley, M. T., C. D. Thursfield, and J. B. McGuinness. Aspects of noninvasive cardiac monitoring. *Biomed Engineering* April:144-148 (1974).

May, T. H., G. L. Stamm, and J. A. Blodgett. Applications of digital processing to calibrated infrared imagery. *SPIE* 256:55-60 (1980).

McCallion, E. W., D. S. Glad, J. S. Lorenzo, C. M. Parry, and C. W. Clench. Pulse-bias mosaic test data and subassembly configuration. SPIE *225:39-45 (1980).*

McPee, R., G. M. Balue, M. Gerhard. Numerical Diagnosis using "Statrules". *IEEE Trans Biomed Eng* BME-16:27-39 (1969).

McKenzie,. R., R. K. Wadhwa, K. Rajindar, and R. C. Bedger. Noninvasive measurement of cardiac output during laparoscopy. *J Rep Med* 24(6):247-250 (1980).

McKusick, V. A., J. T. Jenkins, and G. N. Webb. The acoustic basis of the chest examination. *Am Rev Resp Dis* 72:12-34 (1955).

McRae, L. P., J. A. Cadwallader, III, and M. M. Kartchner. Oculoplethysmography and carotid phonoangiography for the noninvasive detection of extracranial carotid occlusive disease. *Med Instrum* 13:87-91 (1979).

Meldrum, S. J. The principles underlying Dinamap-a microprocessor based instrument for the automatic determination of mean arterial pressure. *J Med Eng Tech* 2:243-244 (1978).

Miller, B. D., and D. Bruce. A computerized pulmonary spectral phonograph. *6th New England Bioeng Conf Proc* 79-82 (1978).

Modesto, J. P., and K. M. C. da Silva. Drift-free electronic integrator for respiration studies. *Med Biol Eng & Comput* 20:457-460 (1982).

Mori, M., K. Kinoshita, H. Morinari, T. Shiraishi, S. Koike, and S. Murao. Waveform and spectral analysis of crackles. *Thorax* 35:843-850 (1980).

Moss, A. A., K. Y. Herbert, and A. C. Brito. Use of thermography to predict intestinal viability and survival after ischemic injury--A blind experimental study. *Thermography* 16:24-29 (1981).

Murphy, R. L. H. Human factors in chest auscultation, pp. 73-88. *In* Human factors in health care. Pickett, R. M., T. J. Triggs (Ed). Lexington, Mass: DC Heath & Co., 1975.

Murphy, R. L. H. Jr., S. K. Holford, and W. C. Knowler. Visual lung-sound characterization by time-expanded wave-form analysis. *J New England Med* 296:968-971 (1977).

Murphy, R. L. Auscultation of the lung--past lessons, future possibilities. *Thorax* 36:99-107 (1981).

Nakayama R., and T. Azuma. Noninvasive measurement of digital arterial pressure and compliance in man. *Am J Physiology* 233:H168-H179 (1977).

Nath, A. R., and L. H. Capel. Inspiratory crackles--early and late. *Thorax* 29:223-227 (1974).

Nath, A. R., and L. H. Capel. Inspiratory crackles and mechanical events of breathing. *Thorax* 29:695-698 (1974).

Newman, P., and N. H. Davis. Thermography as a predictor of sacral pressure sores. *Age and Aging* 10:14-18 (1981).

Nyirjesy, I. Breast thermography. *Clin Obstet and Gynec* 25(2):401-408 (1982).

Ochoa, W., and I. Ohara. The effect of hematocrit on photoelectric plethysmogram. *Tohoku J Experi Med* 132:413-419 (1980).

O'Donnell, D. M., and S. S. Kraman. Vesicular lung sound amplitude mapping by automated flow-gated phonopneumography. *J Appl Physiol* 53:603-609 (1982).

O'Donnell, T. F. Jr., S. G. Pauker, A. D. Callow, J. J. Kelly, K. J. McBride, and S. Korwin. The relative value of carotid noninvasive testing as determined by receiver operator characteristic curves. *Surgery* 87:9-19 (1980).

Olson, W. H., D. R. Schmincke, and B. L. Henley. Time and frequency dependence of disposable ECG electrode skin impedance. *Med Instrum* 3:269-272 (1979).

Orton, C. G.(Ed.) Progress in Medical Radiation Physics: Vol 1, pp. 295-317. C. G. Orton (Ed.) New York: Plenum Press, 1982.

Pantazatos, P., and M. M. Chen. Computer aided tomographic thermography: a numerical simulation. *J Bioeng* 2:397-410 (1978).

Pardee, N. E., C. J. Martin, and E. H. Morgan. A test of the practical value of estimating breath sound intensity. *Chest* 70:341-344 (1976).

Paulus, D. A. Noninvasive blood pressure measurement. *Med Instrum* 15:91-94 (1981).

Pedersen, P. C., C. C. Johnson, C. H. Durney, and D. G. Bragg. An investigation of the use of microwave radiation for pulmonary diagnostics. *IEEE Trans Biomed Eng* BME-23:410-412 (1976).

Piraino, D. W., G. L. Zick, and G. A. Holloway. An instrumentation system for the simultaneous measurement of transcutaneous oxygen and skin blood flow. *IEEE Front Eng in Health Care*. pp55-58 (1979).

Ploysongsang, Y., R. R. Martin, W. R. D. Ross, R. G. Loudon, and P. T. Macklem. Breath sounds and regional ventilation. *Am Rev Resp Dis* 116:187-199 (1977).

141

Ploysongsang, Y., P. T. Macklem, and W. R. D. Ross. Distribution of regional ventilation measured by breath sounds. *Am Rev Resp Dis* 117:657-664 (1978).

Pykett, I. L. NMR imaging in medicine. *Scientific Am* 246:78-88 (1982).

Rajapakse, C., D. M. Grennan, C. Jones, L. Wilkinson, and M. Jayson. Thermography in the assessment of peripheral joint inflammationa re-evaluation. *Rheumat Rehab* 20:81-87 (1981).

Reynolds, M. I., and J. Knox. A simple device for measuring mean skin temperature. *J Med Eng Tech* 2:244-246 (1978).

Rich, R., and M. R. Neuman. Preliminary clinical evaluation of a miniature dry surface electrode, for obtaining heart rate of infants. *29th ACEMB* Nov:329 (1976).

Richardson, P. C., and R. M. Adams. Electric-field disturbances near the human body. *J Appl Physiol* 26:838-840 (1969).

Riddle, H. C., W. E. Brydon, and D. A. Willoughby. A capacitance plethysmograph for measuring small volume changes. *Biomed Eng* 9:301-303 (1974).

Ring, E. F. J. Quantitative medical thermography. *SPIE* 110:78-84 (1977).

Ring, E. F. J., P. A. Dieppe, and P. A. Bacon. The thermographic assessment of inflammation and anti-inflammatory drugs in osteoarthritis. *Br J Clin Practice* 263-264 (1981).

Ritchie, W. G. M., M. S. Lapayowker, and R. L. Soulen. Thermographic diagnosis of deep venous thrombosis—anatomically based diagnostic criteria. *Diag Rad* 132:321-329 (1979).

Roberts, V. C. A review of non-invasive measurement of blood flow. *Biomed Eng* 9:332-335 (1974).

Robicsek, F., T. N. Masters, and R. H. Svenson. The application of thermography in the study of coronary blood flow. *Surgery* 84:858-864 (1978).

Rodriguez F., G. Bierzwinsky, and M. Nassar. Use of noninvasive monitoring in hemorrhagic shock. *Crit Care Med* 1:141-144 (1973).

Rollo, F. D. Future vistas in cardiovascular nuclear medicine. *Cardiovascular Nuclear Med* 6:1-9 (1981).

Romani, G. L., S. J. Williamson, L. Kaufman, and D. Brenner. Characterization of the human auditory cortex by the neuromagnetic method. *Exp Brain Res* 47:381-393 (1982).

Rosi, P. S., H. Yokochi, S. Deller, A. G. Greenbury, S. Rabin, S. Blatt, F. J. Lewis, and J. E. Jacobs. Noninvasive automatic patient monitoring. *Surg Forum* 20:234-236 (1969).

Ruggera, P. S. An EMC test procedure for an electroencephalograph (EEG) using human subjects and simulated electronic patients. *IEEE Int Symp Electromag Compat* 200-206 (1980).

Rush, S., and D. A. Driscoll. EEG electrode sensitivity--an application of reciprocity. *IEEE Trans Biomed Eng* BME-16:15-22 (1969).

Sakamoto, K., K. Muto, H. Kanai, and M. Iizuka. Problems of impedance cardiograph. *Med Bio Eng & Comput* 17:697-709 (1979).

Salter, M. G. Fabrication of lithium chloride-balsa wood electrodes for electrocardiographic monitoring. SAM-TR-69-51, USAF School of Aerospace Medicine, Aerospace Medical Division, Brooks Air Force Base, Tex., 1969. (AD-697380)

Sances, A. Jr., and S. J. Larson. Evoked potential recording:an adjunct to human stereotactic surgery. *IEEE Trans Biomed Eng* BME-14(3):162-165 (1967).

Saunders, M. G. Comment "On the sufficiency of autocorrelation functions as EEG descriptors." *IEEE Trans Biomed Eng* BME-14:204-205 (1967).

Salles-Cunha, S. X., R. E. Halbach, J. H. Battocletti, and A. Jr. Sances. The NMR blood flowmeter applications. *Med Phys* 8:452-457 (1981).

Seelentag, W. W. Electrostatic X-Ray Imaging, pp. 1-56. *In* Medical Imaging Techniques. Watson, B. W.(Ed.) New York: Peter Peregrinus Ltd. (1979).

Shafer, W. A. Further Development of the Field Effect Monitor. *Aero Med Assoc Proc* 1:125-126 (1967).

Shafer, W. A. Non-contact Physiological Sensing, pp. 137-141. *Proc Natl Biomed Sci Instrum Symp*, 4th, Albuquerque, 1967.

Shafer, W. A. Telemetry on Man without Attached Sensors. *NY State J Med*, 2832-2837 (1967).

Siegel, L. A computer-controlled stereotaxic system. *IEEE Trans Biomed Eng* BME-16:197-204 (1969).

Silverstein, M. E., and J. Worman. A portable multi-sensor telemetry system for a rural health network. *IEEE Front Eng in Health Care*: 260-266 (1979).

Singer, J. R. Measuring fluid velocity by nuclear resonance. *Electronics* 77-78 (1960).

Singer, J. R. Flow rates using nuclear or electron paramagnetic resonance techniques with applications to biological and chemical processes. *J Applied Physics* 31:125-127 (1960).

Smith, J. R. Automatic analysis and detection of EEG spikes. *IEEE Trans Biomed Eng* BME-21:1-7 (1974).

Spaiser, L. H. An infra-red photoplethysmograph coupler. *Psychophysiology* 14:75-77 (1977).

Spodick, D. H., and J. R. St.Pierre. Pulsus alternans: physiologic study by noninvasive techniques. *Am Heart J* 80:766-777 (1970).

Sramek, B. B. Electrical bioimpedance. *Med Electronics* 95-105 (1983).

Stanton, P. E., D. A. McClusky, and P. A. Lamis. Hemodynamic assessment and surgical correction of kinking of the internal carotid artery. *Surgery* 84:793-802 (1978).

Stein, P. D., and E. F. Blick. The potential usefulness of arterial tonometry for the measurement of instantaneous changes of aterial blood pressure. *Med Instrum* 6:272-275 (1972).

Steketee, J. The influence of cosmetics and ointments on the spectral emissivity of skin. *Phys Med Biol* 21:920-930 (1976).

Stevenson, J. G., I. Kawabori, and W. G. Guntheroth. Noninvasive detection of pulmonary hypertension in patent ductus arteriosus by pulsed doppler echocardiography. *Circulation* 60:355-359 (1979).

Stucki, P.(Ed.) Advances in Digital Image Processing, pp. 125-161. New York: Plenum Press, 1979.

Takatani, S., P. W. Cheung, and E. A. Ernst. A noninvasive tissue reflectance oximeter. *Ann Biomed Eng* 8:1-15 (1980).

Tichauer, E. R. The objective corroboration of back pain through thermography. *J Occup Med* 19:727-731 (1977).

Truxal, C. Watching the brain at work. *IEEE Spectrum* 52-57 (1983).

Weed, H., M. Sauter, R. Roberts, G. Vossius, and H. Kwee. Relationship of acoustic heart sound frequency shift to heart function. *Front Eng Health Care* 386-389 (1981).

Weinman, J. An appraisal of some noninvasive cardiovascular techniques. *Med Biol Eng* 10:496-503 (1972).

Weinman, J., A. Hayat, and G. Raviv. Reflection photoplethysmography of arterial-blood-volume pulses. *Med Biol Eng & Comput* Jan:22-31 (1977).

Weiss, E. B., and C. J. Carlson. Recording of breath sounds. *Am Rev Resp Dis* 105:835-839 (1972).

Wells, P. N. T. A review of medical imaging methods. *Australian Phys & Eng Sci Med* 4:33-39 (1981).

Wesseling, H. Karel, B. Wit, and J. E. W. Beneken. Arterial haemodynamic parameters derived from noninvasively recorded pulsewaves, using parameter estimation. *Med & Biol Eng* Nov:724-731 (1973).

Wieland, J. A. An evaluation of current status of medical thermography and the diagnostic value of presently available medical thermographs. *SPIE* 191-205 (1971).

William, H. Spectral analysis of arterial sounds--a noninvasive method of studying arterial disease. *Med & Biol Eng* Sept:700-705 (1975).

Williams, T. L. Standard reference lenses for the infrared. *SPIE* 98:16-20 (1976).

Wolthuis, R., D. McAfoose, D. Hull, and J. Fischer. Portable blood measurements using the Korotkov sound technique--a study of measurement accuracy. *Biomed Sci Instrum* 15:101-104 (1979).

Wooten, F. T., W. W. Waring, M. Wegmann, W. F. Anderson, J. D. Conley. Method for respiratory sound analysis. *Med Instrum* 2:254-257 (1978).

Wouda, A. A. Raynaud's phenomenon. *Acta Med Scand* 201:519-523 (1977).

Yakush, S. A., T. J. Willey, T. C. Park, and G. Maeda. Mutiprocessor architecture for rapid EEG frequency analysis. *IEEE Trans Biomed Eng* BME-29:55-56 (1982).

Zimmerman, J. T., M. Reite, and J. E. Zimmerman. Magnetic auditory evoked fields--dipole orientation. *Electroenceph Clin Neurophy* 52:151-156 (1981).

END

DTIC

6 — 86